Tecnologia Meccanica

Two-stroke engine for model aircraft

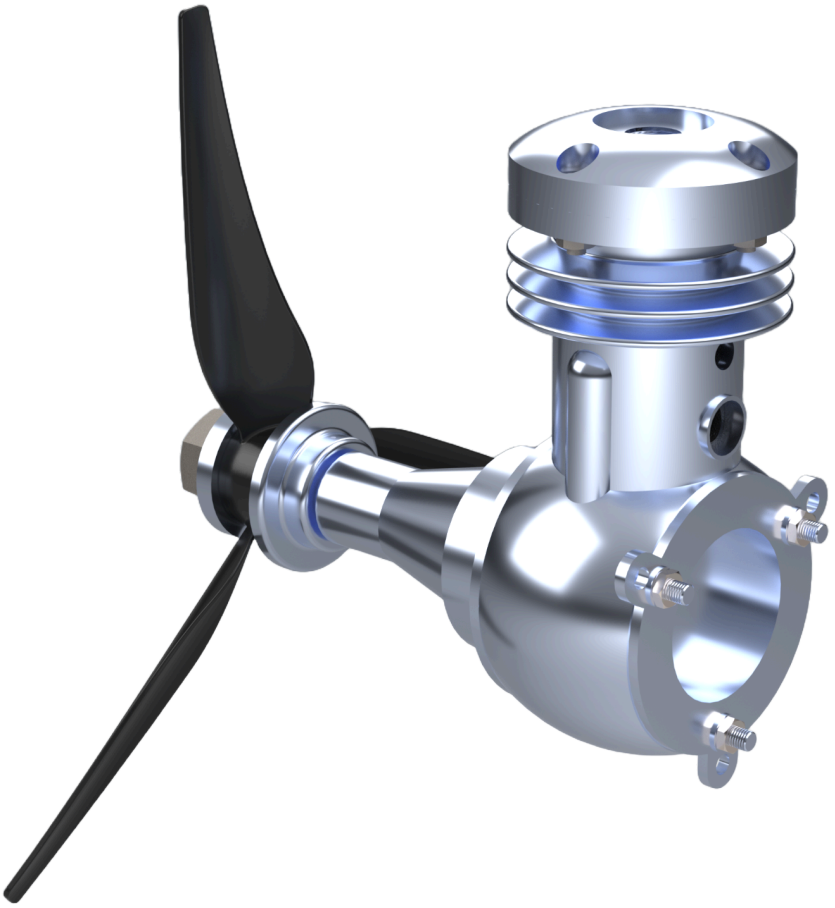

Edited by Michele Spinelli and Sofia La Spina

C.d.L in Ingnegneria per Il Design Industriale A.A. 2024/2025

SUMMARY

1. Project goal

The objective of this project is to define the manufacturing process for certain components of a chosen product and to document the entire study in a technical report. Once the product has been selected and its assembly designed, the manufacturability of some of its components will be analyzed. These components will also be studied using their respective digital reproductions in CAD software. Furthermore, photorealistic renders of the individual components, the exploded view, and the CAD assembly will be included. The process then continues with the drafting of the technical drawings for the components studied and the overall assembly. The analysis of the manufacturing processes will include an examination of some of the most widely used industrial processes today, such as casting, plastic deformation, 3D printing, chip removal, and welding. During the design phase, both the costs and the times associated with production will be evaluated.

1.1 Object's choice

The choice fell on a two-stroke engine for model aircraft.
We became aware of it specifically during an old modeling course, which showed us its operation and geometry, given the high number of components and the various functions they will have to perform we consider this choice appropriate due to the numerous types of machining operations.

2. Assembly drawing

The technical drawing of the assembly, shown below, was created to display the main dimensions (the specific ones will be present in the technical drawings of the components studied) and the names/quantities of the total components.

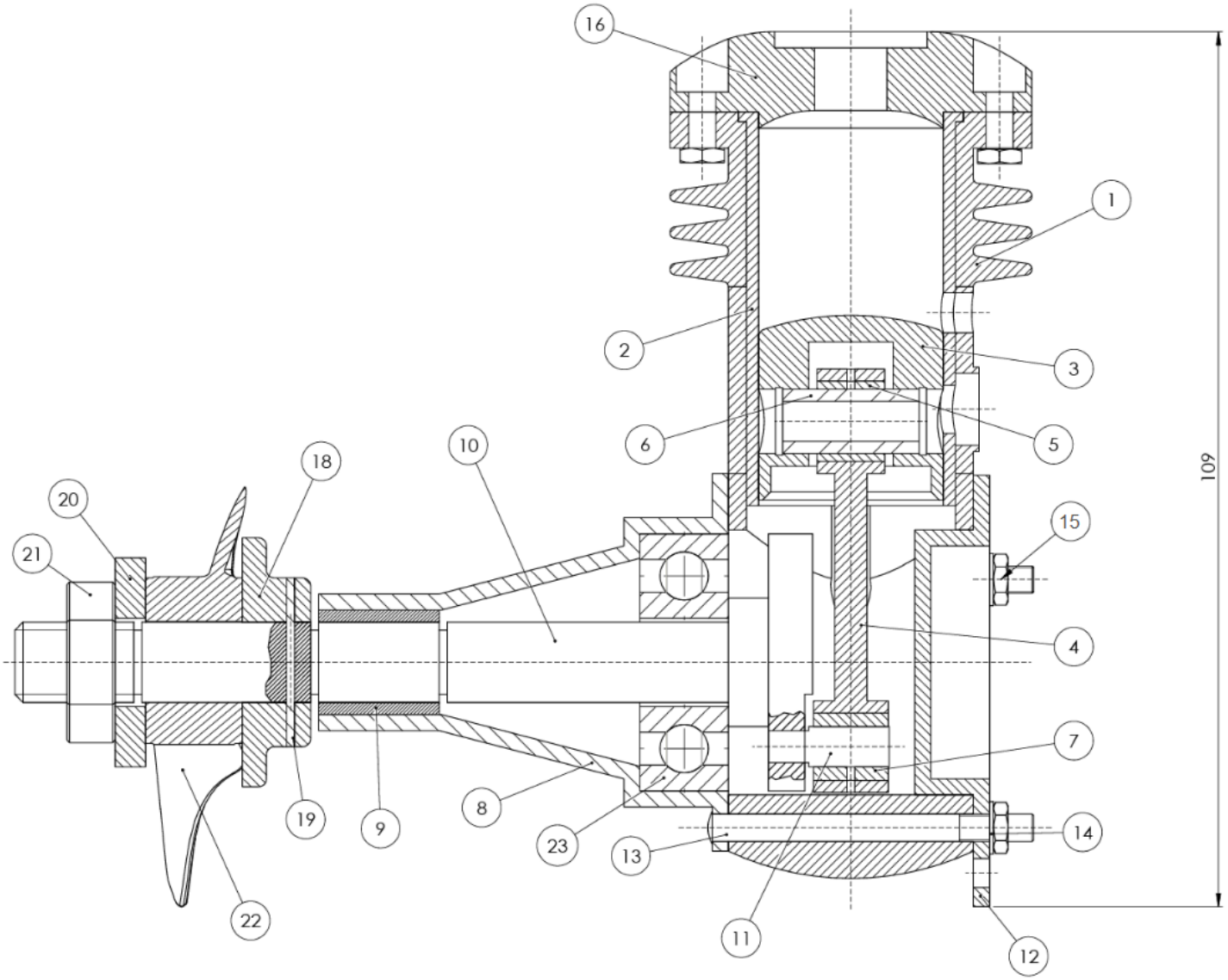

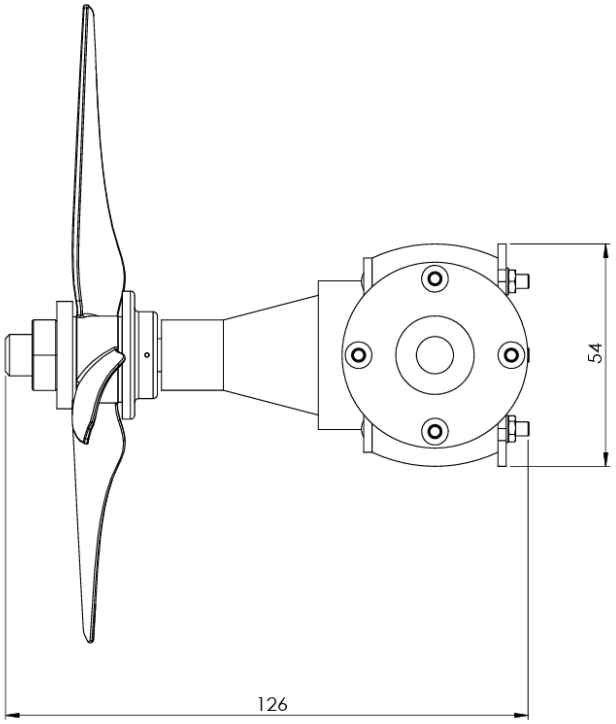

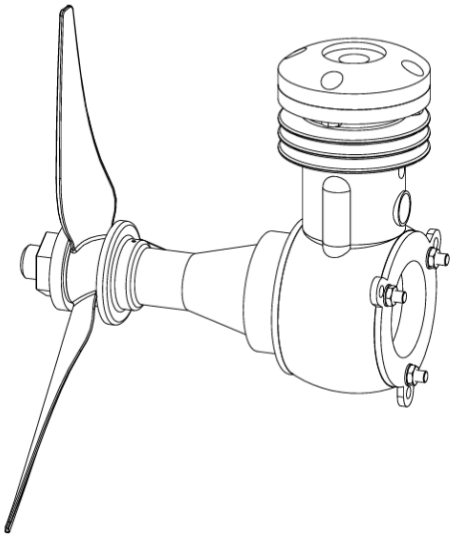

No.	Name	Quantity	No.	Name	Quantity
1	Casing	1	13	Dowel Screw	3
2	Liner	1	14	Washer	3
3	Piston	1	15	M3 Nut	7
4	Connecting Rod	1	16	Cylinder Head	1
5	Bushing	1	17	M3x10 Screw	4
6	Piston Pin	1	18	Support	1
7	Bushing	1	19	Spring Pin	1
8	Support	1	20	Washer	1
9	Bushing	1	21	M10 Nut	1
10	Crankshaft	1	22	Propeller	1
11	Crank Pin	1	23	Ball Bearing	1
12	Cover	1			
Overall Designation: Two-stroke engine for model aircraft					
Drafters: Spinelli Michele, Sofia La Spina					

3. 3D rendering of the components

Below are represented the 3D renders of the most "relevant" components of the entire assembly created in SolidWorks; the components that will be studied in the project, along with their respective manufacturing processes, will be highlighted.

Component 1. ***Crankcase***

Component 2. Liner

Component 3. Piston

Component 4. Connecting Rod

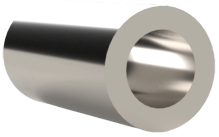

Component 6. Bushing

Component 8. Support

Component 10. ***Crankshaft***

Component 11. ***Crank Pin***

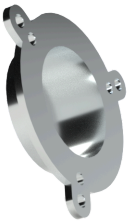

Component 12. ***Cover***

1

Component 16. Cylinder Head

Component 18. Support

Component 22. ***Propeller***

Unmodeled components: n. 5,7,9,13,14,15,17,19,20,21,23

4. Exploded view of the assembly

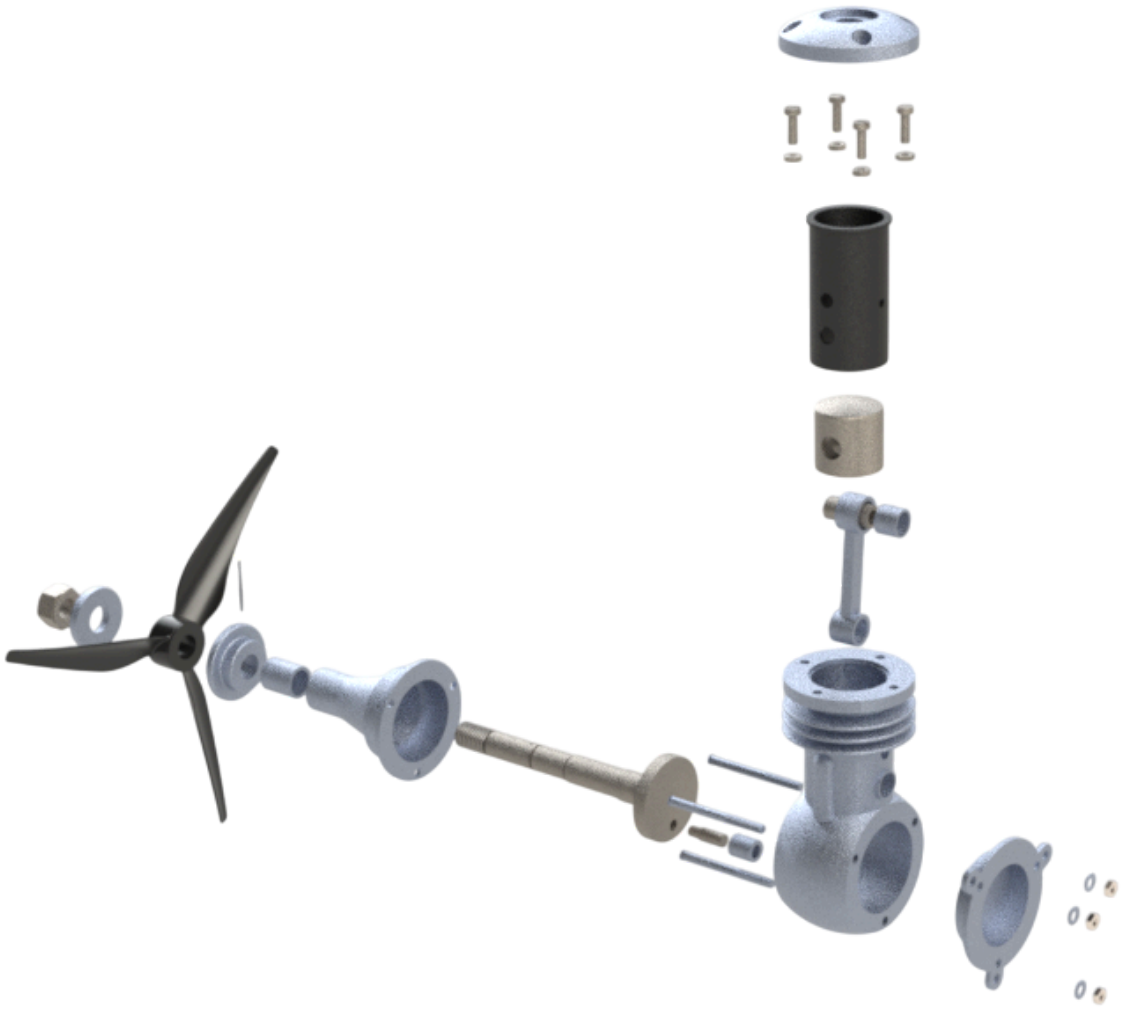

5. Customer requirements

Analyzing the model aircraft market, we have identified the following selection of potential candidates who could serve as buyers/clients:

- **Hobbyists and Model Aircraft Associations**: amateur modelers represent a significant part of the market, these users look for reliable, high-performance, and easy-to-maintain engines for their DIY projects or local competitions, meanwhile organizations and clubs dedicated to the hobby may order larger quantities or request specific solutions for events and races.
  Collaborating with these groups can ensure a stable customer base and direct feedback.
- **Educational Institutions and Training Centers**: schools and training centers that use model aircraft for engineering courses or educational activities may be interested in innovative and safe solutions, which are useful for explaining concepts of mechanics and aerodynamics.
- **Production for Kits and Large-Scale Distribution**: this is a viable option only if the engine is intended to be integrated into model aircraft kits by larger manufacturers or distributed through national/international commercial channels.

The production demand estimates are indicative and depend on several factors:

- Actual market demand,
- The price and competitiveness of the product,
- Production capacity and investments in automation,
- The presence of any supply agreements with clubs, schools, or distributors.

We could initially aim for an annual production in the range of 500–2,000 units.
From this, we deduce that we will need 500–2,000 units of each component we produce, given their uniqueness in the assembly, so we have chosen to produce **1,000 units per year of our product**, which falls within our predefined range.

6. Component introduction: Crankcase

The crankcase of a two-stroke engine for model aircraft is an essential component that must withstand several kinds of strain and it also has to perform the main important functions, like: housing and protecting internal components, channeling the air-fuel mixture flow, dissipating heat and supporting the crankshaft.

The most recommended manufacturing process is the casting as it allows for the creation of complex geometries and ensures good mechanical strength of the component.

6.1 Material's selection

These functions must be paired with a manufacturing material that makes the crankcase lightweight, strong and capable of dissipating the heat generated. The material most commonly used for this purpose is aluminium (mostly its alloys such as Al-Si) due several specific advantages: lightness, good mechanical strength and high thermal conductivity.

Following the information displayed on the technical drawing and considering what we mentioned earlier, we selected the material for our crankcase to be **G. Al-Si 13 alloy**. This is a primary aluminium-silicon casting alloy with 13% of silicon, with the following mechanical and physical properties:

- **Yield strength** = 69-108 MPa
- **Tensile strength** = 157-216 MPa
- **Elongation** = 4-10 %
- **Density** = 2,6-2,9 kg/dm^3
- **Young's modulus** = 69-79 GPa
- **Thermal conductivity** = 130-165 $\frac{W}{m \cdot C^{\circ}}$.

Famiglia: Al Si

Denominazione EN : EN AB 44100 - Al Si 12 (b)

Denominazione UNI: UNI 4514 - G Al Si 13

Rev. 0 del 01/09/02

COMPOSIZIONE CHIMICA %

LEGA		ELEMENTI											
		Cu	Mg	Si	Fe	Mn*²	Ni	Zn	Pb	Sn	Ti	Impurezze singole	Impurezze globali
EN AB 44100 - Al Si 12 (b)	min			10,5									
	max	0,10	0,10	13,5	0,55	0,55	0,10	0,15	0,10		0,15	0,05	0,15
UNI 4514 - G Al Si 13	min			12,0									
	max	0,05	0,05	13,5	0,6	0,4	0,01	0,08			0,10		0,15*

** Se Fe >= 0,3 Mn = 0,2 - 0,4%

*Esc.Fe+Mn+Ti

CARATTERISTICHE MECCANICHE RILEVATE SU PROVETTE COLATE A PARTE SECONDO UNI 3039

Stato Fisico Colata	Simbolo	R Carico unitario di rottura		S Carico al limite di snervamento		A Allungamento	HB Durezza Brinell
		Kg/mm2	N/mm2	Kg/mm2	N/mm2	%	
IN SABBIA (Grezzo)	F	17-20	165-195	8-10	80-100	4-8	50-60
Ricotto	T5	16-20	155-195	7-11	70-110	6-10	50-60
IN CONCHIGLIA (Grezzo)	F	18-22	175-215	9-11	90-110	5-7	55-65
Ricotto	T5	17-22	165-215	8-10	80-100	6-10	50-60
SOTTOPRESSIONE (Grezzo)	F	23-27	225-265	13-17	125-165	1,5-2,5	75-95

IMPIEGHI TIPICI

Lega adatta ad applicazioni richiedenti ottima colabilità in tutte le tecniche di colata, per la realizzazione di getti a pareti sottili viene impiegata su particolari che non richiedono elevata resistenza meccanica ma buoni valori di allungamento e carico di rottura.
Utilizzata particolarmente nell'industria tessile, nella meccanica e nel settore elettrico e dei trasporti.

CARATTERISTICHE TECNOLOGICHE

RESISTENZA MECCANICA A CALDO	MEDIA
RESISTENZA GENERALE ALLA CORROSIONE	BUONA
LAVORABILITA' ALL' UTENSILE	CATTIVA
COLABILITA'	OTTIMA
LUCIDABILITA'	MEDIA

FRAGILITA' DI RITIRO	PICCOLA
TENUTA A PRESSIONE	BUONA
SALDABILITÀ ①	BUONA
ATTITUDINE ALL'ANODIZZAZIONE DECORATIVA ②	SCARSA
ATTITUDINE ALL'ANODIZZAZIONE PROTETTIVA ②	SCARSA

PROPRIETÀ' FISICHE

PESO SPECIFICO	2,65 Kg/dm³
INTERVALLO DI SOLIDIFICAZIONE E DI FUSIONE ③	577 °C
CALORE SPECIFICO(a100)*	0,23 cal/g °C
CALORE LATENTE DI FUSIONE	93 cal/g
RITIRO LINEARE	~1,30 %
RESISTIVITÀ' A 20°C	4,5 μΩ cm
MODULO ELASTICO	7600 Kg/mm²

CONDUTTIVITÀ' TERMICA a 20°C ④	0,37 cal/cm sec °C
DILATAZIONE TERMICA da 20 a 100°C	$20,0 \times 10^{-6}$/°C
DILATAZIONE TERMICA da 20 a 200°C	$20,5 \times 10^{-6}$/°C
DILATAZIONE TERMICA da 20 a 300°C	$21,5 \times 10^{-6}$/°C
TEMPERATURA MASSIMA DI FUSIONE	780 °C
INTERVALLO OTTIMO DI COLATA	
°in sabbia	700-750 °C
°in conchiglia	700-750 °C
°sottopressione	640-700 °C

COMPARAZIONE CON NORMATIVE ESTERE EQUIVALENTI O SIMILARI

	ITALIA	GERMANIA (Din1725/5-86)	FRANCIA (NFA57-105)	G.B.R. (BS1490-88)	USA (ASTM B179-82)	ISO (3522-84)	GIAPPONE (JIS H2211-92)	SPAGNA (UNE38200)
Equivalenti	413.1	230.1	AS 13	LM 6	A 413.2	Al Si 12		
Similari				L 33	SAE 305		AC 3 A	L-2520

TRATTAMENTI TERMICI

Ricottura dei getti in sabbia e conchiglia a 360-400 °C per 4-8 ore a regime.

(Schedule of the G.Al-Si 13's property)

6.2 Manufacturing technique's selection: casting

Based on the geometry of the component, the presence of undercuts and internal cavities, the most suitable process that gives us more freedom for manufacturing the crankcase is indeed the casting process.

The permanent mold casting techniques offer numerous advantages in various industrial contexts, which are well-suited to both the component's functional requirements and the aluminium alloy's properties.
However these techniques also show certain drawbacks such as difficulty as thermal deformation and high tooling costs, and considering we aim to manufacture only around 1000 crankcase units the permanent mold solutions are not very cost-effective, the cost of the molds would significantly increase overall expenses without requiring a mass production capacity.

On the other hand we find a valid solution in transitional mold casting techniques, especially in shell molding, this process offers good dimensional accuracy and better surface quality making it ideal for technical components such a crankcase.
Moreover it provides good repeatability and allows for a certain level of process automation, making it economically available for a medium scale production around 1000 units; although the equipment is more expensive compared to sand casting we have to consider the costs will be depreciated over the expected production volume, making shell molding the optimal choice in terms of balancing quality and cost.

6.3 Allowance definition

Now we have to identify where we have to add the machining allowance in the areas that will require additional machining after the die casting process.

The surfaces where machining allowance must be applied will be:

- holes: that will need to be drilled and threading later;
- upper part of the crankcase: to be lathe to achieve the desired shape;
- crankcase head opening: that'll be mill in order to obtain perfectly flat and smooth surfaces considering that it'll be the sealing area with the other components.

For the machining allowance inside the upper hole of the crankcase head we decided to put it with 1 mm thickness considering that the material chosen wan an aluminium alloy and the dimension of the crankcase are 95 mm.

Dimensioni nominali (mm)	**Sovrametalli di lavorazione** (mm)	**Tolleranze** (mm)
≤ 50	0,5 ÷ 1	± 0,1 ÷ 0,25
50 ÷ 175	0,5 ÷ 1	± 0,16 ÷ 0,42
175 ÷ 300	1 ÷ 2	± 0,29 ÷ 0,67
300 ÷ 450	1,3 ÷ 2,5	± 0,71 ÷ 0,83

(In the left is attached the 3D image with the allowance highlighted in red)

(Below is attached the raw casting drawing)

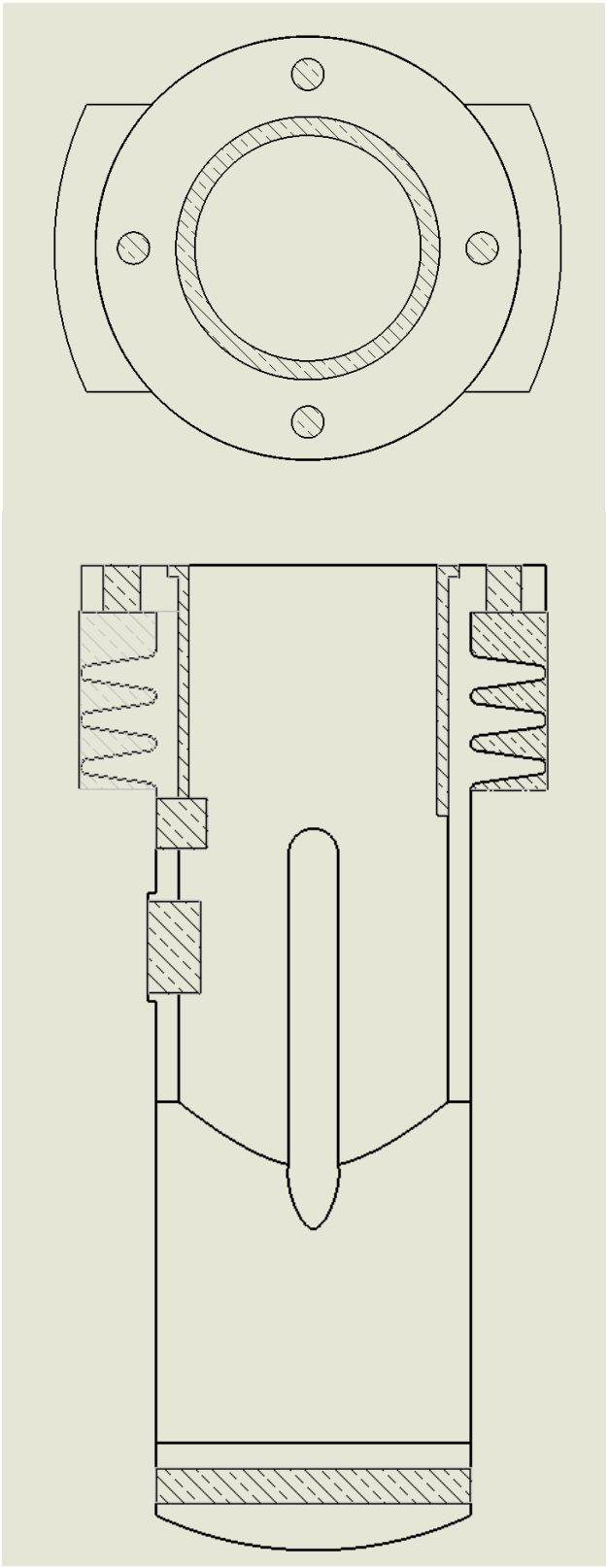

6.3.1 Hole elimination

The only holes that'll be removed from the casting will be the three on the upper part of the crankcase (M3) and the 6 on the lower part (M5), if we attempt to cast them it could lead to deformations or cracks during solidification.

Furthermore since the upper holes on the head will require threading so the machining allowances would've been necessary anyway.

6.4 Parting surface selection

The main division planes are the 3 shown in the following image.
We chose the right plane because it simplifies the placement of the risers, the results of the fewer draft angles and also this plane divides the component into two symmetrical halves.

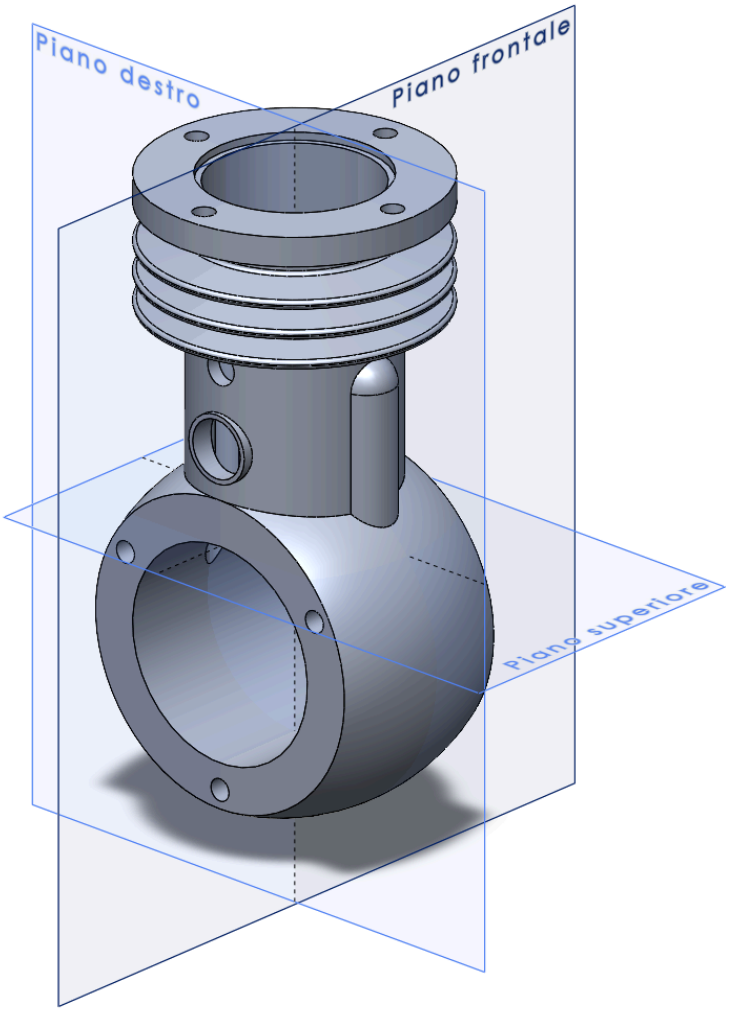

6.5 Draft angles

The surfaces where there will need an additional draft angle are the one highlighted in red, which will be only the upper face of the crankcase where the cylinder head will be placed.

.

VALORI DELLO SFORMO s in mm e in %
dell' ANGOLO di SFORMO β

ALTEZZA del MODELLO (mm)	SFORMO		Angolo di sformo β
	s (mm)	(%)	
fino a 40	0.5	1.25	1'30"
40 - 59	0.75	1.8 - 1.2	1'
60 - 119	1	1.7 - 0.8	40"
120 - 159	1.5	1.7 - 0.8	40"
160 - 199	1.75	1.1 - 0.9	40"
200 - 249	2	1.0 - 0.8	30"
250 - 299	2.5	1.0 - 0.8	30"
300 - 399	3	1.0 - 0.75	30"
400 - 499	3.5	0.9 - 0.8	30"
>= 500	4	<= 0.8	30"

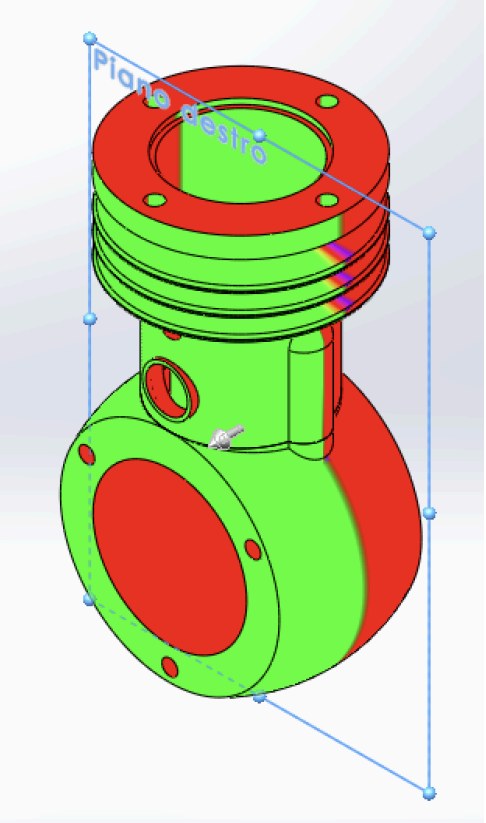

Considering that the crankcase has a height of 95 mm we'll apply a draft angle of 40'', so we'll have to incline the surface by this angle along the same direction of the draft, so the surface will aim to grow away from the extraction direction.

These modifications were not included in the original design as the manufacturing process had not affected the functionality of the component, so we assume they'll be approved.

6.6 Fillet radius

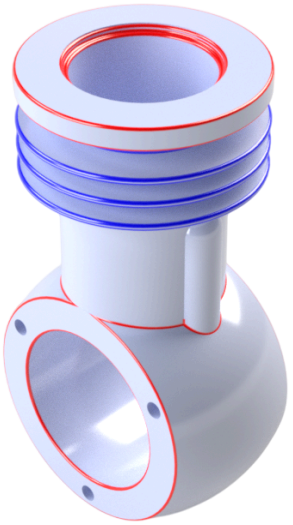

The fillets are applied along the corners that generate convex angles, so the same corners that protrude and could be more exposed to erosion.

In the image beside we highlighted the edges most at risk, these include all the edges of the core and the machining allowances, the fillet radius will match the thickness of the machining allowances.

- Red fillets: represent the manual added radii of 0,5 mm, introduced to improve the mechanical properties;
- Blue fillets: the ones originally included on the design.

6.7 Raw casting enlargement

To compensate for the shrinkage of the casting during cooling the model is scaled up based on material's average linear shrinkage coefficient, which represents the overall behavior of the material throughout the entire cooling process.

Considering the component is made of aluminium alloy, the average linear shrinkage coefficient γ for the alloy G. Al-Si 13 is typically between 1,2-1,3 %.

Therefore the scaling factor s is calculated using the following equation:

$$1 : (1 - \gamma) : s : 1$$

$$s = \frac{1}{1 - \gamma} = \frac{1}{1 - 0{,}012} \simeq 1{,}01$$

6.8 Core forming and design

Considering the selected casting process for the part, namely shell molding, the core forming technique should also be chosen from the group of expendable mold methods, therefore it is advisable to use the same process adopted for the crankcase, both for economic reasons (avoiding the need to increase machining allowances through a different process and making use of the existing equipment) and for mechanical reasons (as shell molding ensures a shape with excellent strength).

A total of four cores will be needed: one cylindrical core coaxial with the parting plane, one cylindrical core perpendicular to the parting plane, and two cores corresponding to the respective grooves.

Regarding the core prints, for the two cores inserted into the holes, considering the small dimensions of the part (95 mm in height), four core prints with a diameter of 6 mm will be sufficient.

The chosen parting plane is the same as the one used for the crankcase, namely the right-hand plane.

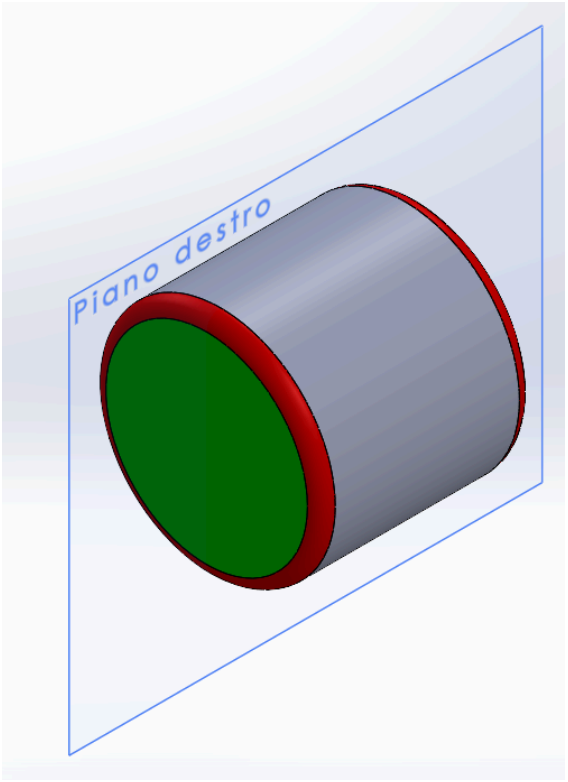

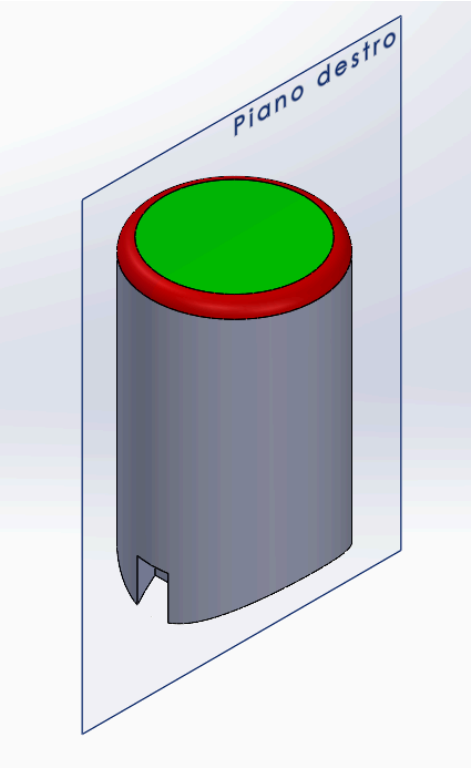

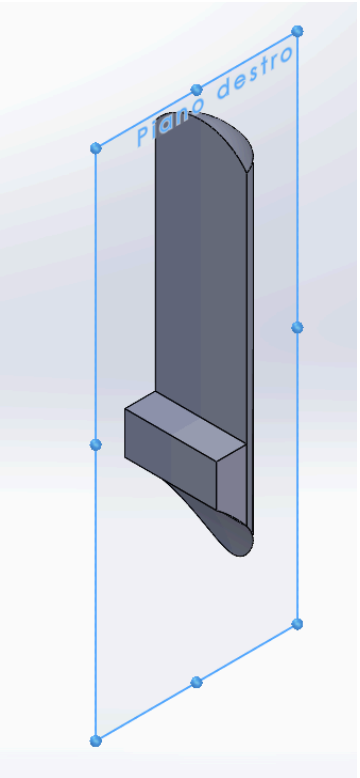

For the cores we designed an interlocking system between the two groove's cores and the core for the coaxial hole to the parting plane, this allows them to be removed without requiring additional machining and without excessively deforming the inner part of the crankcase.

The removal sequence would therefore be as follows: first, the cylindrical core for the hole perpendicular to the parting plane is extracted; then, by applying slight pressure to the other cylindrical core, the two groove cores will detach and fall to the bottom of the crankcase; finally, the cylindrical core for the upper hole can be removed as the two grooves cores.

6.9 Theoretical study of solidification aspects

6.9.1 Calculation solidification modulus

To calculate the cooling modulus we'll need to simplify the casting by dividing it into three parts, in order to approximate it using three elementary solids.The cooling modulus is defined as:

$$M = V / SST$$

Where V is the volume and SST is the thermal exchange surface area, these values are provided by the CAD model with the latter obtained by summing the areas of the non-highlighted surfaces.

N.°	S1 (mm*2)	S2	S3	V (mm*3)	M (mm)
Mv	1059,5	2985,7	786,2	23033,6	4,7
Mr	2700,7			11628,3	4,3
Ma	879,6	4503,5	879,6	26829,2	4,2

Therefore the sprue will be placed in the upper part of the crankcase.

6.9.2 Solidification simulation via software

Considering that the previously used methods were aimed at identifying the last point of solidification, the foundry software Inspire Cast by Altair will be used to verify their accuracy.

After importing the CAD file, it will be necessary to set several parameters to carry out the simulation:

- As the material we selected aluminum AC-21200, this alloy also belongs to the aluminum-silicon category and is the one that most closely matches the composition and properties of the alloy used for our component;.
- The pouring temperature is set to the default suggested by the software, namely 1021.15 K;
- As for the process, it was necessary to select the investment casting option, configuring the mold as silica sand with a thickness of 20 mm.

At this point it is possible to perform the solidification analysis, which will display the evolution of the solid fraction parameter. Below several images are provided to illustrate the simulation process.

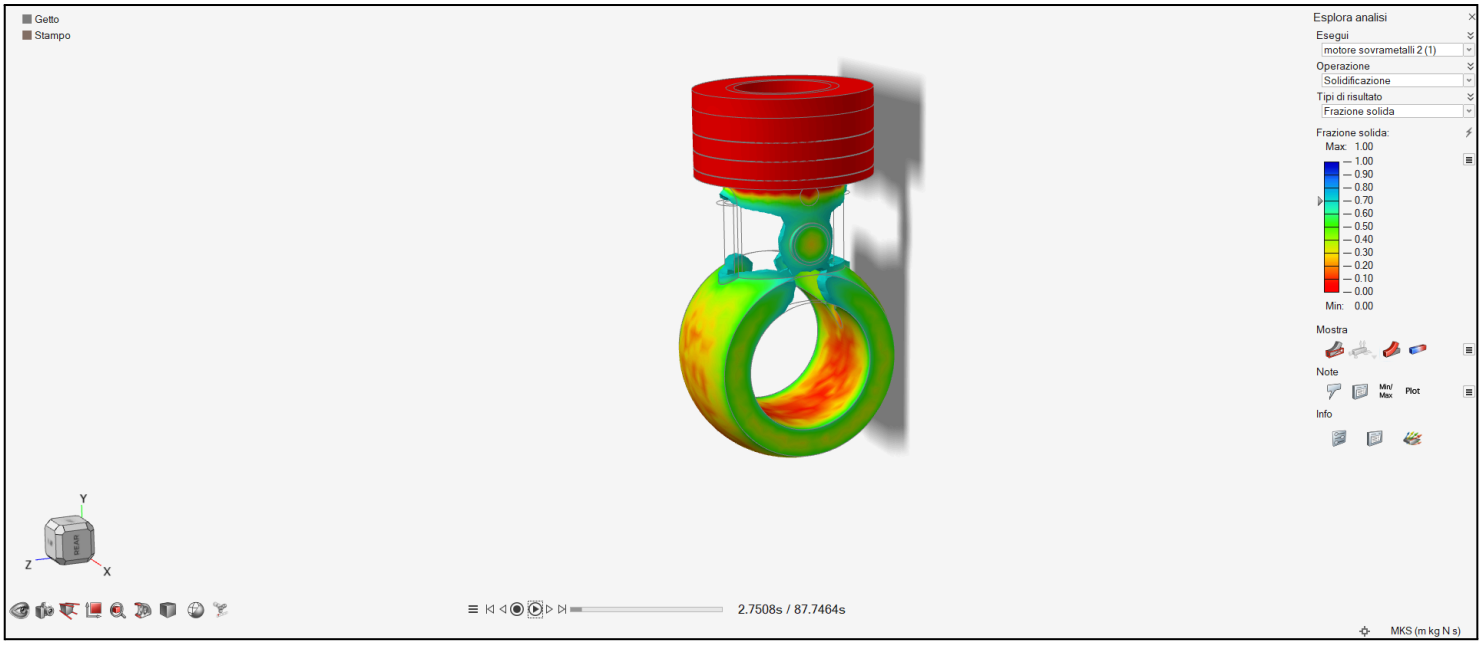

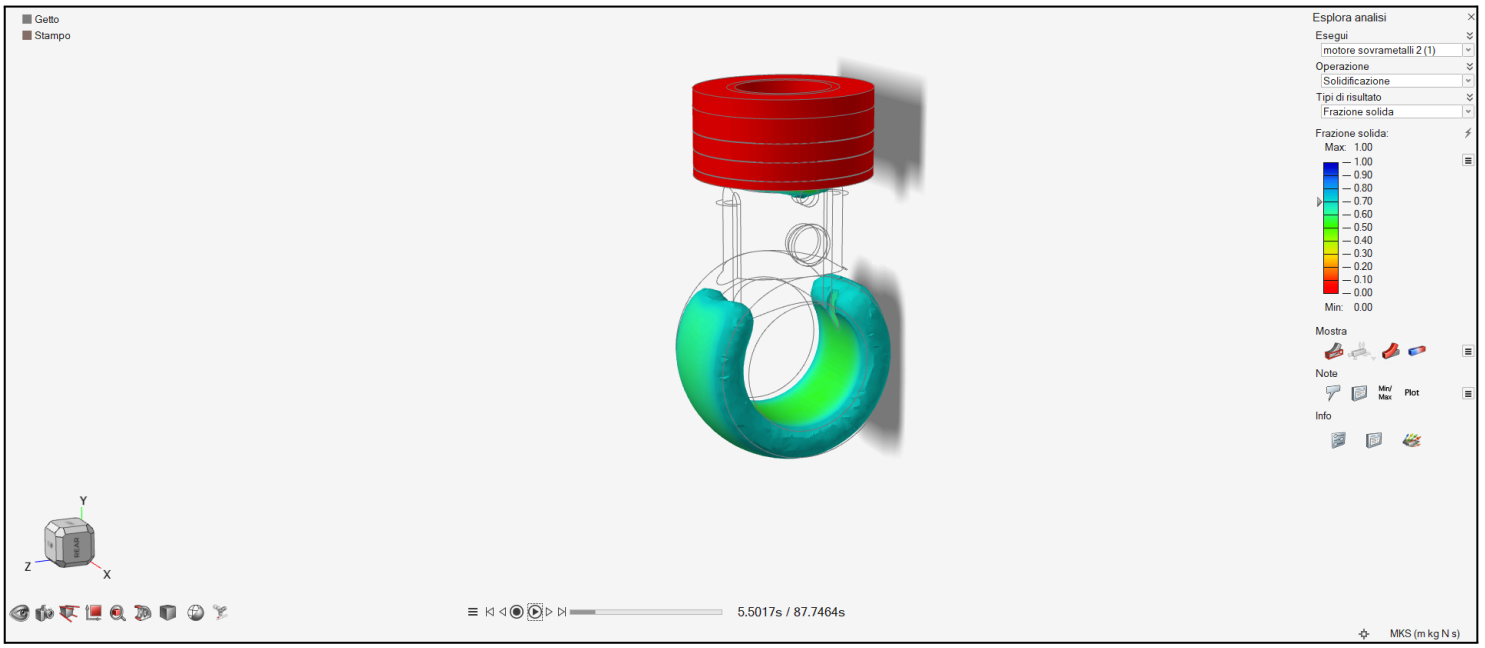
Getto
Stampo
Esplora analisi
Esegui
motore sovrametalli 2 (1)
Operazione
Solidificazione
Tipi di risultato
Frazione solida
Frazione solida:
Max: 1.00
1.00
0.90
0.80
0.70
0.60
0.50
0.40
0.30
0.20
0.10
0.00
Min: 0.00
Mostra
Note
Min/Max
Plot
Info
Y
Z
X
REAR
5.5017s / 87.7464s
MKS (m kg N s)

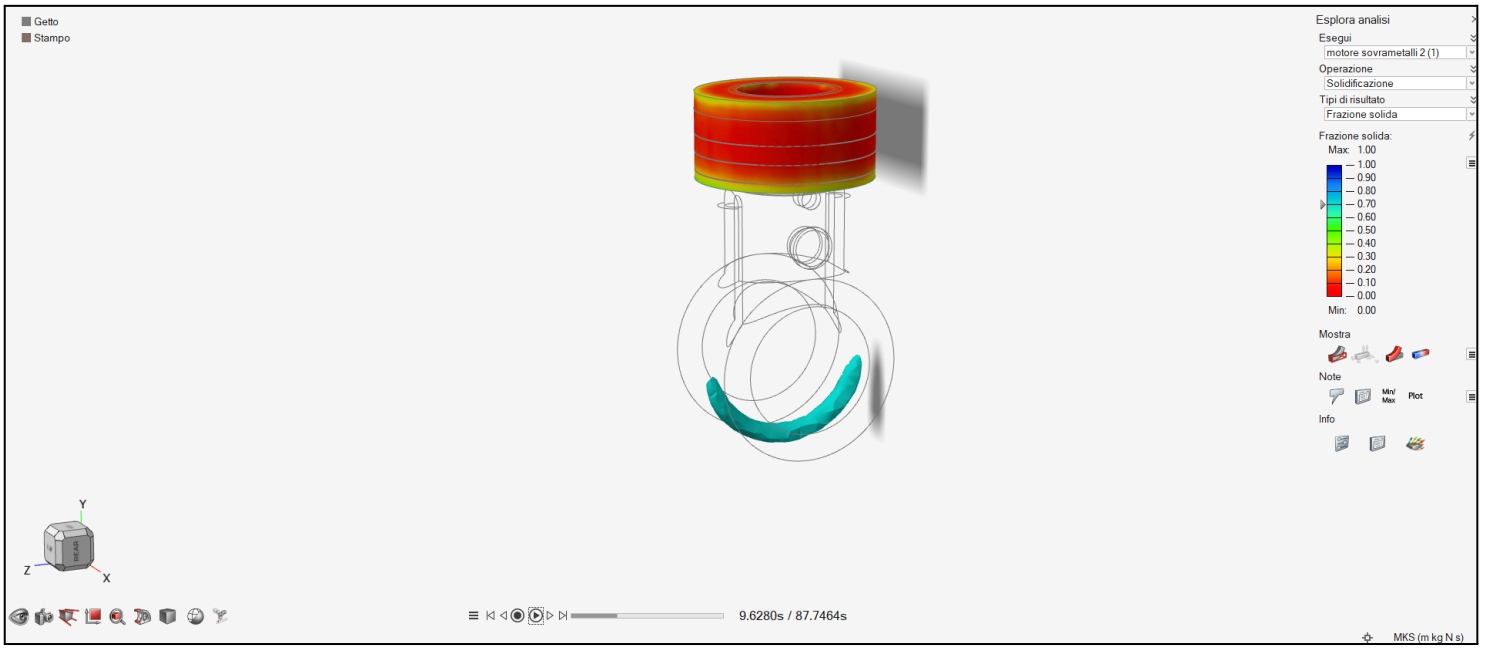
Getto
Stampo
Esplora analisi
Esegui
motore sovrametalli 2 (1)
Operazione
Solidificazione
Tipi di risultato
Frazione solida
Frazione solida:
Max: 1.00
1.00
0.90
0.80
0.70
0.60
0.50
0.40
0.30
0.20
0.10
0.00
Min: 0.00
Mostra
Note
Min/Max
Plot
Info
Y
Z
X
REAR
9.6280s / 87.7464s
MKS (m kg N s)

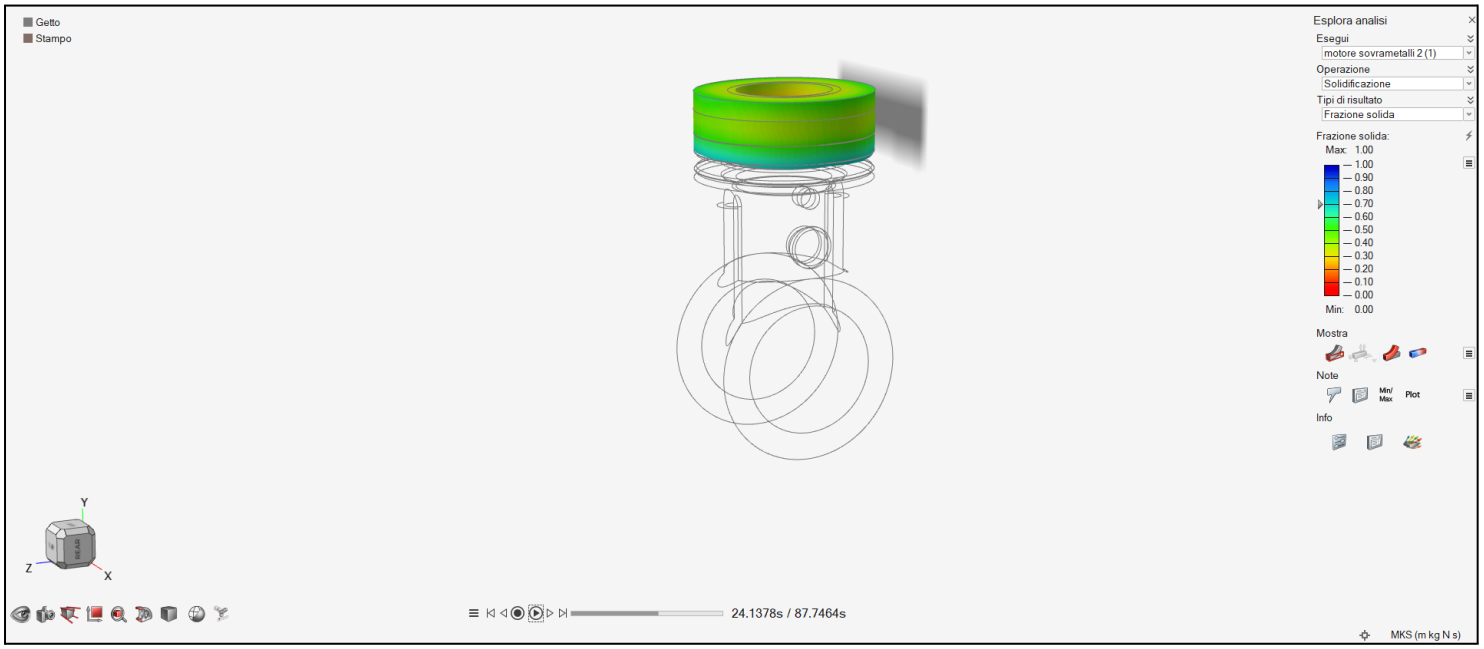

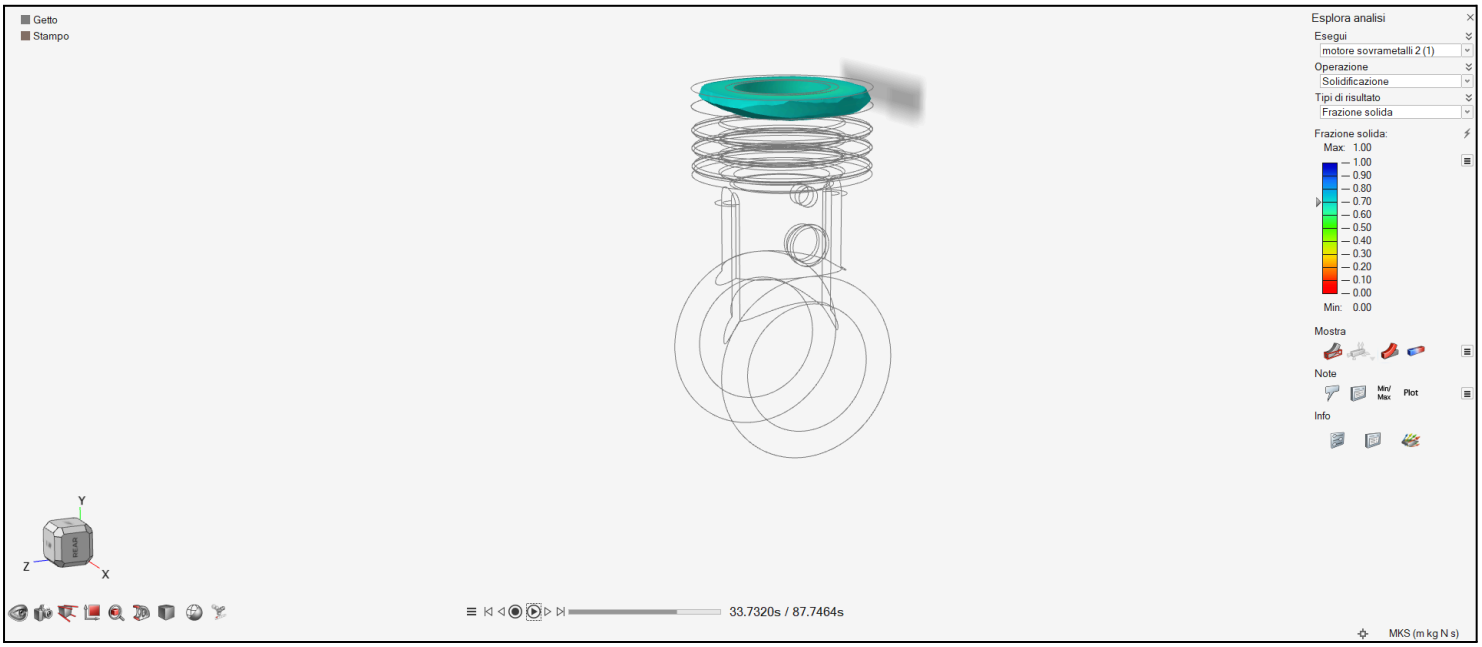

In the final image we can notice that the area most susceptible to shrinkage cavities is shown on the upper face of the crankcase, this result can also be verified through the porosity analysis at the end of solidification with the corresponding image provided below.

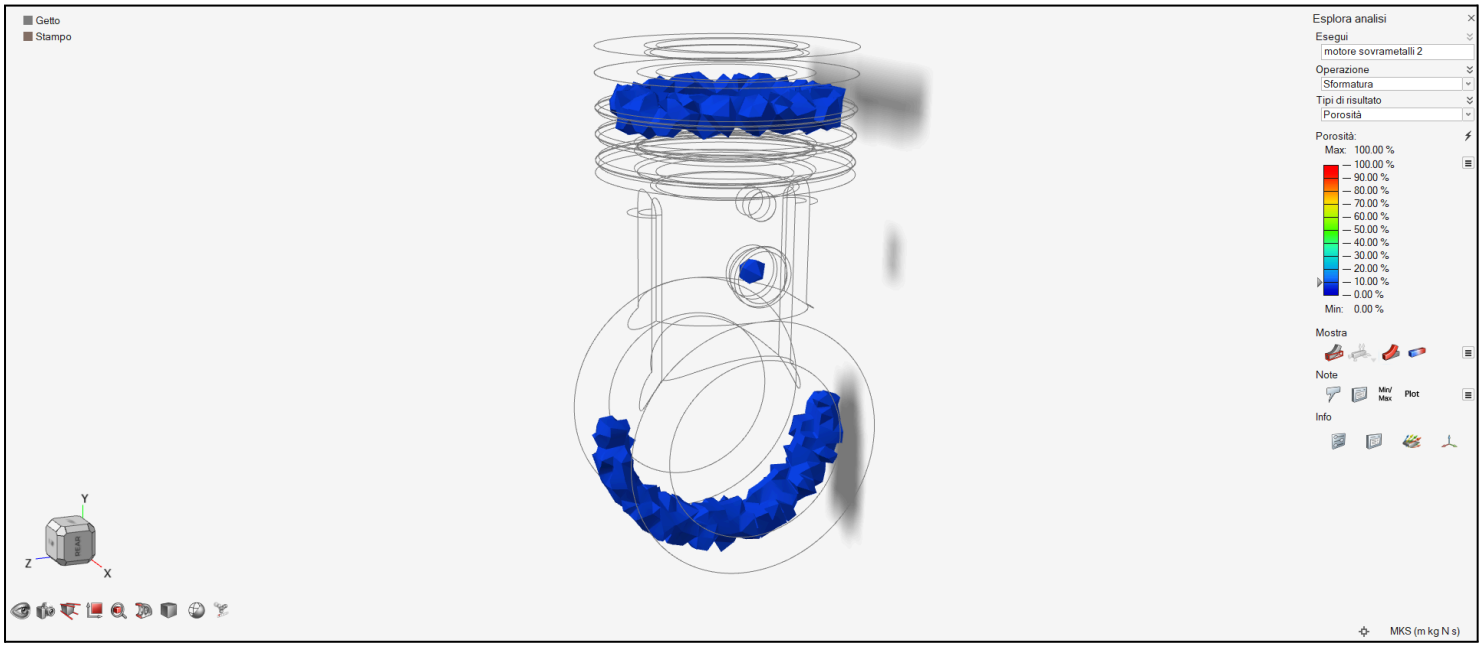

Meanwhile, from the cooling modulus analysis, we can observe that the area with the

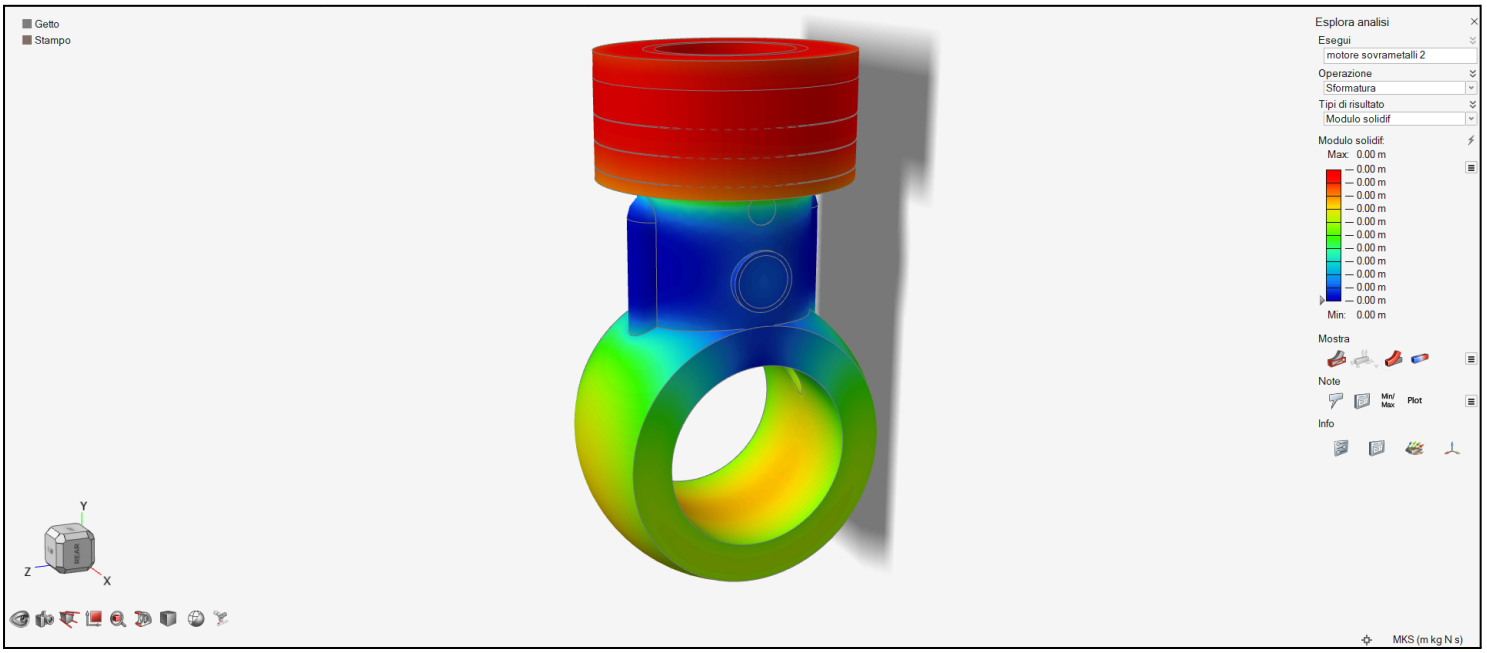

The highest value, highlighted in red, is indeed the upper one, thereby validating the results obtained through the initial cooling modulus calculation method.

There are other methods to understand how solidification occurs, such as Heuvers' circles method, however given the geometric simplicity of the part and considering both the cooling modulus calculations and the software-based analysis, it is not necessary to perform further analyses.

6.10 Riser's design

After studying the solidification of the casting it is necessary to analyze how to prevent shrinkage cavities.

One thing we have to consider is the dimensions of the riser neck must be verified for the chosen position and it must be ensured that the proposed solution does not cause issues later in the casting process.

The design of the riser involves the following steps: positioning the riser and designing the riser neck.

6.10.1 Riser's placement

The riser must be placed on the surface closest to the last solidification zone, which is the upper or lateral surface of the previously selected green part.

Following the cooling modulus calculations and solidification process analysis via software the surface we were initially considering for the riser placement would have been the upper one; however, considering the cross-section measurements, the riser neck should not have a diameter greater than 10 mm, which is too small given the subsequently calculated dimensions of the riser.

Therefore, we've opted for the lateral surface for the riser's placement, which provides more space for the rise gate.

Considering that we chose the shell molding process, it is not necessary to keep the riser in line with the parting plane, as pressure can be maintained between the two mold halves using a mechanical system.

6.10.2 Riser's sizing

To determine the sizing of the riser we must first calculate the modulus it needs to solidify last

$$M_{riser} \geq 1{,}2 \cdot M_{flow} = 6{,}24$$

Given the simplicity of the casting we're considering an open-top cylindrical riser, this design uses less material and is easier to produce, we will also assume the height (h) equals the diameter (d) to minimize the volume while maintaining the required modulus.

Several factors must be considered for the riser's final dimensions, including:

M_p=cooling modulus of the adjacent section = 4,6

V_m= riser's volume

V_M= maximum riser's feeding capacity

D = riser diameter

H = riser height

b = volumetric shrinkage coefficient of the material (in percent)

- *riser's sizing*

Considering a cylindrical riser, we know that:

$$V_m = \pi \frac{d^2}{4} h \quad \text{e} \quad S = \pi dh + \pi \frac{d^2}{4}$$

Given $k = \frac{h}{d}$ => h = kd

By substituting h and simplifying the formulas for volume and surface area, we get:

$$V_m = \pi \frac{d^3}{4} k \quad \text{e} \quad S = \pi d^2 k + \pi \frac{d^2}{4}$$

We can now substitute the simplified volume and surface area formulas into the one used for the cooling modulus:

$$M = \frac{V_m}{S} = \frac{dk}{4k+1}$$

Knowing that k = $\frac{h}{d}$ and h=d we can consider k=1, treating d as the unknown, we get:

$$d = \frac{M(4k+1)}{k} = 31{,}2 \text{ mm} = h$$

Now we can calculate the riser's volume and surface area:

$$V_m = 0.78\, d^3 = 23{,}8 \cdot 10^3\ mm^3 \quad \text{e} \quad S_m = 3{,}8 \cdot 10^3\ mm^2$$

Another value to calculate is the maximum riser's feedable capacity to ensure proper sizing, especially if it's larger than the total volume of the entire casting

$$V_M = V_m \frac{14-b}{b} = 71{,}4 \cdot 10^3\ mm^3$$

The value b, which is the volumetric shrinkage coefficient of the material in percentage, is 3.5% for an aluminum-silicon alloy

Valori di *b*	
MATERIALE	*b*%
Acciai non legati	7
Acciai legati	10
Ghisa bianca	6
Ghisa grigia	
$C_{eq} = 3{,}5\%$	2-3
$C_{eq} = 4{,}1\%$	1-2
$C_{eq} > 4{,}1\%$	1-0.4
Bronzo	4.5
Ottone	6.7
Rame-alluminio	4
Alluminio-silicio	3.5
$C_{eq} = C + \frac{1}{3}(Si + P)$	

The volume of the entire part, calculated using the SolidWorks software is:
$V_p = 72{,}6 \cdot 10^3 mm^3$

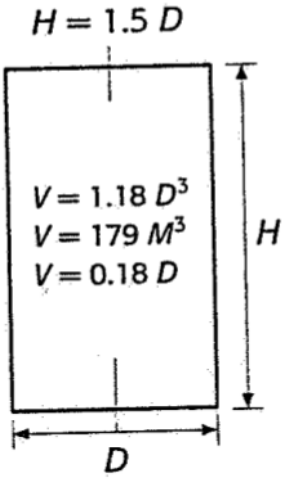

As we can see the maximum volume is slightly less than the riser's one, therefore we've decided not to keep the height and diameter as equal values, instead we'll set the height to $H = 1{,}5 \cdot D$

Recalculating the diameter will be D = 31 mm and consequently the height will be H = 46,5 mm.

As a result the riser's volume and it's maximum feeding capacity will be:

$$V_m = 35 \cdot 10^3 \, mm^3$$
$$V_M = 105 \cdot 10^3 mm^3$$

The riser will now be able to feed the entire part.

Before calculating the volume of the riser neck and the gating system, we must ensure that their combined volume doesn't exceed the surplus between the maximum feedable capacity and the part's volume, which is:

$$\Delta = V_M - V_p = 32{,}4 \cdot 10^3 \, mm^3$$

This check ensures that the liquid metal supplied by the riser is sufficient.

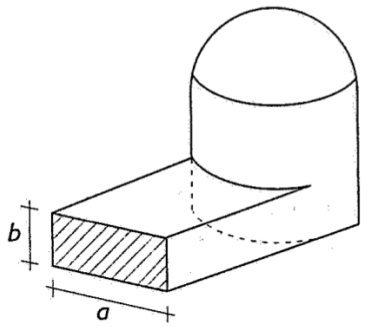

$$M \text{ collare} = \frac{a \cdot b}{2\,(a + b)}$$

- *riser neck*

Considering a neck with a rectangular base and a height no greater than 21.74 mm, we will use a rectangular base with the following dimensions:

a = 20 mm
b = 15 mm

Given these values, the cooling modulus can be calculated:

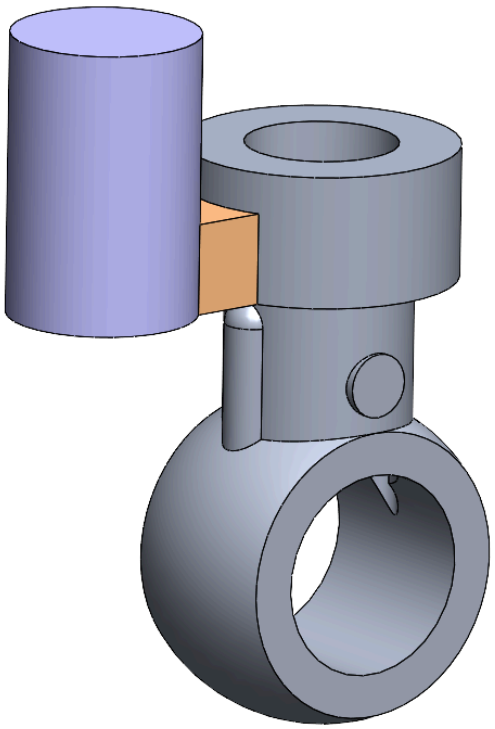

$$M_c = \frac{a \cdot b}{2\,(a \cdot b)} = 4{,}2$$

(In the attached image on the left are illustrated the results of these calculations)

6.11 Gating system

The elements that make up the entire gating system are:

- Pouring basin,
- casting channel,
- distributor channel,
- gate.

6.11.1 Gating system and sprue sizing

Now we only need to calculate the dimensions for the sprue and the gate.

- *gating system*

First, for the sprue, we must calculate the pouring time, which needs to be short enough to prevent parts of the casting from solidifying before pouring is complete. We'll consider the density of aluminum to be 2,9 Kg/dm^3 , while the total volume (including the neck and riser) from the CAD model is V_T= 98,2 · 10^3 mm^3.

$$G = \varrho \cdot V = 0{,}3 \text{ Kg}$$

Next, we can calculate the filling time using the following formula:

$$T[s] = 3.2\sqrt{G} \simeq 1{,}7$$

Now we can calculate the cross-sectional area of the sprue:

$$S = \frac{Q}{v} = \frac{V/T}{v} = 192{,}5\ mm^2$$

Consequently, the minimum diameter of the gating system will be:

$$d = 2\sqrt{\frac{S}{\pi}} \simeq 15 \text{ mm}$$

Here, v is the approximate velocity of the fluid in the sprue, calculated with the following formula:

$$v \simeq \sqrt{2gh} \simeq 0{,}3 \cdot 10^3\ mm^3/s$$

With h corresponding to the pouring height, which we'll consider to be 15 mm, equal to the dimension b of the neck.

To perform the subsequent solidification analysis using the software, we'll also need to calculate the casting flow rate:

$$K = \frac{G}{T} = 0{,}17$$

- *sprue*

For simplicity of molding, we'll choose a square cross-section for the gate. Therefore, the side length of this section will be

$$l = \sqrt{S} = 13{,}8 \text{ mm}$$

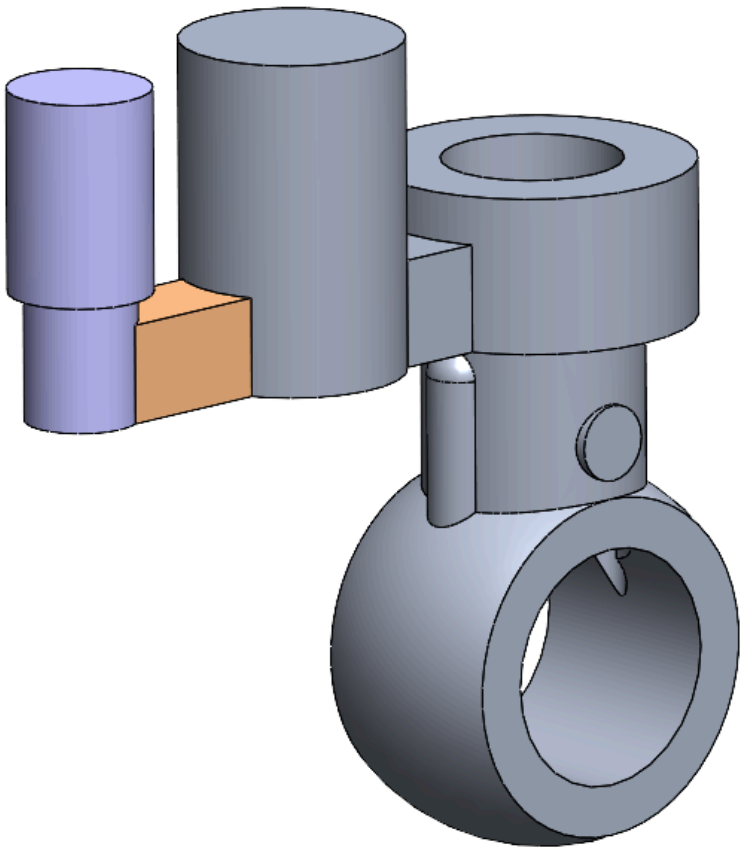

6.11.2 Flasks and modeling plates

After creating the complete model, we can proceed with selecting the flasks and pattern plates.

- *pattern plates:*

For our purposes—mass production of small/medium-sized castings—we'll use a pattern plate with two mold halves made of sand bonded with a thermosetting resin.

Given the small dimensions of our component the best solution is to create a mold that can accommodate at least two patterns simultaneously.

The final designs for both pattern plates have been included in the appendix. These drawings also show the riser, the gating system and the respective draft angles and fillet radii.

- *flasks:*

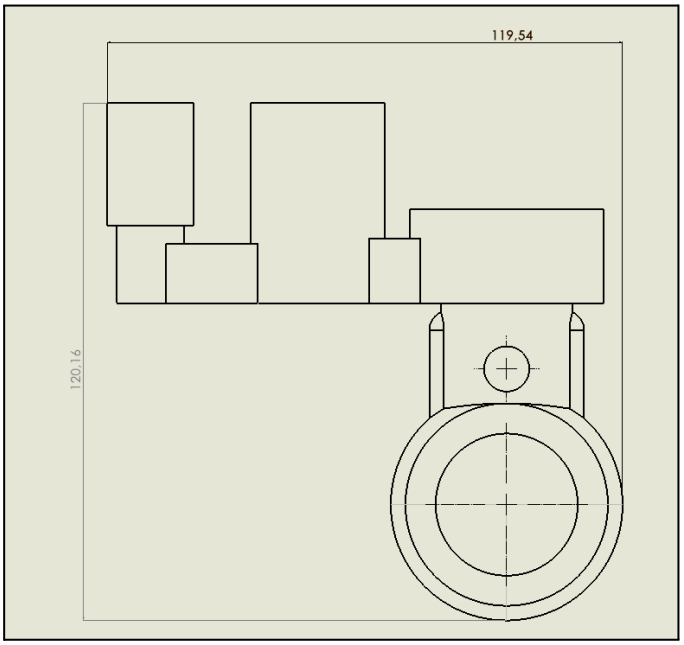

For the two flasks, since the parting plane symmetrically divides the raw carter, including the riser and gating system, the heights of the two flasks will be the same.

As the dimensions of the carter, riser, and gating system are very small (119 mm x 120 mm), it's possible to accommodate multiple patterns simultaneously, so assuming a mold that holds at least two patterns the required size would be 240 mm x 120 mm. According to UNI 6765-70 standards we can select two flasks measuring 250 mm x 315 mm.

Furthermore, considering that the distance between the top of the carter and the parting plane is 22.5 mm, we will choose the smallest possible height for the flasks, which is H = 50 mm.

Upper flask = lower flask = 250x315x50

a	b	H											
250	315	50	63	80	100	125	160	200					
280	355	50	63	80	100	125	160	200	250				
315	400	50	63	80	100	125	160	200	250	300			
355	450	--	--	80	100	125	160	200	250	300			
400	500	--	--	--	100	125	160	200	250	300	355		
450	560	--	--	--	100	125	160	200	250	300	355		
500	630	--	--	--	100	125	160	200	250	300	355	400	
560	710	--	--	--	100	125	160	200	250	300	355	400	
630	800	--	--	--	100	125	160	200	250	300	355	400	
710	900	--	--	--	--	125	160	200	250	300	355	400	500
800	1000	--	--	--	--	125	160	200	250	300	355	400	500
900	1100	--	--	--	--	--	160	200	250	300	355	400	500
1000	1300	--	--	--	--	--	--	200	250	300	355	400	500
1100	1400	--	--	--	--	--	--	200	250	300	355	400	500
1200	1500	--	--	--	--	--	--	--	250	300	355	400	500
1300	1600	--	--	--	--	--	--	--	250	300	355	400	500
1400	1700	--	--	--	--	--	--	--	--	300	355	400	500
1500	1800	--	--	--	--	--	--	--	--	300	355	400	500

6.11.3 Casting and solidification simulation

The parameters used for the simulation are the same as the one used in the previous section where porosity was calculated, with the exception of the mold, casting dimensions, and shell (which are now known values).

The parameters under consideration are:

- Pouring temperature,
- Solid fraction during solidification,
- Final porosity,
- Solidification time,
- Filling time.

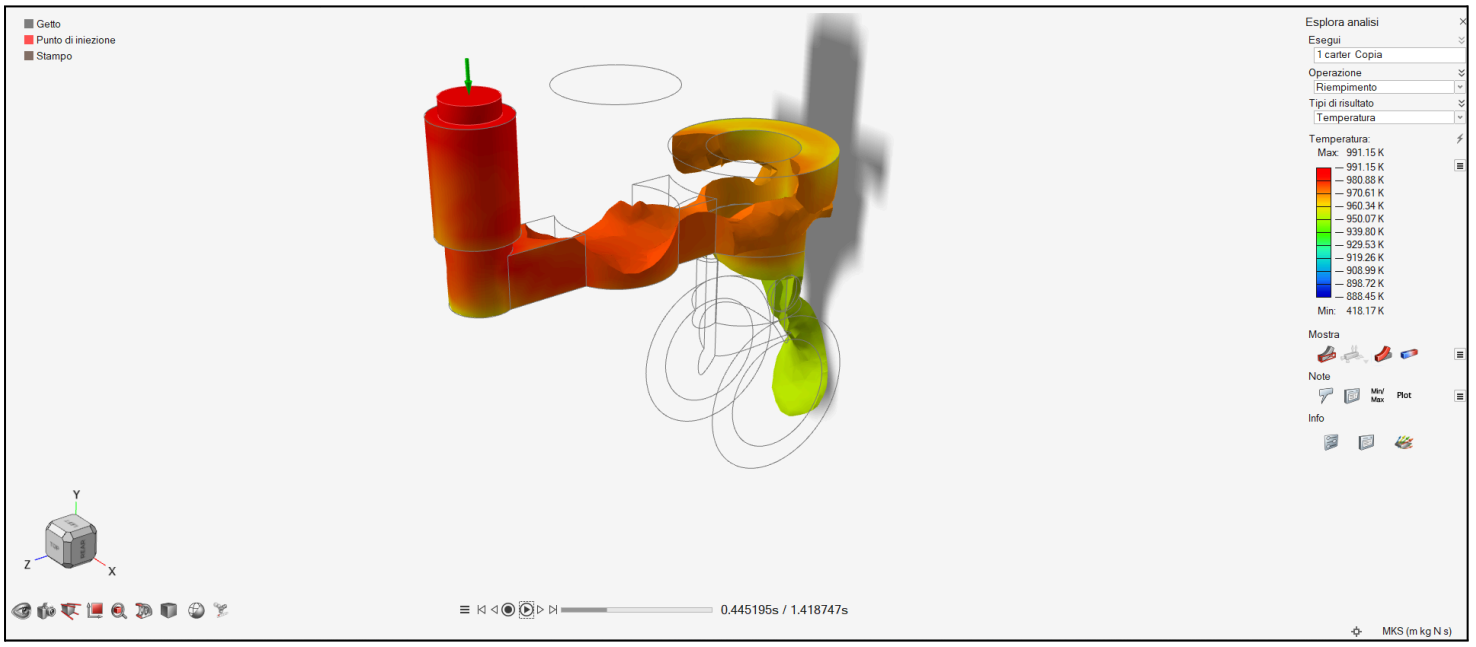

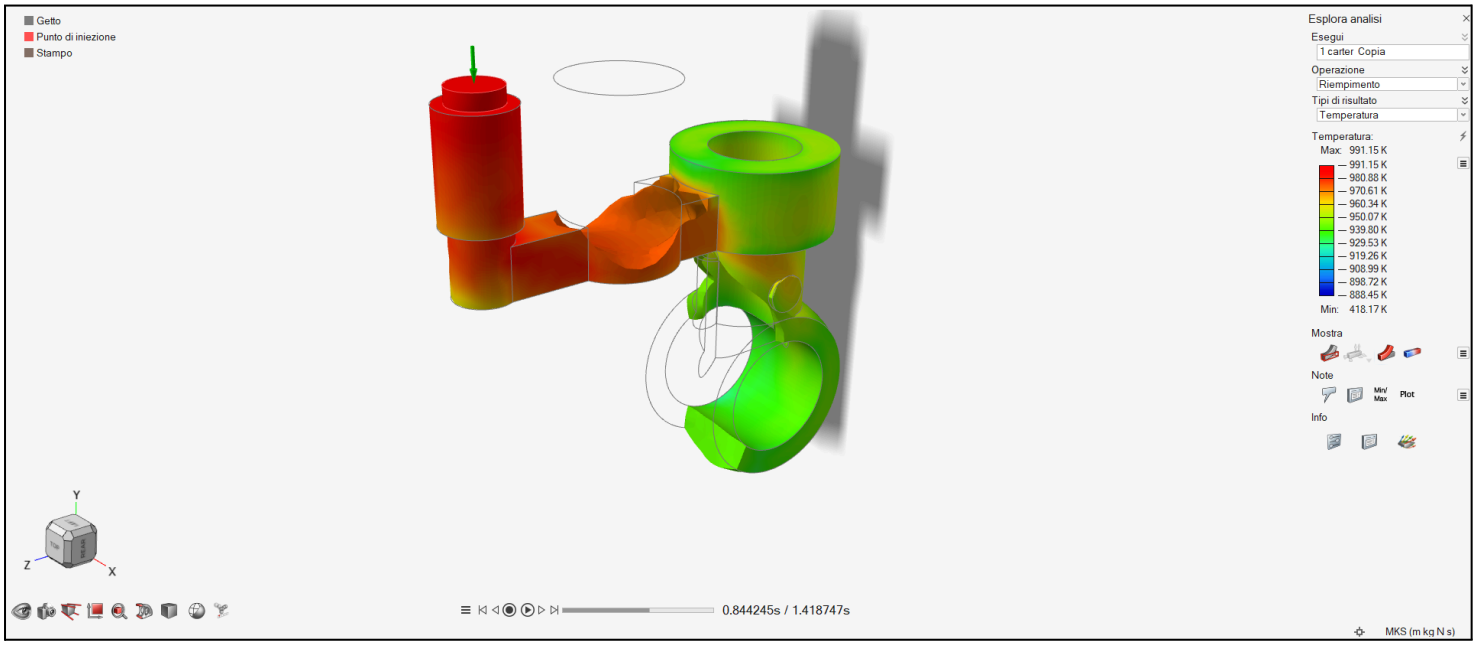
Getto
Punto di iniezione
Stampo
Esplora analisi
Esegui
1 carter Copia
Operazione
Riempimento
Tipi di risultato
Temperatura
Temperatura:
Max: 991.15 K
991.15 K
980.88 K
970.61 K
960.34 K
950.07 K
939.80 K
929.53 K
919.26 K
908.99 K
898.72 K
888.45 K
Min: 418.17 K
Mostra
Note
Min/Max
Plot
Info
Y
Z
X
0.844245s / 1.418747s
MKS (m kg N s)

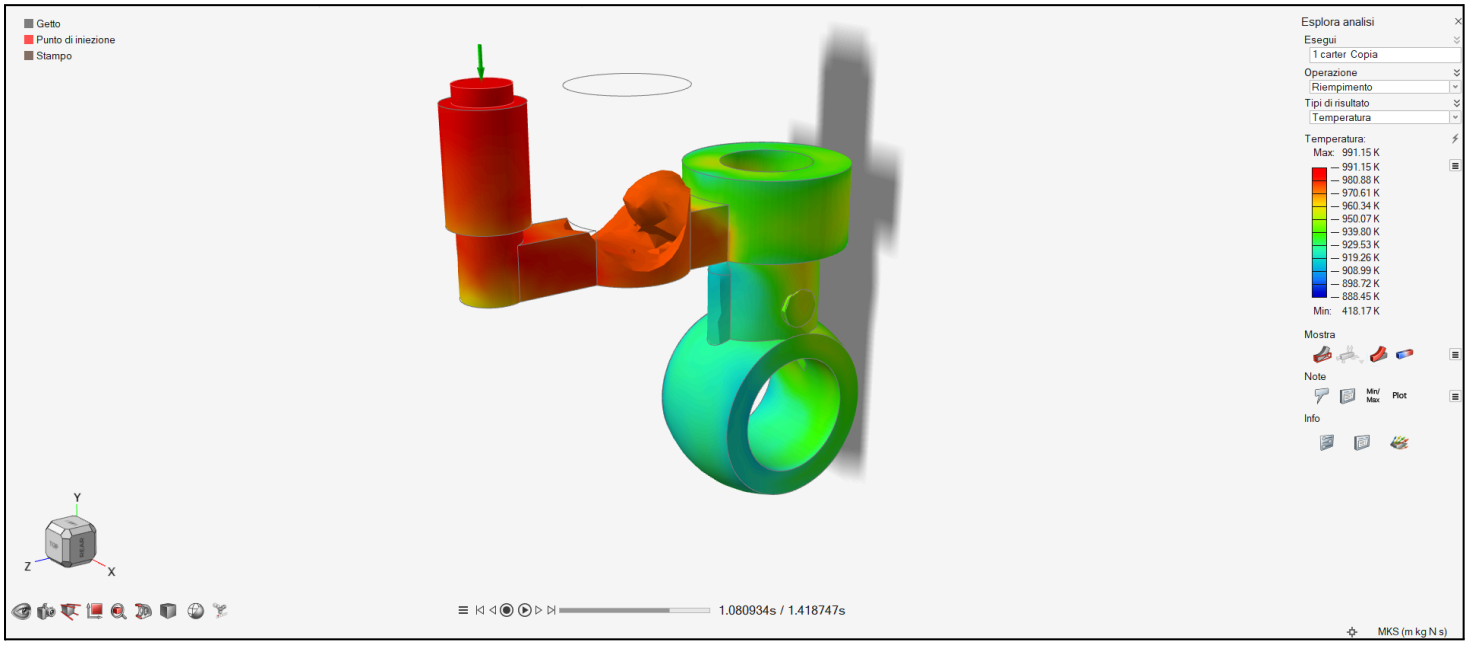
Getto
Punto di iniezione
Stampo
Esplora analisi
Esegui
1 carter Copia
Operazione
Riempimento
Tipi di risultato
Temperatura
Temperatura:
Max: 991.15 K
991.15 K
980.88 K
970.61 K
960.34 K
950.07 K
939.80 K
929.53 K
919.26 K
908.99 K
898.72 K
888.45 K
Min: 418.17 K
Mostra
Note
Min/Max
Plot
Info
Y
Z
X
1.080934s / 1.418747s
MKS (m kg N s)

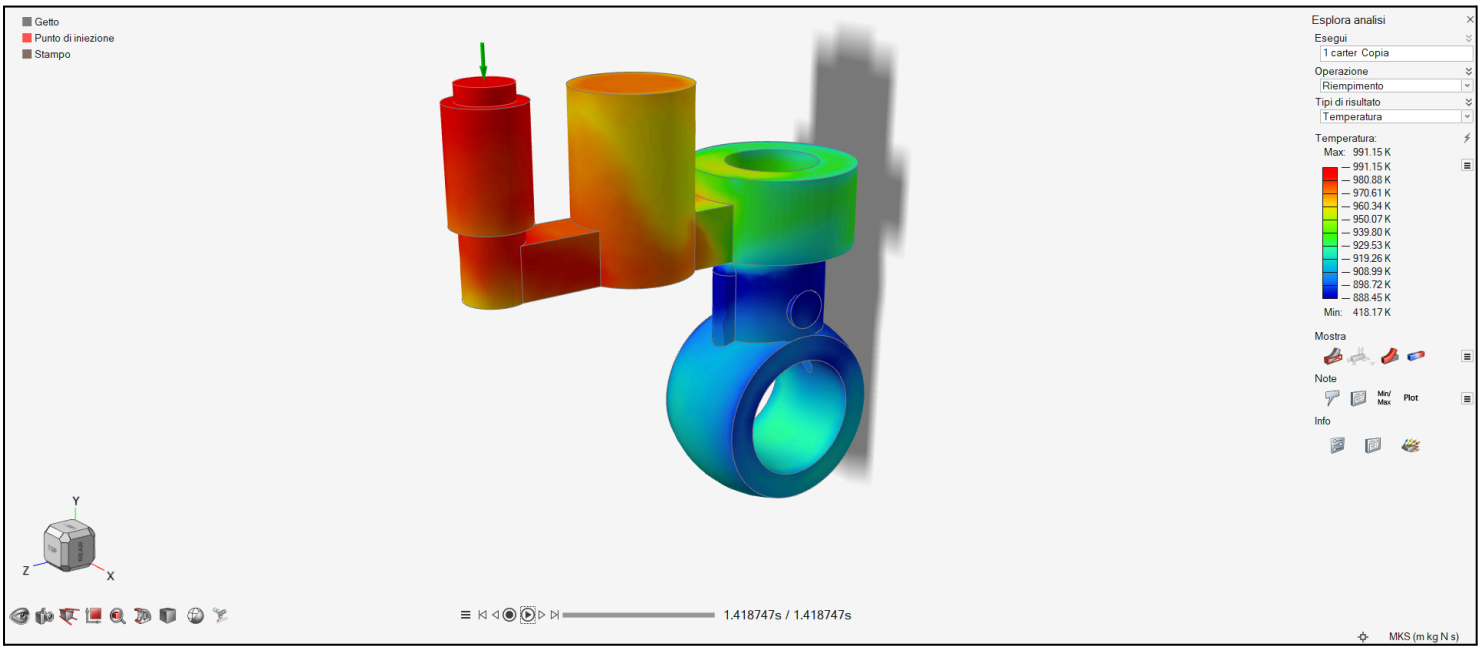

Pouring temperature: as can be seen from the previously attached images, the placement of the riser and the gating system with their respective collars ensures good filling and, consequently, good solidification.

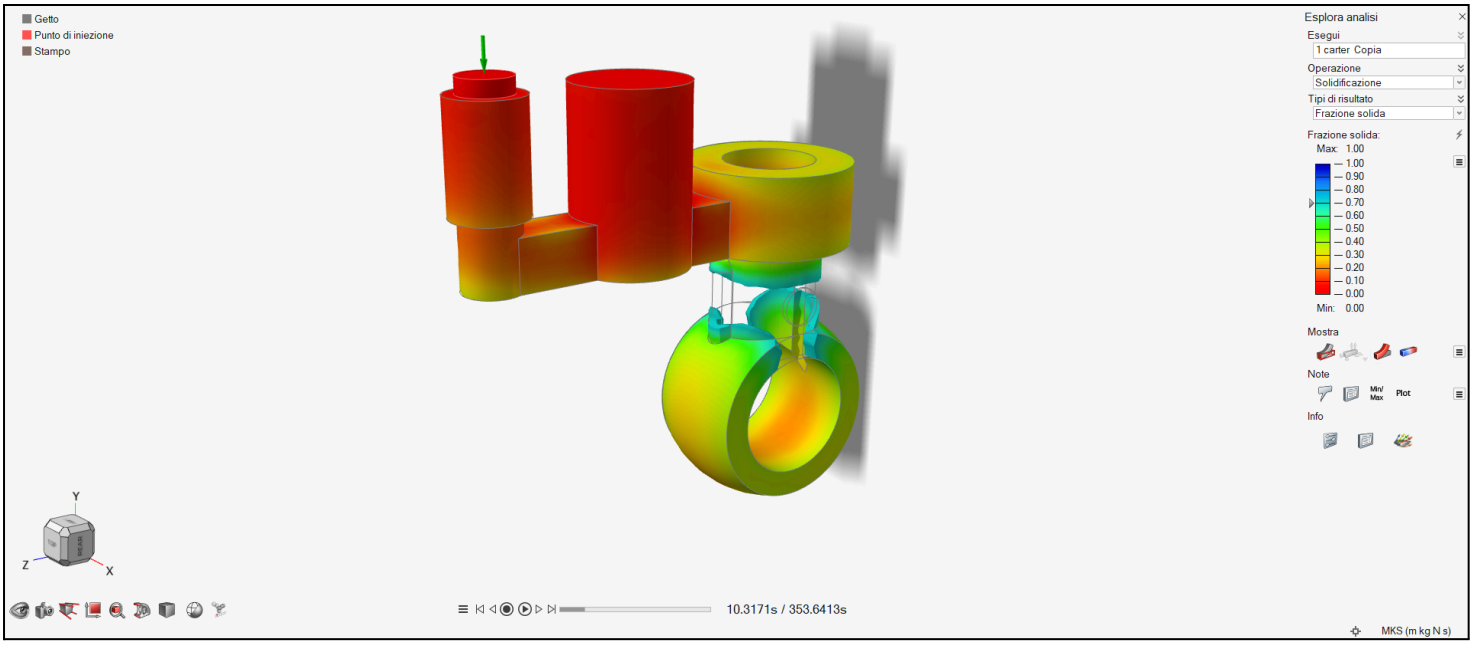

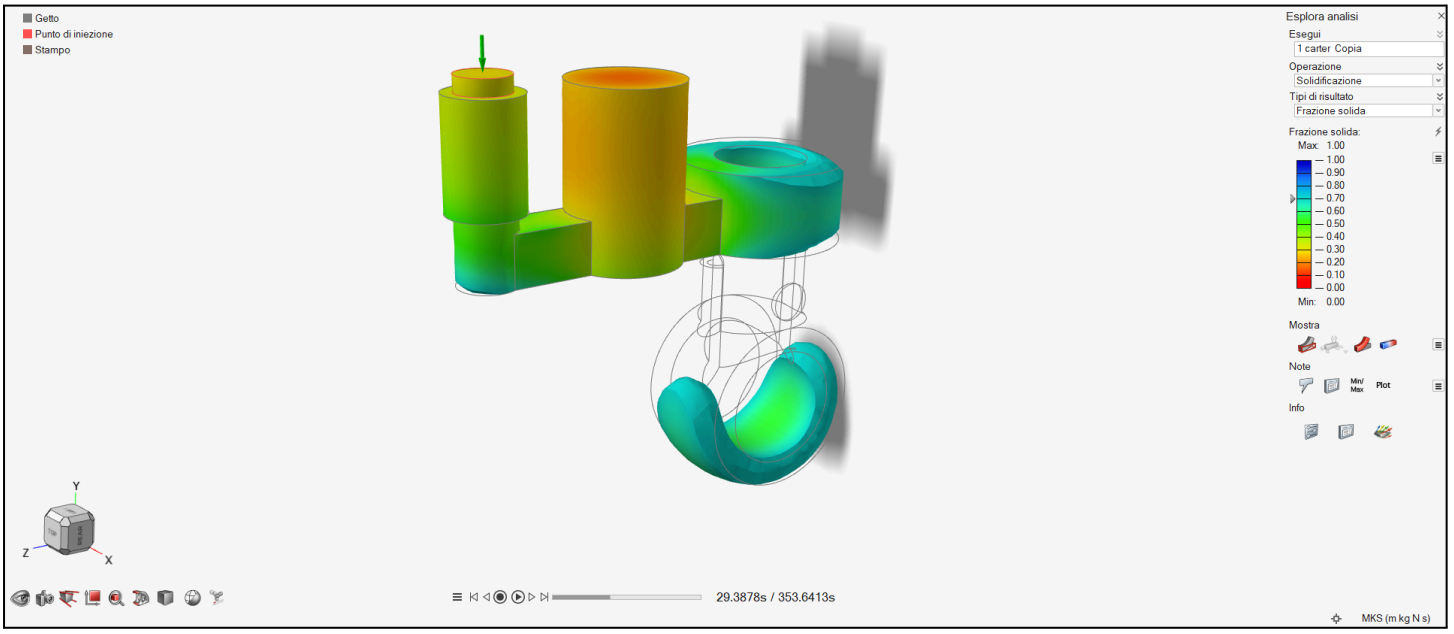
Getto
Punto di iniezione
Stampo
Esplora analisi
Esegui
1 carter Copia
Operazione
Solidificazione
Tipi di risultato
Frazione solida
Frazione solida:
Max: 1.00
1.00
0.90
0.80
0.70
0.60
0.50
0.40
0.30
0.20
0.10
0.00
Min: 0.00
Mostra
Note
Min/Max
Plot
Info
Y
Z
X
29.3878s / 353.6413s
MKS (m kg N s)

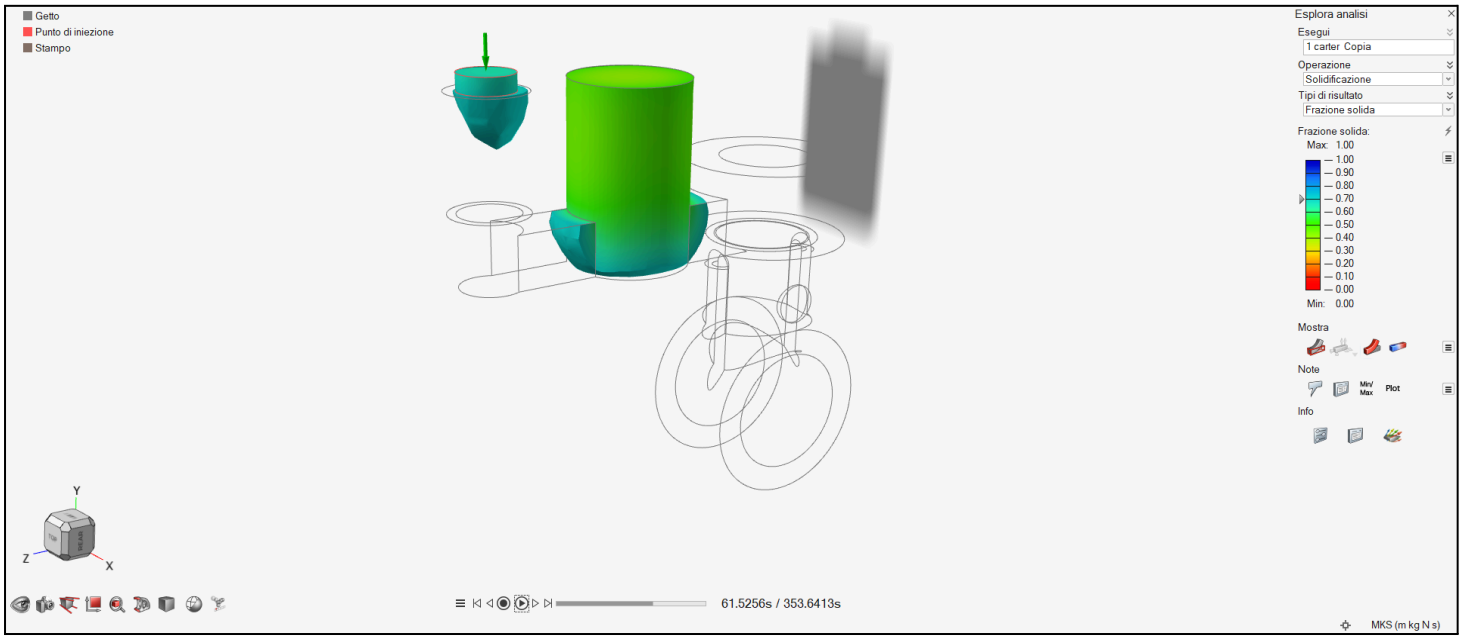
Getto
Punto di iniezione
Stampo
Esplora analisi
Esegui
1 carter Copia
Operazione
Solidificazione
Tipi di risultato
Frazione solida
Frazione solida:
Max: 1.00
1.00
0.90
0.80
0.70
0.60
0.50
0.40
0.30
0.20
0.10
0.00
Min: 0.00
Mostra
Note
Min/Max
Plot
Info
Y
Z
X
61.5256s / 353.6413s
MKS (m kg N s)

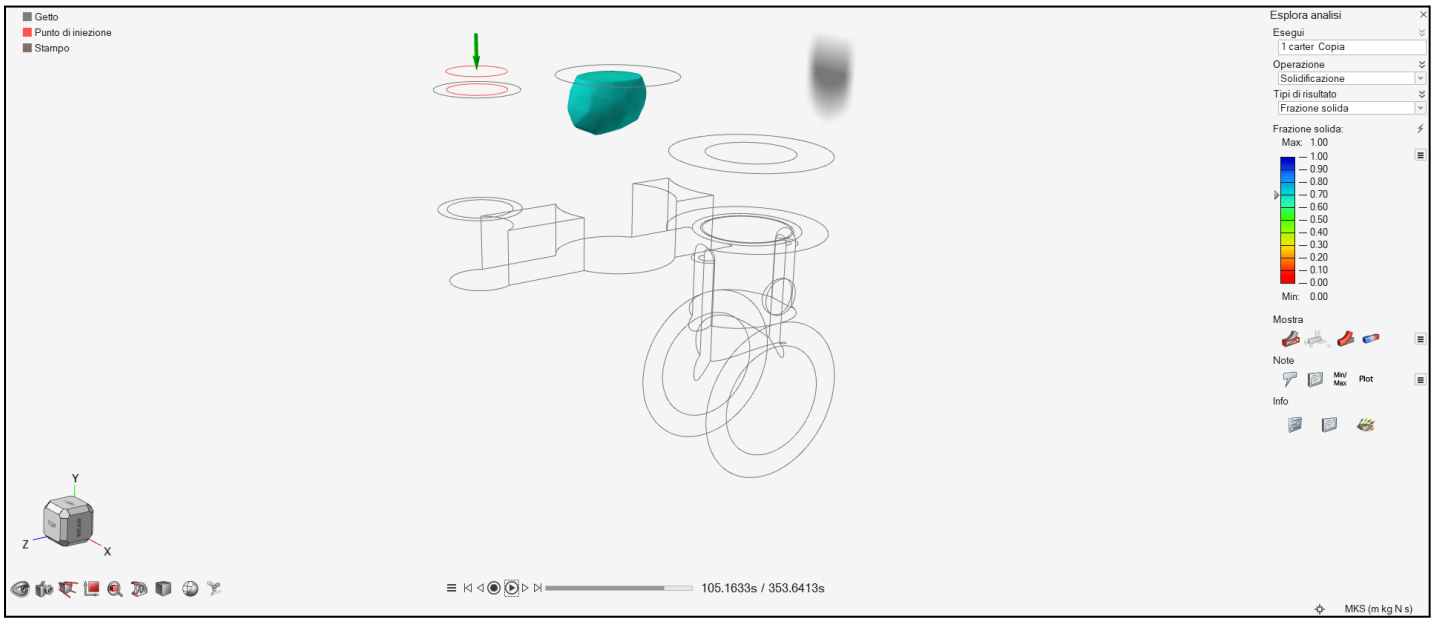

Solid fraction during solidification: this shows us that the solidification is occurring in the desired direction.

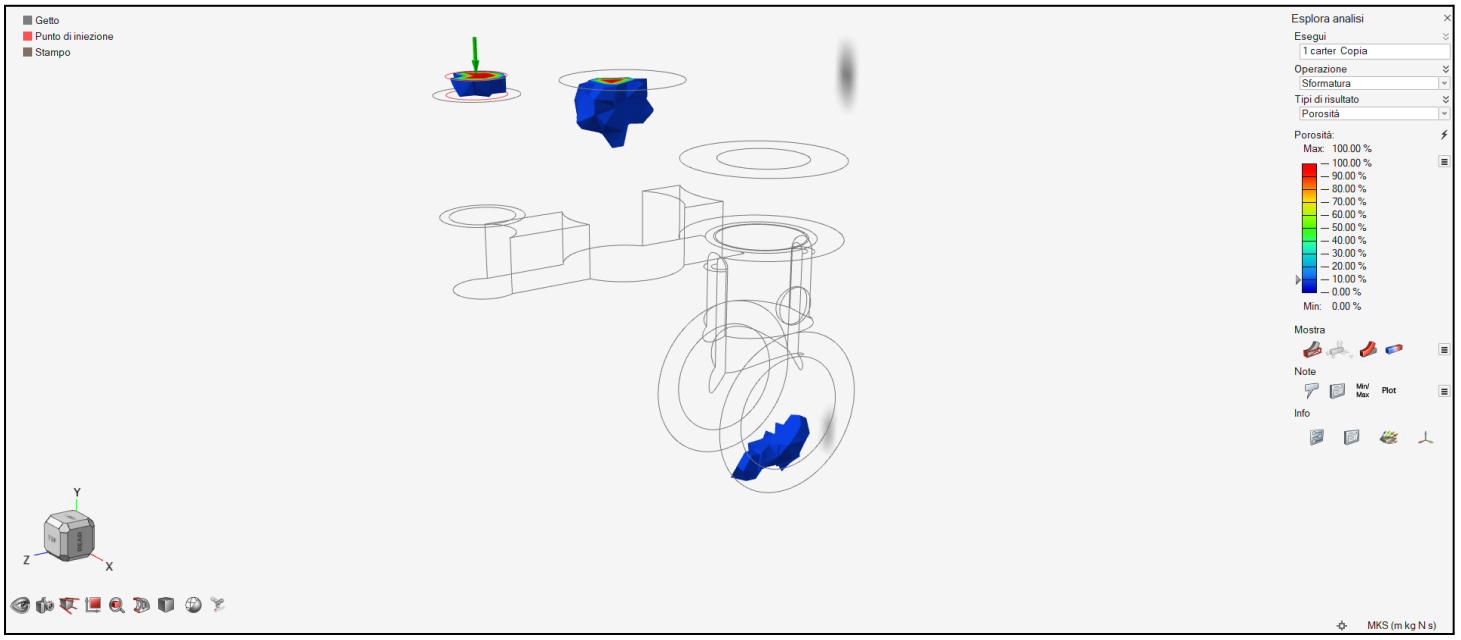

Final porosity: it can be noted that even at the lowest percentage, as seen in the image above, the largest porosity forms on the riser, while the secondary porosity is present in the lower part of the carter, but its maximum porosity is less than 10%..

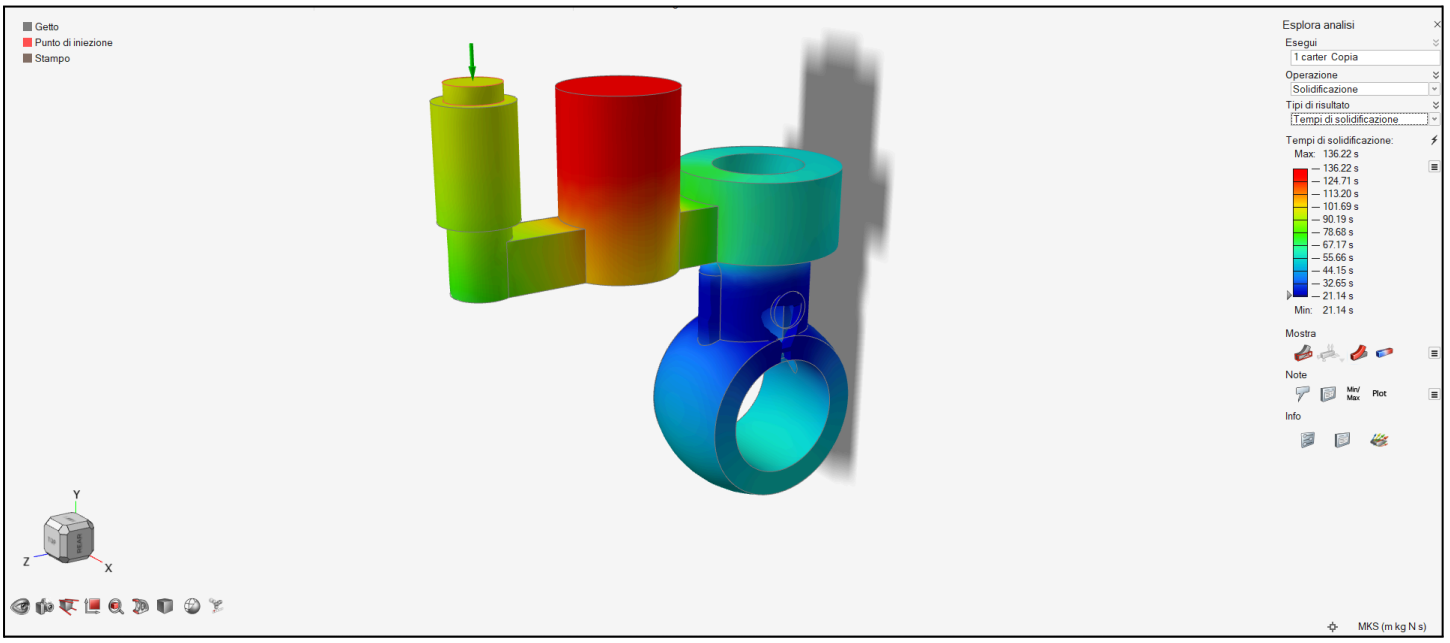

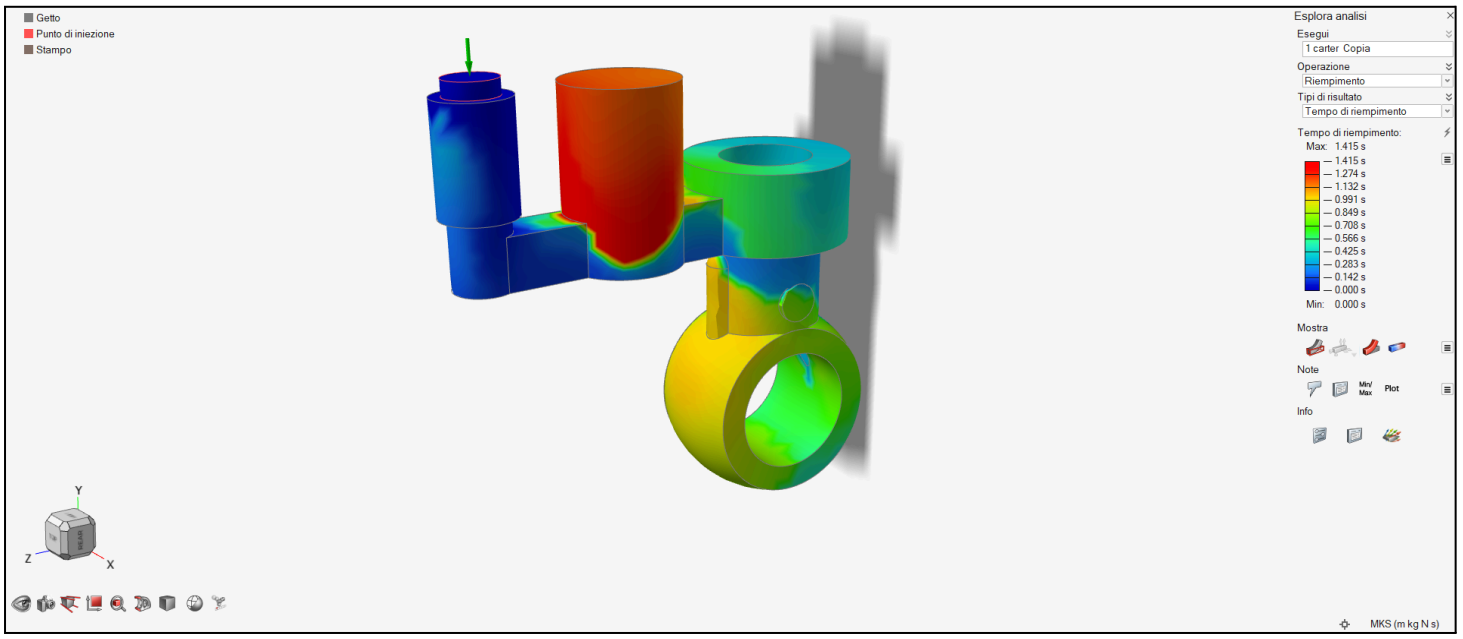

Filling time: it is noted that the time estimated by the software is slightly lower than the calculated time, at 1.4 s.

6.12 Timing and costs

6.12.1 Casting's timing

1. Operative times:

    - Pouring time = 1.7 s
    - Casting solidification time = 136.2 s = 2.2 min

2. Inactive times:

    - Furnace loading = 40 min
    - Alloy melting = 40 min
    - Shell heating = 30 min
    - Shell preparation = 20 min
    - Assembly = 25 min
    - Casting extraction = 20 min (includes cooling and part removal)

The total time, in this case considering two parts simultaneously, will be 3 hours.

6.12.2 Casting's costs

1. Material costs:
    - shell = Considering the price of silica sand is €0.8/kg and the mass is 10.4 kg, the cost is negligible;
    - Aluminum Alloy G. Al-Si 13: The density is 2.65 g/cm3, and the material price is €3.4/kg. Therefore, the cost per single part is €0.8, while the total cost for a production run of 1,000 parts will be €800.

2. Labor costs:
    - Active Times: These include furnace loading, shell preparation, pouring, extraction, and trimming times, totaling 1 hour and 45 minutes.
    - Passive Times: These include alloy melting and solidification, totaling 1 hour and 10 minutes.

We'll assume the operator's hourly wage is €25. Over a 3-hour shift, 2 parts are produced, making the labor cost €75 per full shift. For a production run of 1,000 parts, the total labor cost will be €37,500.

The total cost per single carter amounts to €38.3. The total cost for 1,000 parts is €38,300.

7. Component introduction: Propeller

The propeller represents an essential component of our model aircraft engine, as it converts mechanical energy into aerodynamic thrust, allowing the model to move. It must therefore be light, well-balanced, and aerodynamically efficient, in addition to having a geometry optimized to ensure high performance at a low weight. For its production 3D printing was chosen since a technology that is well-suited for creating complex shapes, such as the propeller blades, which have curved profiles with varying thickness and inclination, difficult to obtain with traditional low-cost machining. Furthermore, 3D printing allows for the rapid production of single parts or small series, which is perfect for the production planned for this project.

7.1 Material selection

As plausible materials for a 3D-printed propeller, we have considered **nylon and ABS**. Comparing them, we see that nylon is a more difficult material to print than ABS as it absorbs a lot of moisture from the air. Furthermore, nylon has low adhesion to the print bed, and it is more flexible and "soft" than ABS, so thin geometries or those with small details tend to be less precise or more deformed. We won't focus on the temperatures required for printing, as the 3D printer we will choose will allow for printing with both materials without issues.

The main implications for the manufacturing of a model aircraft propeller—namely, being rigid, lightweight, well-balanced, and not tending to deform during rotation—have led us to choose **ABS**, as it is more rigid and stable, better able to maintain dynamic balance and shape under load. Here are some of its most important mechanical properties.

Shrinkage	Medium-high
Print speed	30 – 60 mm/s
Density	1.04 g/cm³
Hardness (Rockwell)	R95 – R110
Tensile strength	35 – 50 MPa
Modulus of elasticity (E)	1.8 – 2.3 GPa
Elongation at break	10 – 50%

7.2 Selection of the manufacturing technique (3D Printing)

For the production of the propeller, **FDM (Fused Deposition Modeling)** 3D printing technology was adopted, as it represents an effective, economical, and easily accessible solution for the production of lightweight components with complex geometry. FDM allows for building the part layer by layer, depositing a molten thermoplastic material (in our case, ABS), and is particularly suitable for elements that are not subjected to high structural loads but require precision in form and a low weight. This type of printing is also advantageous for small-batch production (as in our case), as the unit costs remain low and do not vary significantly with the number of parts.

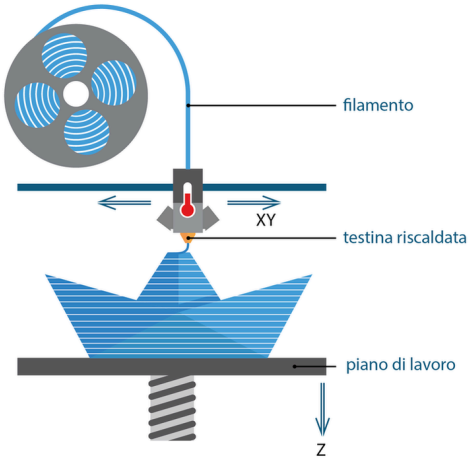

Esempio di funzionamento tecnica FDM

7.3 3D printer selection

The choice fell on the **Snapmaker Artisan FDM 3D printer**, available for use at the University of Pisa. Let's look at its technical specifications.

- **Print temperature:** 300 °C
- **Base/bed temperature:** 110 °C
- **Print volume:** 350 × 400 × 400 mm
- **3D printing:** PLA, ABS, PETG, Soluble PLA, Nylon
- **Shank diameter:** CNC 0.5-6.35 mm

7.4 Printing simulation

Let's now look at the **printing processes** in chronological order, using the Snapmaker Luban software:

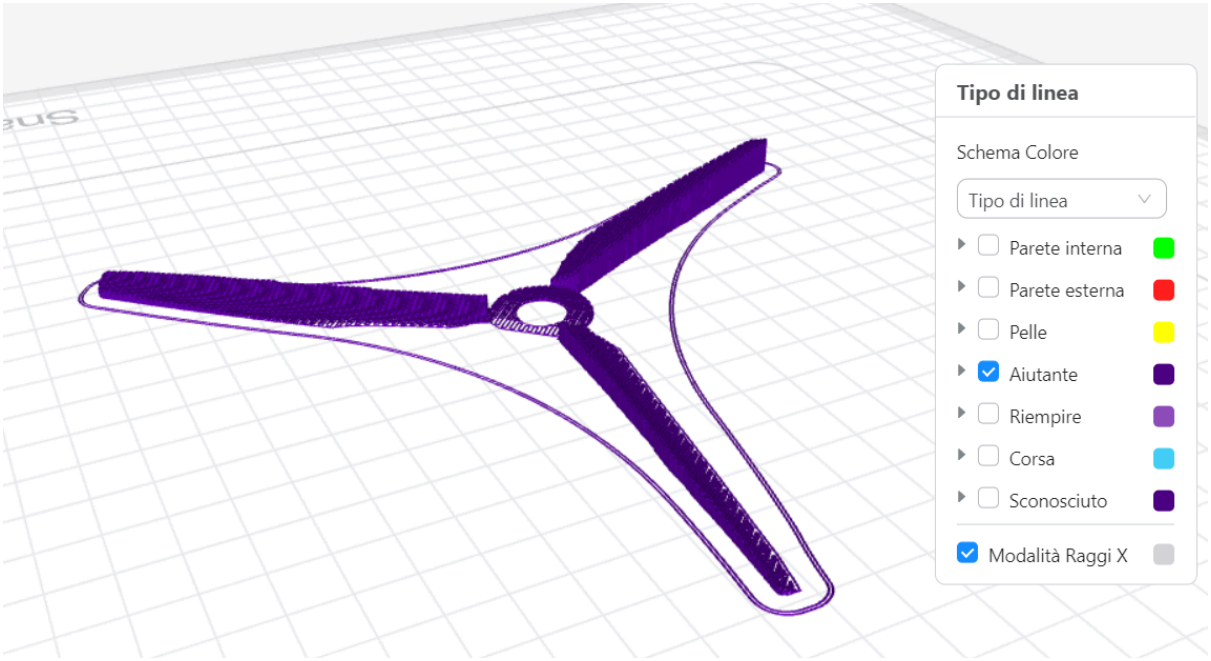

First step: creation of the propeller supports

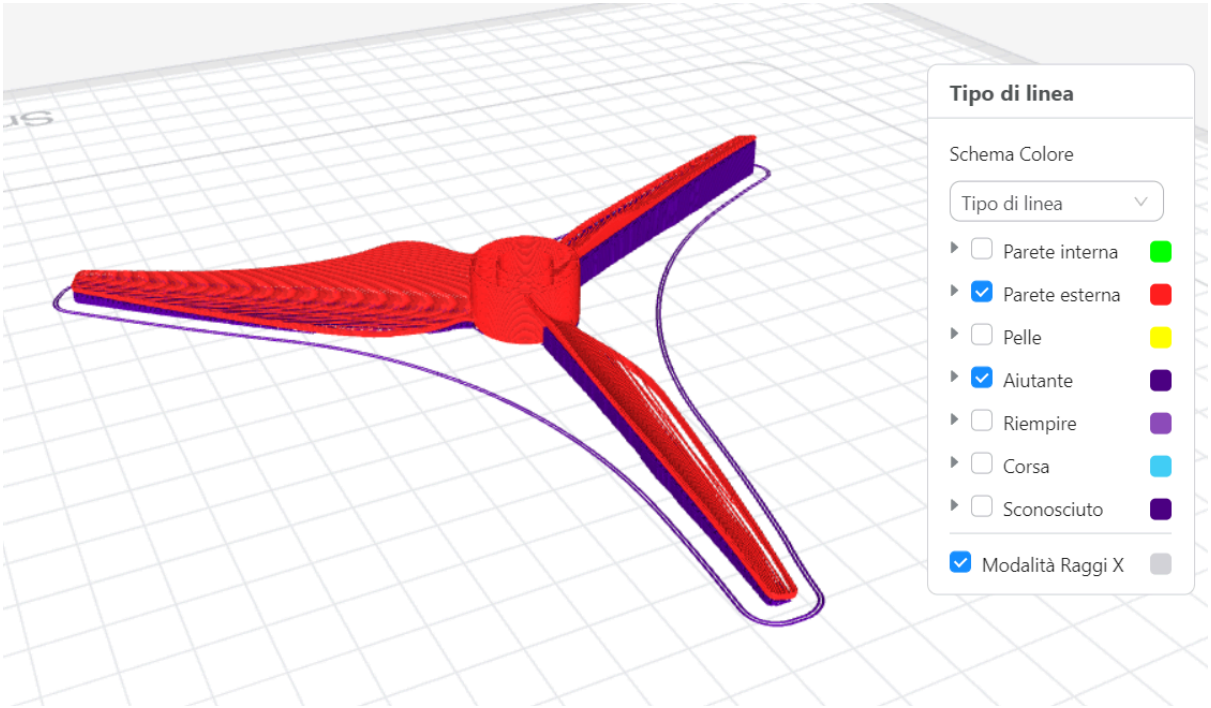

Second step: the outer walls are defined, and the structure begins to form

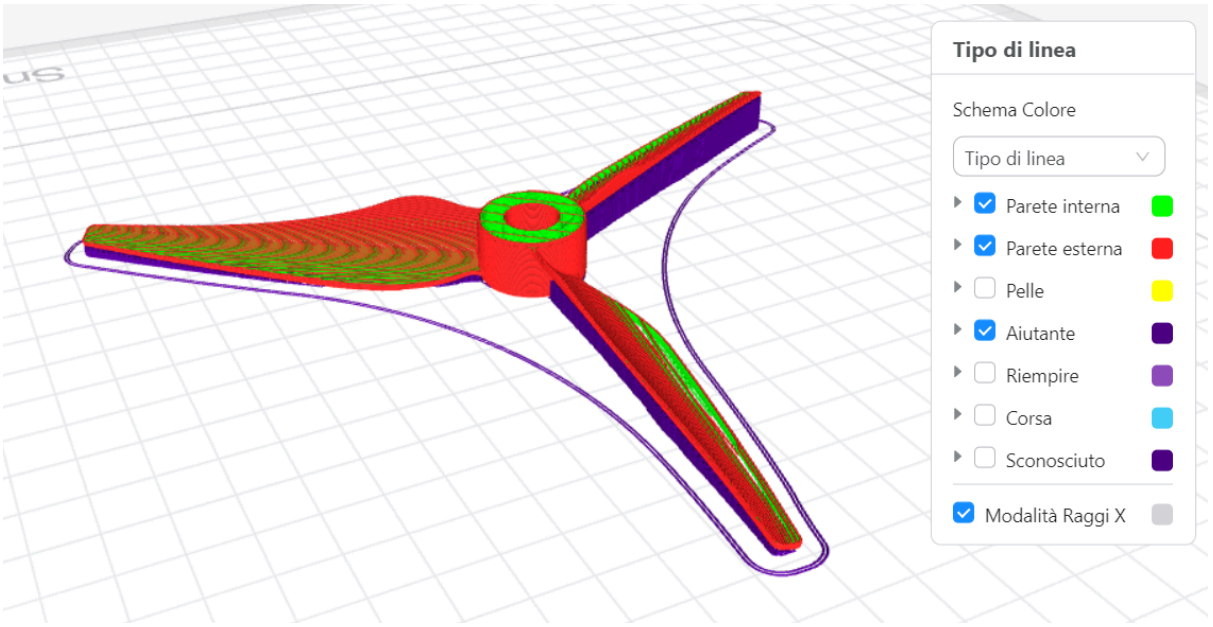

Third step: segments of the inner walls are also defined to increase the rigidity of the structure in the initial phase

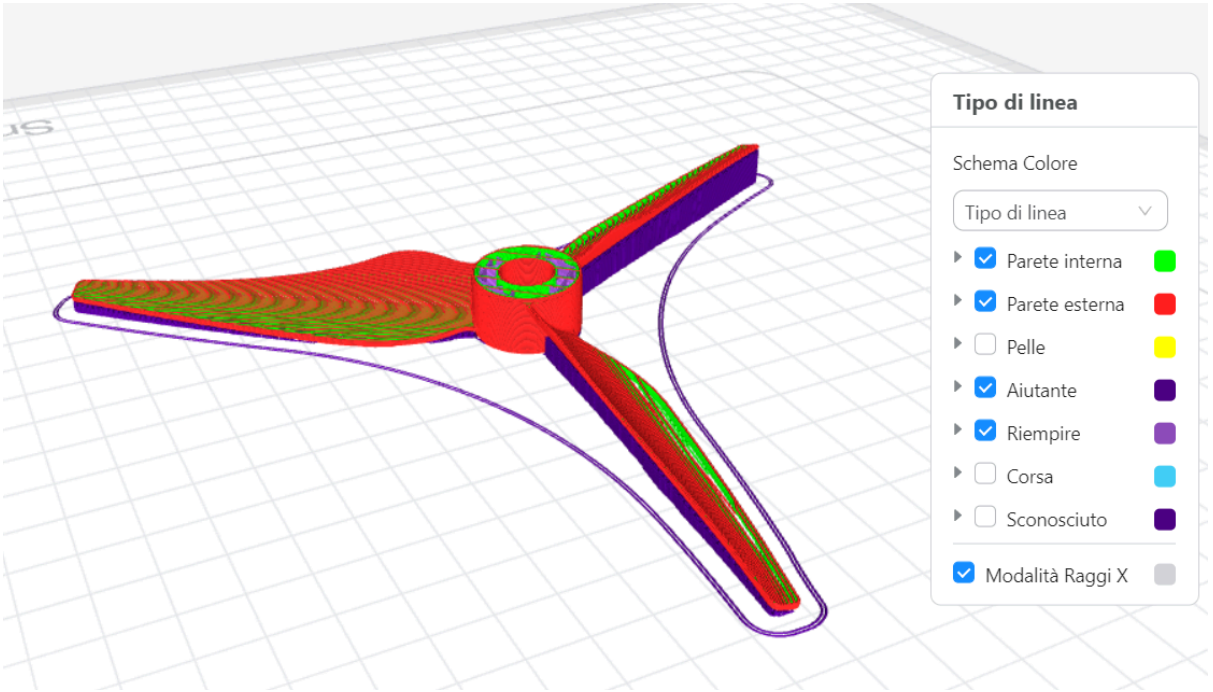

Fourth step: material is added as infill where the structure needs rigidity

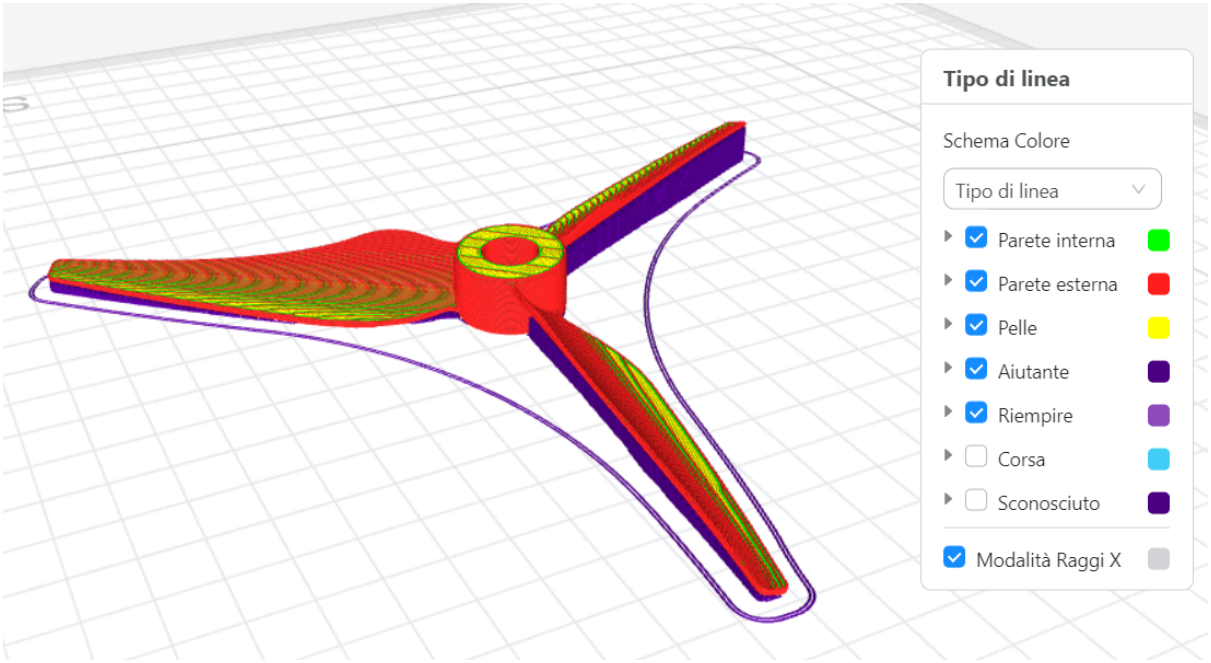

Last step: those parts of the surface that remained uncovered are closed

Below are the prints we made in two different materials. The first print was made with Nylon, highlighting the critical issues of the material and finish. The second print was made with ABS, resulting in an improvement in surface finish and the overall structure.

3D printing in ABS

3D printing in Nylon

However, the component printed with the FDM technique **probably cannot be used in operation due to the low surface finish**, which would influence its behavior and fluid dynamics, likely decreasing lift. Therefore, we have decided to use FDM printing only with the goal of verifying the general dimensions and aesthetics of the component. In the event that we wanted the propeller to be part of a prototype intended to function properly, the choice of 3D technique would fall on MSLA printing or equivalents, which provide a superior surface finish that does not affect the component's aerodynamics.

7.5 Calculation of production costs and times

For the calculation of costs and times, we used also the native 3D printer software, Snapmaker Luban. This software allows you to load the 3D file of the propeller, select the print heads, material, supports, etc. The supports were placed under the respective blades of the propeller, providing the necessary foundation. The central part of the propeller, however, rested on the print bed and therefore did not need supports.

The cost of the Snapmaker Artisan printer owned by UNIPI (which we used) is approximately €3000, but this is a hybrid machine (laser cutting, 3D printing, and mechanical machining), so the cost could be influenced by these aspects. The filament (ABS) used weighed 11.2 g, the required filament length was 3.7 m, and the time needed for completion was 1 hour and 5 minutes, which we approximate to one hour for simplicity in our calculations.

We perform the cost calculation based on:

- **Printer cost** (considering a useful life of 10 years, 15 working hours per day, and 300 days of use per year) = 45,000 hours / €3000 = €0.067/hour * 1 hour = €0.067 per part
- **Filament cost per kg (ABS)** = approximately €18.
- **Filament cost per part produced** = €0.2 per part
- **Operator cost** (€15/hour) = (approx. 8 minutes of effective work) = €2 per part
- **Energy cost**: 0.18 kWh * €0.28/kWh = €0.05 per part
- **Single part cost**: 0.067 + 0.2 + 0.05 + 2 = €2.317
- **Cost for 1000 parts** = €2317

The timelines are:

- **Machine setup time** (PASSIVE): Estimated 5 minutes
- **Project loading time on PC** (PASSIVE): 30 seconds
- **Printing tim**e (ACTIVE): 1 hour
- **Part removal time from the base** (PASSIVE): Estimated 30 seconds
- **Support removal time** (PASSIVE): 2 minutes
- **Filament reloading tim**e (PASSIVE): 1 minute

Total time per single part = 5 + 2 + 2 + 60 = 1 hour and 9 minutes
Total time for 1000 parts = 69 min * 1000 = 69000/60 = 1150 hours

8. Component introduction: Crankshaft

In our two-stroke internal combustion engine, the crankshaft plays a fundamental role. It is the element that converts the reciprocating motion of the piston into rotational motion, which can then be used to drive the propeller.

8.1 Selection of the manufacturing technique

The manufacturing process selected for this component is machined by **chip removal** on machine tools. First of all, the geometry of the shaft is simple and regular, consisting mainly of coaxial cylinders with different diameters. This type of shape is highly compatible with turning operations, both manual and CNC. The holes (axial and radial) can also be easily produced using standard drilling operations. Furthermore, the component diameters (from 10 mm to 32 mm) fall within the ranges commonly machinable with standard tools and equipment. No complex geometries are present that would require special techniques. Machining is also the best choice in terms of cost, precision, and availability, especially for small-batch production as in our case. The shaft, at the hole located on the flange, will also undergo a welding operation with the “Crank Pin” component. Therefore, the choice of the raw material will also be evaluated considering this aspect.

8.2 Quantity of parts to be produced

As stated in paragraph 5, "Customer Requirements," given the hypothetical demand for 1000 two-stroke model aircraft engines, we will need to produce the same quantity for all the parts we are studying (each is present only once in the overall assembly). We will therefore need to produce **1000 "Crankshaft" components**.

8.3 Raw material selection

The crankshaft must be made from materials that guarantee strength, durability, and the ability to withstand the stresses and high temperatures generated during operation. Our choice falls on S355JR steel, a low-carbon (approximately 0.2%) non-alloy structural steel widely used in mechanical and civil engineering, where it is highly valued for its combination of mechanical strength, weldability, and good machinability.

It has the following characteristics:

- **Yield strength (Re):** ≥355 MPa
- **Tensile strength:** 470–630 MPa
- **Elongation at break:** 22%
- **Weldability:** Excellent
- **Density:** 7.85 g/cm 3

The type of raw material we will use will be a hot-rolled S355JR round bar (given the predominantly cylindrical axial section of the shaft), which is more economical. It is assumed that the initial Ra of the bar is in a range between 10-25 μm.

8.4 Machines used

In the selection of machine tools, we opted for models that, once purchased, can also be used for other productions besides the one studied in this project. By considering only a machine specifically tailored for the machining of our shaft, we risk ending up with a machine that is not very robust or powerful and would not be used for future operations. We are therefore "sacrificing" the short-term economic aspect for a more complete and stable machine with a useful life of approximately 20-30 years, one that can be used in multiple contexts.

8.5.1 Lathe

The choice fell on the **Damatomacchine Multitech 1000.51 Plus** model.

Multitech 1000.51 Plus	
Distance Between Centers	1000 mm
Center Height	180 mm
Spindle Speed	From 90 to 2000 rpm
Motor Power	2.2KW
Cross Travel of the Tool Post	160 mm
Price	7000€

8.5.2 Milling machine

As a second machine, to create the holes and the facing on the flange of our shaft, we will opt for a milling machine. The choice fell on the **Damatomacchine Orion 7.5 Universal Milling Machine** model.

Orion 7.5 Universal Milling Machine	
Max. Drilling Diameter	30 mm
Spindle Stroke	110 mm
Motor Power	2,2 kW
Spindle Speed	100-2000 rpm
Price	9000€

8.5.3 Band saw

As a third machine, a band saw will be useful for the cutoff phase of the raw steel bar. The choice falls on the HBM Metal Bandsaw model, priced at €549. The metal arms cost €20.

8.5.4 Grinding machine

We will need a grinding machine and a subsequent grinding wheel to achieve the desired roughness on two surfaces of our shaft. These surfaces will come into contact with other components (supports and bushings), which are not included in this project's study but are present in the original assembly.

For the grinding machine model, the **RIBON RUR 1000 UNIVERSAL GRINDING MACHINE** was chosen.

RIBON RUR 1000 UNIVERSAL GRINDING MACHINE	
Center Height	160 mm
Distance Between Centers	800 mm
Grinding Wheel Spindle Speed	1750 rpm
Max. Grinding Wheel Diameter	410 mm
Price	4500€

As for the abrasive grinding wheel model, taking into account that the two surfaces are between 15 mm and 21 mm long and have a diameter of 10 mm, we will choose the most suitable wheel from the TYROLIT catalog.

The choice falls on the grinding wheel with dimensions 300x40x76.2, with the name **89A 802 J5A V217 50**, and a price of €80.

8.6 Manufacturing cycle

8.6.1 Numbering of the various surfaces

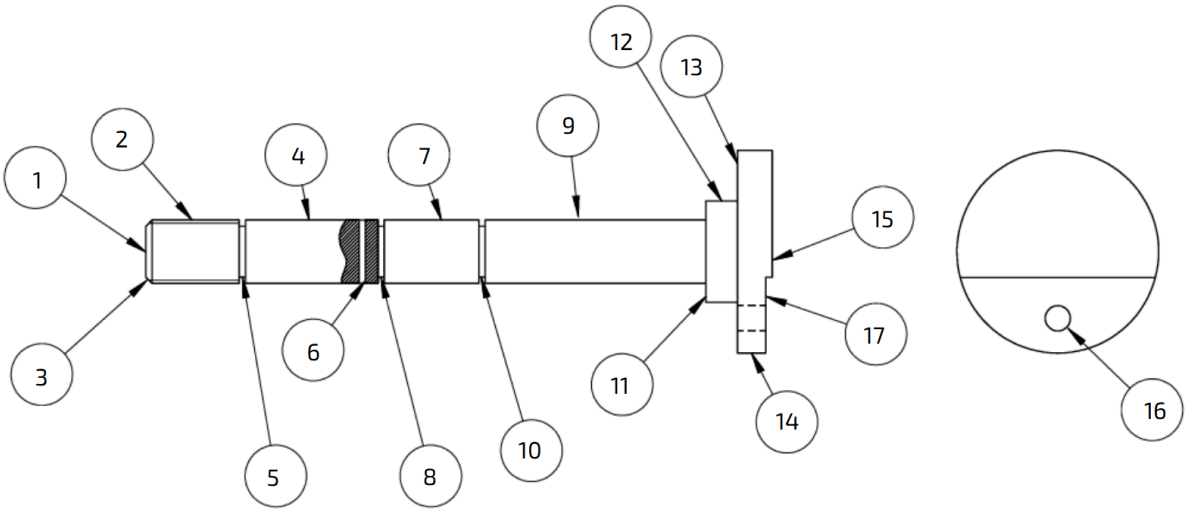

Surface No.	Surface Type	Possible Processes
2-4-5-7-8-9-10-12-14	Coaxial External Cylindrical Surfaces (c.e.c.)	Turning
1–11-13-15-17	Plane Orthogonal to the Axis	Turning/Milling
3	External Chamfer	Chamfering
16	Coaxial Internal Cylindrical Surfaces	Drilling
6	Orthogonal Internal Cylindrical Surfaces	Drilling

8.6.2 Grouping of the various surfaces

Surface No.	Process
1-2-3-4-5-8-10-7-11-12-13-14-15	Turning
6-16-17	Milling

8.6.3 Precedence constraints

The first surfaces to be made are the external coaxial ones that define the axis of our shaft, specifically surfaces 14 and 12; the other coaxial surfaces follow accordingly. Obviously, the drilling surfaces must be executed only after defining surfaces 4 and 17. Also, the creation of the grooves and the threading will be done once the surface that includes surfaces 2, 4, and 7 is completed.

8.6.4 Possible cycles

Machining Cycle			
Phase	**Sub-phase**	**Process**	**Surfaces**
10	Parting-off		
20	A	Facing Roughing Finishing	Sur. 1 Sur. 9 Sur. 9
	B	Roughing Finishing	Sur. 12 Sur 12
	C	Grooving	Sur. 5-8-10
	D	Chamfering	Sur. 3
	E	Threading	Sur. 2
	F	Facing Roughing Finishing	Sur. 15 Sur. 15 Sur. 14
30	A	Drilling	Sur. 6
	B	Surfacing Finishing	Sur. 17 Sur. 17
	C	Drilling	Sur. 16
40	A	Grinding	Sur. 4-7

8.6.5 Selection of Inserts and Tools

The facing, roughing, and chamfering operations will be carried out using the **CNMG 12 04 16-MR 4405** insert from Sandvik Coromant.

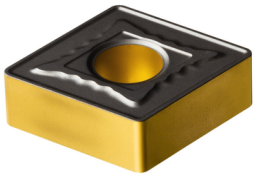

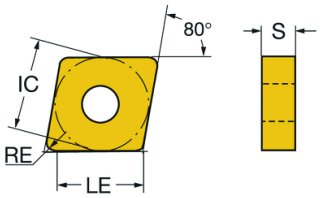

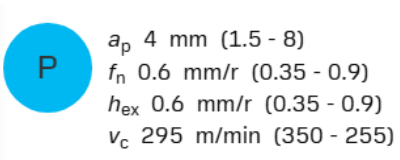

- **Insert thickness (S)**: 4.7625 mm
- **Inscribed circle diameter (IC)**: 12.7 mm
- **Effective cutting edge length (LE)**: 11.2 mm
- **Corner radius (RE)**: 1.5875 mm
- **Price**: €13.39

The tool holder is the **DCLNR 2020K 12** from Sandvik Coromant.

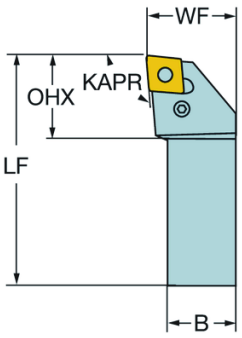

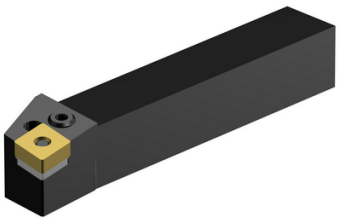

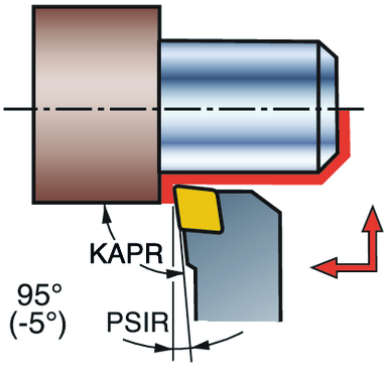

- **Tool cutting-edge angle (KAPR)**: 45°
- **Shank width (B)**: 20 mm
- **Functional length (LF)**: 125 mm
- **Functional width (WF)**: 25 mm
- **Price**: €96

The finishing operations will use the **DCMX 07 02 08-WF 1125** insert from Sandvik Coromant.

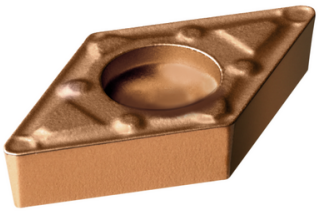

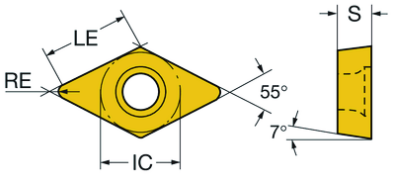

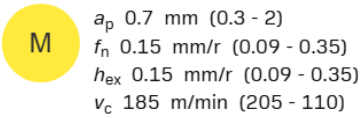

- **Insert thickness (S)**: 2.38 mm
- **Inscribed circle diameter (IC)**: 6.35 mm
- **Effective cutting edge length (LE)**: 6.9 mm
- **Corner radius (RE)**: 0.79 mm
- **Price**: €11.70

The tool holder is the **SDJCL 12 3B** from Sandvik Coromant.

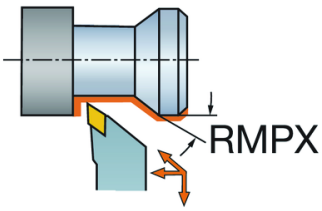

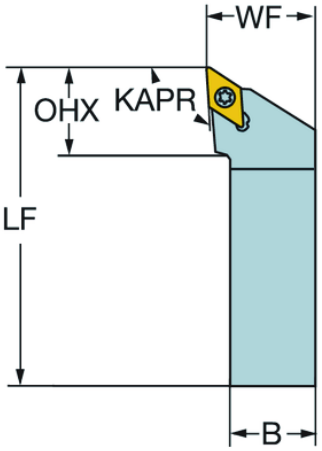

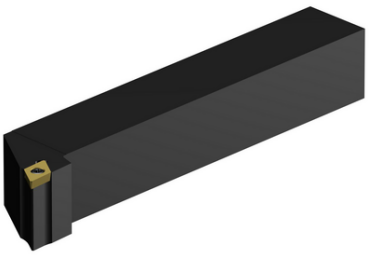

- **Tool cutting-edge angle (KAPR)**: 93°
- **Shank width (B)**: 20 mm
- **Functional length (LF)**: 125 mm
- **Functional width (WF)**: 25 mm
- **Price**: €117

The threading operation will be carried out using the **266RG-16MM02A150M 112** insert from Sandvik Coromant.

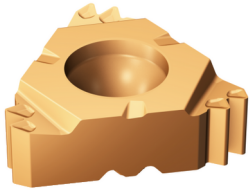

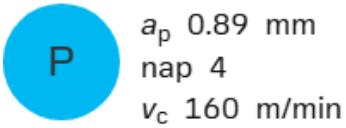

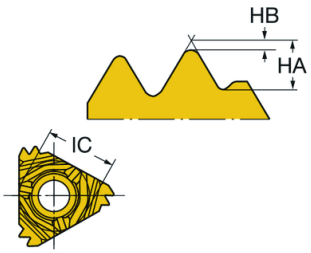

- **Inscribed circle diameter (IC)**: 9.5 mm
- **Theoretical thread height (HA)**: 1.12 mm
- **Thread height difference (HB)**: 0.22 mm
- **Price**: €44

The threading operation will be carried out using the 266RFA-2020-16 tool holder from Sandvik Coromant.

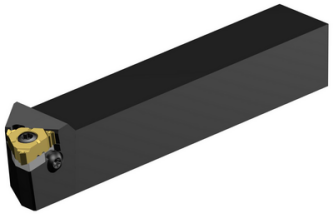

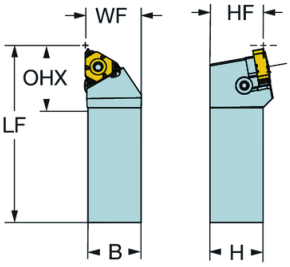

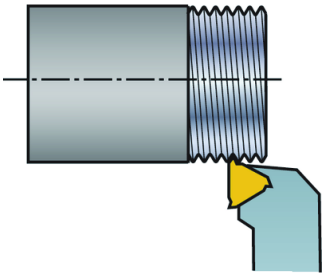

- **Maximum overhang (OHX)**: 21.6 mm
- **Shank width (B)**: 20 mm
- **Functional length (LF)**: 125 mm
- **Functional width (WF)**: 20.5 mm
- **Price**: €168

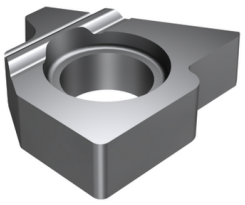

The threading operations will be carried out with the 5322 391-13 support from Sandvik Coromant, with a price of €25.

The grooving operation will be carried out using the **N123T3-0100-0000-GS 1125** insert from Sandvik Coromant.

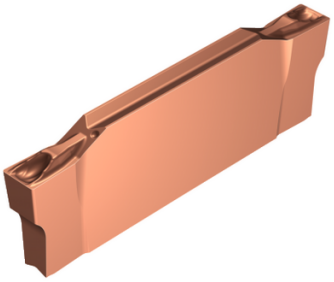

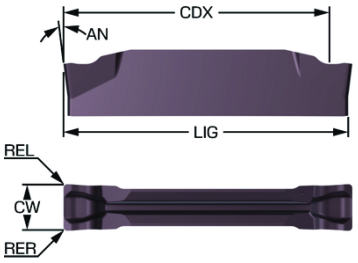

- **Maximum cutting depth (CDX)**: 13.5 inches
- **Main relief angle (AN)**: 5°
- **Cutting width (CW)**: 1.5 mm
- **Price**: €37

The grooving operation will be carried out using the **N123K55-25A2** tool from Sandvik Coromant.

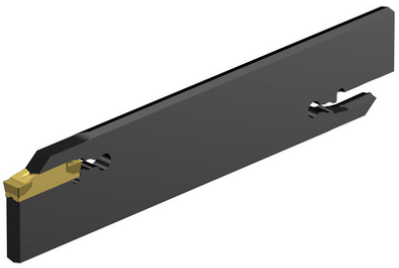

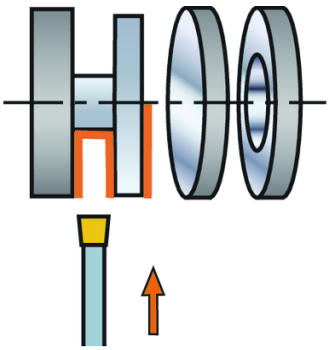

- **Functional length (LF)**: 150 mm
- **Functional width (WF)**: 5.75 mm
- **Maximum cutting depth (CDX)**: 55 mm
- **Price**: €133

The spot drilling and marking operations will be carried out using the **Dormer A100 Ø3.15 mm DIN 333-A center drill**, with a cost of €2.70, to mark both the Ø1 mm and Ø5 mm holes.

The drilling and face milling operations will be carried out with the **2P342-0500-PA P2BM** end mill from Sandvik Coromant.

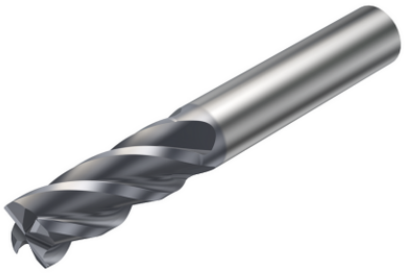

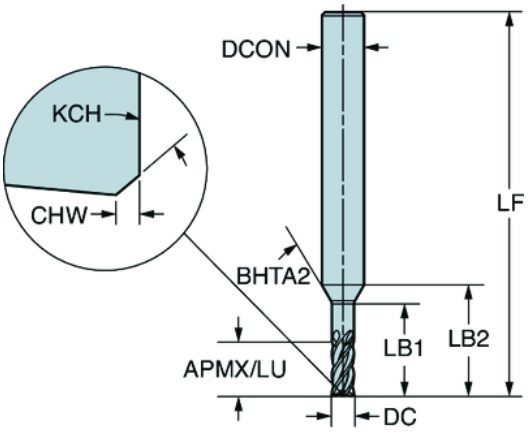

- **Cutting diameter (DC)**: 5 mm
- **Useful length (LU)**: 11 mm
- **Tip length (PL)**: 0.74 mm
- **Maximum cutting depth (APMX FFW)**: 11 mm
- **Functional length (LF)**: 57 mm
- **Price**: €85

The drilling operation that will define the internal surface 6 will then be completed with the micro drill bit 13, at a price of approximately €2.60 each.

8.6.6 Selection of cutting parameters

- Turning
  - $D \rightarrow$ Average Machining Diameter (mm)
  - $ap \rightarrow$ Tool Cutting Depth (mm)
  - $Vc \rightarrow$ Cutting Speed (m/min)
  - $Ra = \frac{a^2}{8 \cdot RE} * 1000 \rightarrow$ Roughness
  - $RE \rightarrow$ Tool Corner Radius (mm)
  - $a \rightarrow$ Theoretical Feed per Revolution (mm/rev)
  - $n = \frac{Vc*1000}{\pi D} \rightarrow$ Spindle Speed (rev/min)
  - $1/n \rightarrow$ Kronenberg constant
  - $Rm \rightarrow$ Tensile Strength of Steel
  - $\beta \rightarrow$ Insert cutting angle
  - $Ps = 2,4 \cdot Rm^{0,454} \cdot \beta^{0,666} \rightarrow$ Specific Cutting Pressure
  - $S = a \cdot ap \rightarrow$ Chip Cross-Section
  - $Pt = Ps \cdot S^{-1/n} \rightarrow$ Cutting Pressure
  - $Ft = Pt \cdot S \rightarrow$ Cutting force
  - $Pc = \frac{Ft \cdot Vc}{1000 \cdot 60} \rightarrow$ Theoretical cutting power
  - $Pm = \frac{Pc}{\eta} \rightarrow$ Machine power (kW)

- Milling
  - $D \rightarrow$ Milling cutter diameter (mm)
  - $Z \rightarrow$ Number of cutting edges
  - $np \rightarrow$ Number of passes
  - $ap \rightarrow$ Tool depth of cut (mm)
  - $Vc \rightarrow$ Cutting speed (m/min)
  - $Va \rightarrow$ Theoretical feed per revolution (mm/rev)
  - $n = \frac{Vc*1000}{\pi D} \rightarrow$ Spindle speed (rpm)
  - $1/n \rightarrow$ Kronenberg constant
  - $Rm \rightarrow$ Tensile Strength of Steel
  - $\beta \rightarrow$ Insert cutting angle
  - $Ps = 2,4 \cdot Rm^{0,454} \cdot \beta^{0,666} \rightarrow$ Specific Cutting Pressure
  - $S = a \cdot ap \rightarrow$ Chip Cross-Section
  - $Pt = Ps \cdot S^{-1/n} \rightarrow$ Cutting Pressure
  - $Ft = Pt \cdot S \rightarrow$ Cutting force
  - $Pc = \frac{Ft \cdot Vc}{1000 \cdot 60} \rightarrow$ Theoretical cutting power
  - $Pm = \frac{Pc}{\eta} \rightarrow$ Machine power (kW)

- Grinding
  - $S \rightarrow$ Grinding wheel thickness (mm)
  - $D \rightarrow$ Grinding wheel diameter
  - $ap \rightarrow$ Tool depth of cut (mm)
  - η → Efficiency
  - k → Grinding coefficient
  - $Vc \rightarrow$ Cutting speed (m/min)
  - $Vf \rightarrow$ Feed Rate (f*n)
  - f → Theoretical feed per revolution (mm/rev)
  - $n = \frac{Vc*60000}{\pi D} \rightarrow$ Spindle speed (rpm)
  - v → Material Removal Rate ($ap*S*Vf$)
  - $Pc = 0,155 * k * \sqrt{V * S} * \sqrt{\frac{Vc}{30}} \rightarrow$ Theoretical Cutting Power
  - $Pm = \frac{Pc}{\eta} \rightarrow$ Machine power (kW)

Cutting parameters for facing surface 1:

Di	$35\ mm$	n	$1000\ giri/min$	Ra	$12,65\ \mu m$	Ft	$516\ N$
Df	$0\ mm$	Rm	$550\ N/mm^2$	a	$0,3\ mm/g$	Pc	$0,473\ kW$
D	$17,5\ mm$	Ps	$779\ \frac{N}{mm^2}$	RE	$1,58\ mm$	Pm	$0,67\ kW$
ap	$2\ mm$	S	$0.6\ mm^2$	β	80°	η	0,7
Vc	$55\ m/min$	Pt	$861\ \frac{N}{mm^2}$				

Cutting parameters for roughing surface 9:

Di	$35\ mm$	n	$737\ giri/min$	Ra	$12,65\ \mu m$	Ft	$557\ N$
Df	$12.5\ mm$	Rm	$550\ N/mm^2$	a	$0,3\ mm/g$	Pc	$0,51\ kW$
D	$23.75\ mm$	Ps	$779\frac{N}{mm^2}$	RE	$1,58\ mm$	Pm	$0,72\ kW$
ap	$2.2\ mm$	S	$0.66\ mm^2$	β	80°	η	0,7
Vc	$55\ m/min$	Pt	$845\frac{N}{mm^2}$				

Cutting parameters for finishing surface 9:

Di	$12.5\ mm$	n	$1415\ giri/min$	Ra	$1.58\ \mu m$	Ft	$40\ N$
Df	$10\ mm$	Rm	$550\ N/mm^2$	a	$0,1\ mm/g$	Pc	$0,03\ kW$
D	$11.25\ mm$	Ps	$670\frac{N}{mm^2}$	RE	$0.79\ mm$	Pm	$0,05\ kW$
ap	$0.3\ mm$	S	$0.03\ mm^2$	β	55°	η	0,7
Vc	$50\ m/min$	Pt	$1336\frac{N}{mm^2}$				

Cutting parameters for roughing surface 12:

Di	$35\ mm$	n	$660\ giri/min$	Ra	$12,65\ \mu m$	Ft	$516\ N$
Df	$18\ mm$	Rm	$550\ N/mm^2$	a	$0,3\ mm/g$	Pc	$0,473\ kW$
D	$26,5\ mm$	Ps	$779\frac{N}{mm^2}$	RE	$1,58\ mm$	Pm	$0,67\ kW$
ap	$2\ mm$	S	$0.6\ mm^2$	β	80°	η	0,7
Vc	$55\ m/min$	Pt	$861\ N/mm2$				

Cutting parameters for finishing surface 12:

Di	$18\ mm$	n	$1311\ giri/min$	Ra	$1.58\ \mu m$	Ft	$40\ N$
Df	$16\ mm$	Rm	$550\ N/mm^2$	a	$0,1\ mm/g$	Pc	$0.05\ kW$
D	$17\ mm$	Ps	$670\frac{N}{mm^2}$	RE	$0.79\ mm$	Pm	$0,07\ kW$
ap	$0.3\ mm$	S	$0.03\ mm^2$	β	55°	η	0,7
Vc	$70\ m/min$	Pt	$1336\ N/mm2$				

Cutting parameters for facing surface 15:

Di	$35\ mm$	n	$1000\ giri/min$	Ra	$12,65\ \mu m$	Ft	$516\ N$
Df	$0\ mm$	Rm	$550\ N/mm^2$	a	$0,3\ mm/g$	Pc	$0,473\ kW$
D	$17,5\ mm$	Ps	$779\ \frac{N}{mm^2}$	RE	$1,58\ mm$	Pm	$0,67\ kW$
ap	$2\ mm$	S	$0.6\ mm^2$	β	80°	η	0,7
Vc	$55\ m/min$	Pt	$861\ \frac{N}{mm^2}$				

Cutting parameters for roughing surface 14:

Di	$35\ mm$	n	$515\ giri/min$	Ra	$12,65\ \mu m$	Ft	$557\ N$
Df	$33\ mm$	Rm	$550\ N/mm^2$	a	$0,3\ mm/g$	Pc	$0,51\ kW$
D	$34\ mm$	Ps	$779\ \frac{N}{mm^2}$	RE	$1,58\ mm$	Pm	$0,72\ kW$
ap	$2\ mm$	S	$0.66\ mm^2$	β	80°	η	0,7
Vc	$55\ m/min$	Pt	$845\ \frac{N}{mm^2}$				

Cutting parameters for finishing surface 14:

Di	$33\ mm$	n	$783\ giri/min$	Ra	$1.58\ \mu m$	Ft	$40\ N$
Df	$32\ mm$	Rm	$550\ N/mm^2$	a	$0,1\ mm/g$	Pc	$0,053\ kW$
D	$32.5\ mm$	Ps	$670\ \frac{N}{mm^2}$	RE	$0.79\ mm$	Pm	$0,08\ kW$
ap	$0.3\ mm$	S	$0.03\ mm^2$	β	55°	η	0,7
Vc	$80\ m/min$	Pt	$1336\ n/mm2$				

Cutting parameters for grooving 5-8-10:

Di	$10\ mm$	n	$1676\ giri/min$	Ra	$3.1\ \mu m$	Ft	$403\ N$
Df	$9\ mm$	Rm	$550\ N/mm^2$	a	$0,1\ mm/g$	Pc	$0,33\ kW$
D	$9.5\ mm$	Ps	$843\ \frac{N}{mm^2}$	RE	$0.4\ mm$	Pm	$0,47\ kW$
ap	$1\ mm$	S	$0.4\ mm^2$	β	90°	η	0,7
Vc	$50\ m/min$	Pt	$1009\ n/mm2$				

Cutting parameters for chamfering surface 3:

Di	$10\ mm$	n	$1508\ giri/min$	Ra	$0.79\ \mu m$	Ft	$122.6\ N$
Df	$9\ mm$	Rm	$550\ N/mm^2$	a	$0,1\ mm/g$	Pc	$0,09\ kW$
D	$9.5\ mm$	Ps	$779\ \frac{N}{mm^2}$	RE	$1,58\ mm$	Pm	$0,13\ kW$
ap	$1\ mm$	S	$0.1\ mm^2$	β	80°	η	0,7
Vc	$45\ m/min$	Pt	$1226\ n/mm2$				

Cutting parameters for threading surface 2:

Di	$10\ mm$	n	$1340\ giri/min$	Ra	$5.68\ \mu m$	Ft	$84.5\ N$
Df	$9\ mm$	Rm	$550\ N/mm^2$	a	$0,1\ mm/g$	Pc	$0,05\ kW$
D	$9.5\ mm$	Ps	$643\ \frac{N}{mm^2}$	RE	$0.22\ mm$	Pm	$0,08\ kW$
ap	$0.8\ mm$	S	$0.08\ mm^2$	β	60°	η	0,7
Vc	$40\ m/min$	Pt	$1057\ n/mm2$				

Cutting parameters for facing surface 17:

D	$5\ mm$	n	$1273\ giri/min$			Ft	$583\ N$
Z	4	Rm	$550\ N/mm^2$	$a\mathbf{z}$	$0,2\ mm/g$	Pc	$0,194\ kW$
		Ps	$531\ \frac{N}{mm^2}$	Va	$1018\ mm$	Pm	$0,27\ kW$
ap	$1\ mm$	S	$0.2\ mm^2$	β	45°	η	0,7
Vc	$20\ m/min$	Pt	$729\ n/mm2$				

Cutting parameters for finishing surface 17:

D	$5\ mm$	n	$1592\ giri/min$			Ft	$160\ N$
Z	4	Rm	$550\ N/mm^2$	$a\mathbf{z}$	$0,15\ mm/g$	Pc	$0,41\ kW$
		Ps	$531\ \frac{N}{mm^2}$	Va	$955\ mm$	Pm	$0,58\ kW$
ap	$0.25\ mm$	S	$0.04\ mm^2$	β	45°	η	0,7
Vc	$25\ m/min$	Pt	$1001\ n/mm2$				

Cutting parameters for drilling surface 16:

D	$5\ mm$	n	$955\ giri/min$			Ft	$2292\ N$
Z	4	Rm	$550\ N/mm^2$	$a\mathbf{z}$	$0,2\ mm/g$	Pc	$0,573\ kW$
		Ps	$531\frac{N}{mm^2}$	Va	$764\ mm$	Pm	$0,81\ kW$
ap	$5.5\ mm$	S	$1.1\ mm^2$	β	45°	η	0,7
Vc	$15\ m/min$	Pt	$521\ n/mm2$				

Cutting parameters for drilling surface 6:

D	$1\ mm$	n	$1592\ giri/min$			Ft	$1076\ N$
Z	2	Rm	$550\ N/mm^2$	$a\mathbf{z}$	$0,2\ mm/g$	Pc	$0,08\ kW$
		Ps	$309\frac{N}{mm^2}$	Va	$1273\ mm$	Pm	$0,12\ kW$
ap	$10\ mm$	S	$2\ mm^2$	β	20°	η	0,7
Vc	$5\ m/min$	Pt	$269\ n/mm2$				

Cutting parameters for grinding surfaces 4-7:

D	300 mm	n	$1273\ giri/min$				
S	1 cm	Rm	$550\ N/mm^2$	**f**	0,1 mm/g	Pc	$0,48\ kW$
		k	7,5	Vf	127 mm/min	Pm	$0,7\ kW$
ap	$0,002\ mm$			V	0.254 cm^3	η	0,7
Vc	$20\ m/min$						

8.6.7 Process sheets

Present in the appendix.

8.6.8 Dimensional inspection

After the relevant machining operations, we need to perform an inspection phase to ensure that the dimensions and roughness are acceptable. We will therefore use:

- **A vernier caliper** is fundamental because it allows you to precisely verify if the dimensions of a part respect the measurements indicated in the technical drawing. Using it means you can immediately identify any deviations from tolerances, thus preventing scrap, rework, and ensuring the quality of the finished part.

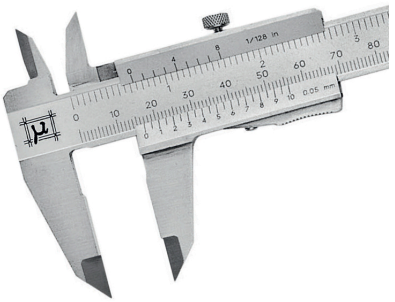

- **A Surface Roughness Tester** is used to measure the surface roughness of a part, which indicates how smooth or irregular the surface is. It is an essential instrument when the surface finish is a functional characteristic of the part.

Rugosimetri
da 935.901 a 935.902

8.7 Calculation of Machining Times

Let's analyze the active times of the different machining operations. $T = \frac{(L+e)}{a \cdot n}$

Parting-off	Sur. 14
Feed (mm/rev)	300
Approach distance	2
Workpiece width	35
Machining time per single pass	0,12

.

Turning	Fac.1	Rou.9	Fin.9	Rou.12	Fin.12	Grov.5-8-10	Cham.3	Thre.2	Fac.15	Rou.14	Fin.14
Feed (mm/rev)	0,3	0,3	0,1	0,3	0,1	0,1	0,1	0,1	0,3	0,3	0,1
Spindle Speed (rpm)	1000	737	1415	660	1311	1676	1508	1340	1000	515	1273
Approach distance	2	2	2	2	2	2	2	2	2	2	2
Workpiece Length	17,5	89	89	5	5	1,5*3	1	15	17,5	6	6
Number of Passes	1	6	5	5	4	1*3	1	1	1	1	2
Single Pass Time	0.065	0.41	0.64	0,03	0,05	0,04	0,019	0,12	0,065	0,05	0,06
Total Pass Time	0.065	2.46	3.2	0,15	0,21	0,12	0,019	0,12	0,065	0,05	0,12
TOTAL	6.5										

Milling	Dri. sur. 6	Surfacing. sur. 17	Fin. sur. 17	Dri. sur. 16
Feed (mm/rev)	1592	1273	1592	955
Approach distance	2	2	2	2
Workpiece Length	10	32	32	6
Number of Passes	1	1	2	1
Single Pass Time	0,06	0,033	0,035	0,025
Total Pass Time	0,06	0,033	0,07	0,025
TOTAL	0,18			

Grinding	Sur.4	Sur.7
Feed (mm/rev)	127	127
Approach distance	1	1
Workpiece Length	15	21
Number of Passes	4	4
Abrasive Wheel Width	25	25
Single Pass Time	0,12	0,17
Total Pass Time	0,5	0,68
TOTAL	1.18	

The total active time is **8 minutes and 26 seconds**.

Let's analyze the idle times in turning:

- Loading the raw workpiece into the chuck → 50 sec * 2 times → 1 min
- Chuck assembly → 1 min * 1 time → 1 min
- Lathe start/stop → 5 sec * 30 times → 1 min 50 sec
- Inspection time → 20 sec * 9 times → 3 min
- Tool approach and retraction → 20 sec * 30 times → 6 min
- Depth setting → 10 sec * 30 times → 5 min
- Centering → 10 sec * 2 times → 20 sec
- Chuck closing → 10 sec * 2 times → 20 sec
- Tool and insert assembly/disassembly → 40 sec * 18 times → 12 min

Total idle time in turning → 30 minutes and 30 seconds

Let's analyze the idle times in parting-off:

- Workpiece positioning and clamping → 30 sec * 1 time → 30 sec
- Blade start → 20 sec * 2 times → 40 sec
- Blade retraction → 10 sec * 2 times → 20 sec
- Workpiece removal → 30 sec * 1 time → 30 sec

Total idle time in parting-off → 2 minutes

Let's analyze the idle times in milling:

- Workpiece positioning → 30 sec * 2 times → 1 min
- Chuck assembly → 1 min * 1 time → 1 min
- Milling machine start/stop → 5 sec * 5 times → 25 sec
- Inspection time → 20 sec * 4 times → 1 min
- Tool approach and retraction → 20 sec * 5 times → 1 min 40 sec
- Depth setting → 10 sec * 5 times → 50 sec
- Centering → 10 sec * 2 times → 20 sec
- Tool and insert assembly/disassembly → 1 min * 8 times → 8 min
- Hole centering → 40 sec * 2 times → 1 min 20 sec

Total idle time in milling → 15 minutes and 35 seconds

Let's analyze the idle times in grinding:

- Workpiece positioning → 30 sec * 1 time → 30 sec
- Wheel mounting and dismounting → 80 sec * 1 time → 1 min 20 sec
- Grinding machine start/stop → 5 sec * 8 times → 40 sec
- Tool approach and retraction → 20 sec * 8 times → 2 min 40 sec
- Depth setting → 10 sec * 8 times → 1 min 20 sec
- Tool and insert assembly/disassembly → 1 min * 8 times → 8 min
- Inspections → 20 sec * 2 times → 40 sec

Total idle time in grinding → 15 minutes and 10 seconds

Now we have all the data to calculate the total manufacturing time of our shaft on machine tools. We find that producing one shaft takes 70 minutes, or 1 hour and 10 minutes. Since our annual order quantity is 1,000 pieces, the total production time amounts to approximately 1,166 hours.

8.8 Calculation of machining costs

To calculate the labor cost, we assume the hiring of two operators working 8 hours per day on the machines we have purchased. Their labor rate is €20 per hour. We will therefore also calculate the costs of labor, energy, machinery, tools, and inserts.

MACHINE COST (assuming a service life of 20 years and 2,000 operating hours per year)

- **Band Saw**: (12 sec active time + 2 min idle time) * 1,000 = 2,120 min
  €549 / 40,000 h = €0.013 / h
- **Lathe**: (6 min 50 sec active time + 30 min 30 sec idle time) * 1,000 = 37,000 min
  €7,000 / 40,000 h = €0.175 / h
- **Milling Machine**: (20 sec active time + 15 min 35 sec idle time) * 1,000 = 15,550 min
  €9,000 / 40,000 h = €0.2256 / h
- **Grinding Machine**: (1 min 18 sec act. time + 15 min 10 sec idle time)*1,000 = 16,300 min
  €4,500 / 40,000 h = €0.1125 / h

The total hourly cost of our machines is €0.50.
For 1,000 shafts, corresponding to 1,166 hours of use, the total cost is €583.
For a single shaft, the cost is €583 / 1,000 = €0.58.

TOOLS AND INSERTS COST:

The quantity of inserts purchased was calculated for the production of 1,000 shafts, based on an estimate of their usage time, which was determined according to the operations, cutting parameters, and number of cutting edges.

- CNMG120416-MR4405 (roughing, chamfering, facing) (30) / DCLNR2020K12 (1)
  30 * €13 = €390 + €96 = €486
- DCMX 07 02 08-WF 1125 (finishing) (15) / SDJCL 12 3B (1)
  15 * €11.7 = €175.5 + €117 = €292.5
- 266RG-16MM02A150M 112 (threading) (5) / 266RFA-2020-16 (1) / 5322 391-13 (1)
  5 * €40 = €200 + €168 + €25 = €393
- N123T3-0100-0000-GS 1125 (grooving) (8) / N123K55-25A2 (1)
  8 * €37 = €296 + €133 = €429
- Dormer DIN 333-A (centering and marking) (3)
  3 * €2.7 = €8.1
- 2P342-0500-PA P2BM (drilling and surfacing) (5)
  5 * €85 = €425

- Guhring 5514 – HSS-Co Ø1 mm (drilling) (300)
  300 * €2.6 = €780
- Bandsaw (4) = 4 * €20 = €80
- Grinding wheel 89A 802 J5A V217 50 (2) = €160

Total cost = €3,053.6 (estimated for 1,000 pieces)
Cost per single shaft: €3.05

ENERGY COST:

(Grinding machine) 4 kW + (Lathe) 2.2 kW + (Milling machine) 2.2 kW + (Bandsaw) 0.5 kW = 8.9 kW / 4 = 2.2 kW average, therefore:
1,166 hours * 2.2 kW = 2,594 kWh * €0.173 = €448 / 1,000 = €0.48 per shaft

LABOR COST:

The operator is paid €20 per hour. If we estimate 1,000 hours of idle time to produce our 1,000 shafts, the total labor cost is €20,000, which translates to €20 per single shaft.

RAW MATERIAL COST:

Hot-rolled round bars in S355JR steel are usually supplied in standard commercial lengths, which, according to online sources, are 6 m (6,000 mm), with diameters up to 80 mm. Considering a cutting allowance of 2 mm per piece (typical for a bandsaw or cutoff saw), each piece occupies 102 mm (100 mm + 2 mm allowance).

Number of pieces per bar: 6,000 / 102 ≈ 58 → 58 pieces per bar
Number of bars required for 1,000 shafts: 1,000 / 58 ≈ 17.24 → 18 bars of 6,000 mm
Weight of a single bar (Ø 30 mm, 6,000 mm):
Volume = $\pi \times (0.015\ m)^2 \times 6\ m \approx 4.24 \times 10^{-3}\ m^3$
Weight = $4.24 \times 10^{-3} \times 7{,}850 \approx 33.3$ kg per bar
Material price (S355JR) ≈ €1.70/kg
Cost per bar = 33.3 kg × €1.70/kg ≈ €56.61
Cost per shaft = €56.61 / 58 pieces per bar ≈ €0.97 per shaft
Total cost for 18 bars: 18 × €56.61 ≈ €1,019

The total unit production cost of our shaft is €25.
The total cost for producing 1,000 shafts is €25,103.

9 Component Introduction: Cover

The cover component, located at the end of the crankshaft and connecting rod housing, serves to seal this area. There is one piece per engine, so our production batch will consist of 1,000 units.

9.1 Material Selection

Considering that, as previously mentioned, this component primarily serves to cover and protect internal parts, we select the material accordingly. Therefore, it must be a ductile material suitable for our manufacturing process. Aluminum is already a good choice due to its lightweight, so we choose among its alloys the one that offers the best properties. We identify the 1000 and 3000 series alloys and select **3003 aluminium alloy** for a good balance between strength and formability.

9.2 Selection of Manufacturing Technique

The production technique chosen is plastic deformation. The process will consist of deep drawing, which will allow us to create the “shell” shape of our component starting from a raw sheet metal. But by checking the ratio between height and diameter, we obtain 9 / 47 ≈ **0.19**. This value confirms that the process can be performed in a **single drawing operation**. Since our piece is axially symmetrical and circular, we will start with a circular sheet metal. Calculating Next, shearing operations will be performed to obtain the final geometry, and punching will be used to create the holes. Since our piece is axially symmetrical and circular, we will start with a circular sheet metal.

9.3 Machine Selection

Hydraulic Press HBM	
Maximum Load	75 t
Cylinder Stroke	250 mm
Work Width	800 min
Price	2000€

The diameter calculation was performed according to the formula shown in the photo and based on the geometry of the part, resulting in D = √(47² + 4(33*7 + 47*2)) = 59.2
We will use sheets 70 mm in diameter and 2 mm thick.

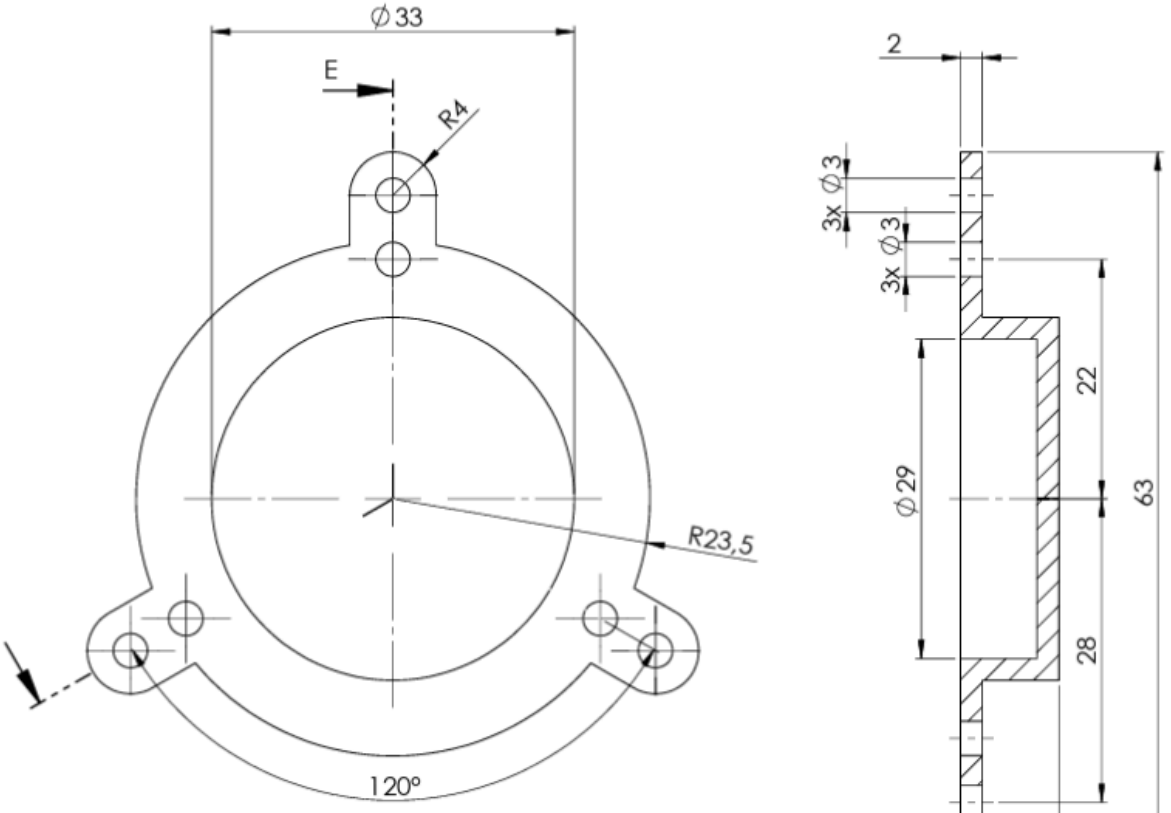

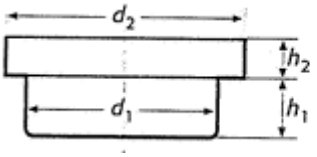

$$D = \sqrt{d_2^2 + 4\,(d_1\,h_1 + d_2\,h_2)}$$

Now we will calculate the clearance between the punch and the die:

$g = 0.002 \times s \times \sigma t^{0,5} = 0.03$ mm

- s = thickness of the blank (2 mm)
- Kt = shear strength of aluminum 3003 (90 MPa)

9.4 Die and Punch

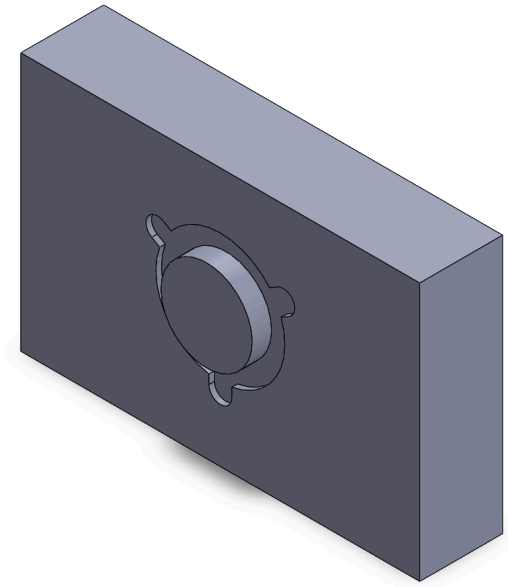

Die

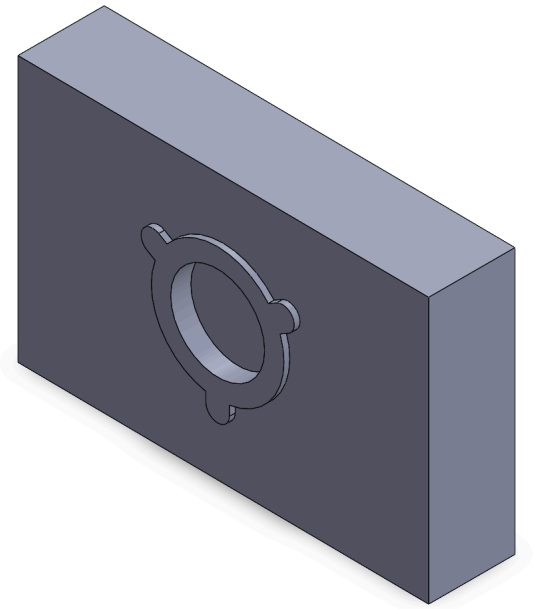

Punch

9.5 Deep Drawing

Force (F) = 0.002 m (s) × 3.14 × 0.07 m (D) × 95 × 10^6 Pa = 41762 N
Power (P) = F × v = 41762 N × 0.03 m/s = 1252 W

- v = punch feed speed (0.03 m/s, typical value)

9.6 Blanking and Punching

Force (F) = 0.002 m (s) × 0.140 m (L) × 90 × 10^6 Pa= 25200 N
Power (P) = F × v = 25200 N × 0.03 m/s = 756 W

- L = perimeter
- τ = specific shear strength

9.7 Cost and Timing

We estimate a machine production time of approximately 25 seconds, to which we add the operator's idle time for positioning the sheet and removing the finished part, estimated at 20 seconds. Therefore, the production time for a single cover is under one minute. Considering that the annual production batch will be 1,000 units, the total production time is 1,000 minutes, or approximately **17 hours**.

The costs include the operator cost, the machine cost, and the material cost.

Starting with the operator, we plan to pay approximately €20/h, which translates to €0.34 per piece (340 minutes / 1,000 pieces).

The material (aluminum 3003, in the blank form we prepared, i.e., a 2 mm thick, 70 mm diameter disc) costs approximately €4.5/kg on the market. Calculating the weight (from mass, density, and volume) as 0.2 kg, the material cost per piece is therefore €0.90.

The machine cost is €2,000. Hourly cost = (2,000 € / 20 years of service) / 260 working days / 8 hours = €0.04/h.

The die and punch cost approximately €2,500–3,000. Assuming a 4-year service life, the annual cost is about €700, and with a production of 1,000 covers per year, the cost per piece is €0.70.

Therefore, the cost per single cover is approximately **€2**, and the total cost for producing 1,000 units is **€2,000**.

10. Component introduction: crankshaft and crankpin

For the welding process we've decided to weld the pin to the shaft's flange.

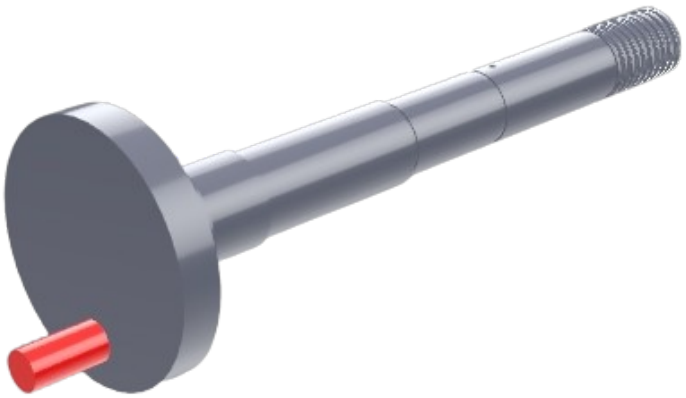

10.1 Manufacturing technique's selection: welding

For the joining of these two components, we have opted for brazing. This process provides greater aesthetic precision by not melting the base metals. Instead, it uses a filler metal that melts at a lower temperature than the two parts to be joined, creating a very strong joint that ensures greater resistance to vibration. Given the small size of our parts, capillary brazing is recommended. It is a process applied to join small components and is particularly suitable for mechanical parts like a shaft and a crank pin. For the filler metal, since both the shaft and the pin are made of steel alloy, the most recommended option is a silver alloy. It provides good mechanical strength and excellent adhesion to steel. However, a valid and more economical alternative is brass alloy (CuZnSi), also known as Silicon brass, which also adheres well to steel but requires more heat. To facilitate adhesion between the two parts and the filler metal, a flux is added. For brazing on steel, we have chosen a flux based on boron chloride and complex fluorides.

10.2 Machine's selection

The choice of machinery is divided into two options:

- Oxy-acetylene micro-torch: Recommended for small, precise joints, with a temperature over 3,000°C. It allows for localized heat control.
- Butane gas torch: A more economical and accessible alternative, also recommended for small steel joints, with a flame temperature between 1,300°C and 1,800°C.

We have opted for the oxy-acetylene micro-torch because, in addition to being more precise, which is crucial for the aesthetic and mechanical quality of our small part, it is also the most versatile and fastest option.

We've selected the Smith Little Torch Acetylene and Oxygen set, which costs around €850. It's excellent for precision brazing, features interchangeable nozzles from 0.2 mm to 1.2 mm, and uses an oxy-hydrogen flame, which is ideal for melting the filler wire.

The most important characteristics of the micro-torch must be:

- Flame type: Neutral, meaning a 1:1 ratio between oxygen and acetylene.
- Flame temperature: Considering that the brass alloy melts between 880°C and 900°C and steel melts at approximately 1,400°C, the flame should heat the joint to about 950°C.

10.3 Brazing's parameters

- Joint clearance: A clearance of 0.11 mm is recommended for a slow, localized flow, which ensures better capillary action.
- Flux: To be applied before heating the joint and the filler material, we have chosen a flux for brass on steel composed of borax and fluorides.
- Filler wire: CuZnSi alloy.
- Crankshaft and crankpin materials: S355JR.
- Filler wire diameter: 1.5 mm.
- Filler wire speed: 0.7 mm/s.
- Feeding method: Manual with a micro-torch.

10.4 Manufacturing phases

The steps in the brazing process are as follows:

- Surface preparation, including cleaning and degreasing.
- Application of flux to both surfaces.
- Joining of the parts.
- Heating of the joint area.
- Application of the filler metal.
- Removal of heat as soon as the brazing material has flowed.
- Allowing the part to cool.

- Cleaning and removing flux residues.

10.5 Timing and costs

10.5.1 Timing

- Preparation of flux and filler metal: 1 min per piece
- Positioning and fastening of parts: 1 min per piece
- Brazing: 3 min per piece
- Cooling: 10 min per piece
- Mechanical cleaning and degreasing: 3 min per piece
- Flux removal: 2 min per piece

Considering the active times, a total of 10 minutes per piece is required, plus the passive time for cooling, which is another 10 minutes per piece. Therefore, for 1,000 pieces, the total optimized time will be 250 hours.

10.5.2 Costs

Labor: labor costs are estimated at €20/h.

Filler Wire: considering that 8 mm of filler wire are needed for each piece, 8 meters of filler wire will be required to produce 1,000 pieces. The CuZnSi alloy wire costs an average of €35/kg.

Gases: oxygen and acetylene cost €70/L and €90/L, respectively.

For a total production run of 1,000 pieces, the total cost for labor and materials will be €5,200, which is approximately €5.2 per piece. The cost of the machinery is not included, as it's considered a versatile asset that can be used for future productions.

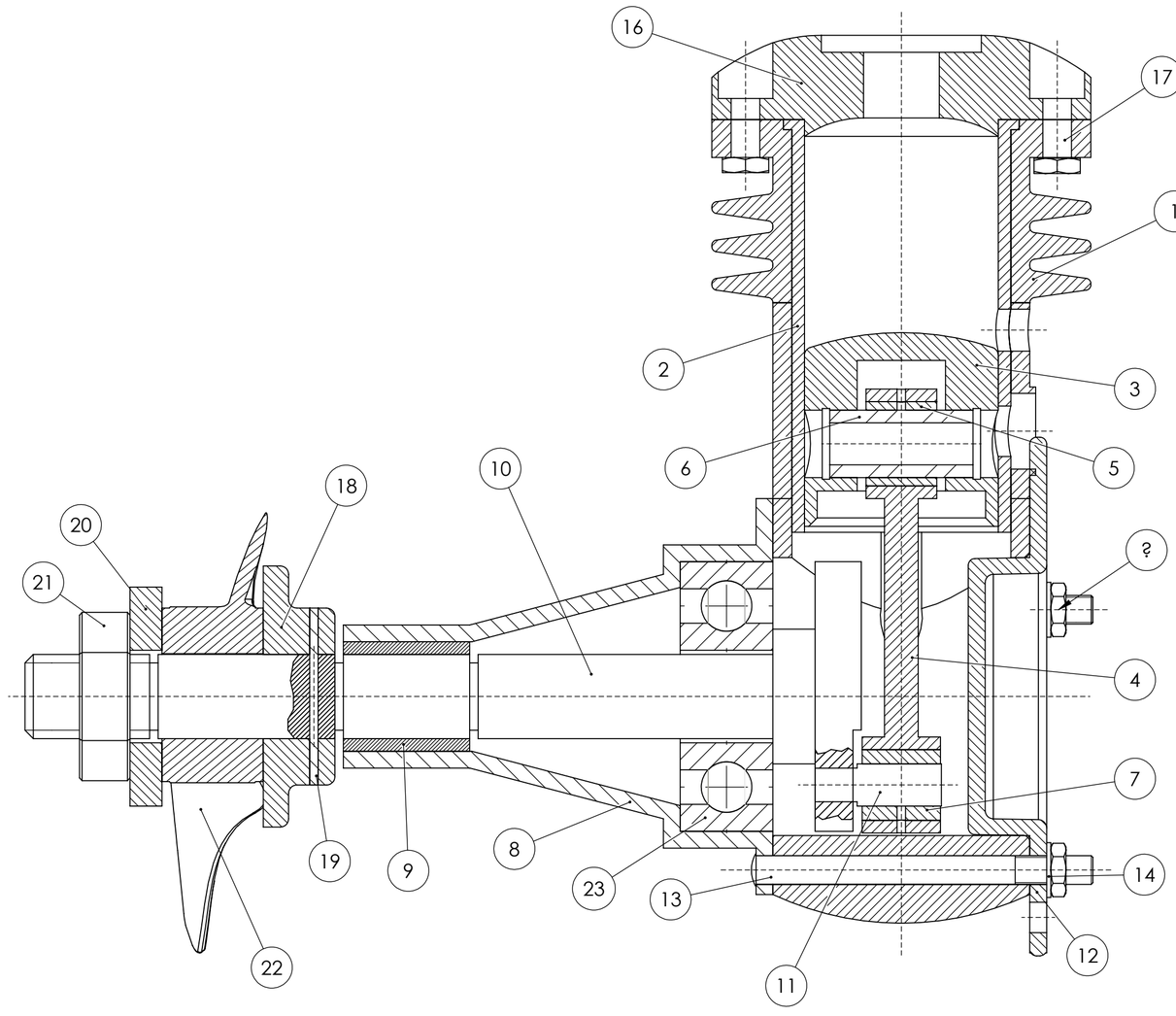

N°	Denominazione	Q.tà	Materiale
23	Cuscinetto	1	
22	Elica	1	ABS
21	Dado M10	1	
20	Rondella	1	Fe420
19	Spina elastica	1	
18	Supporto	1	GAlSi12NMNG
17	Vite M3X10	4	
16	Testata	1	GAlSi12NMNG
15	Dado M3	7	
14	Rosetta	3	
13	Vite di centraggio	3	C40
12	Coperchio	1	Al. Serie 3003
11	Perno di Manovella	1	38NCrMo7
10	Albero	1	S355JR
9	Bronzina	1	P.CuZn37
8	Supporto	1	GAlSi12NMNG
7	Bronzina	1	P.CuZn37
6	Spinotto	1	38NCrMo7
5	Bronzina	1	P.CuZn37
4	Biella	1	P.AlCu3
3	Pistone	1	X12CrTi
2	Camicia	1	GSO-420/15
1	Carter	1	G.Al-Si 13

Università di Pisa - Scuola di ingegneria

Motore a 2 tempi per aeromodelli

Data: 02/06/2025

Scala 2:1

Disegnatori

Spinelli Michele
Sofia La Spina

Foglio 1/1

Tolleranze generali secondo UNI ISO 2768-fH

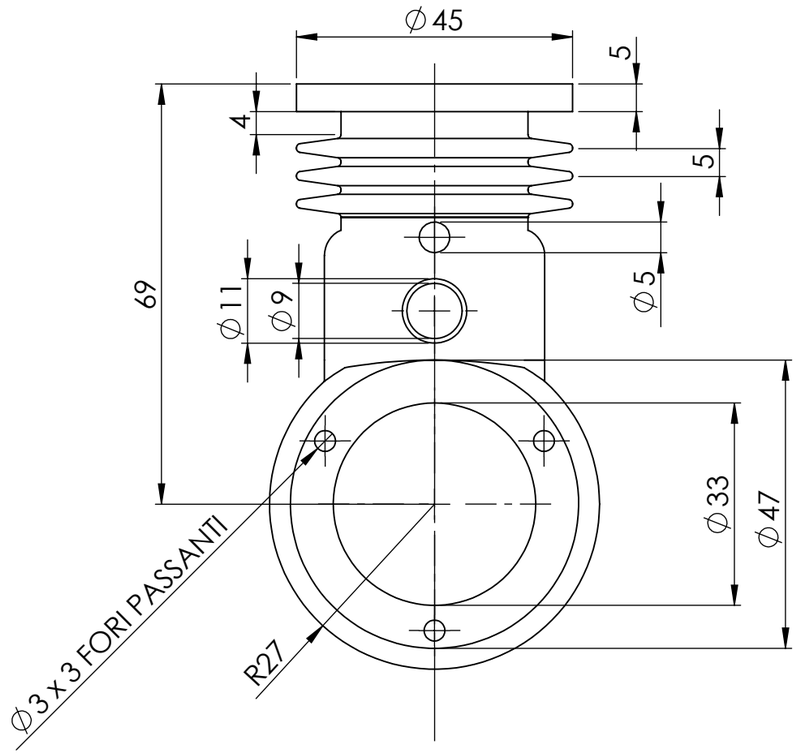

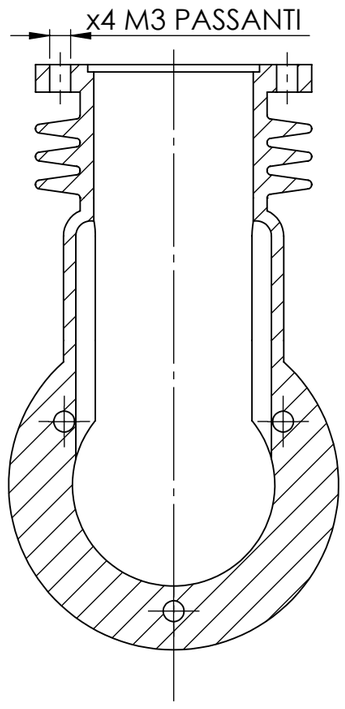

SEZIONE F-F

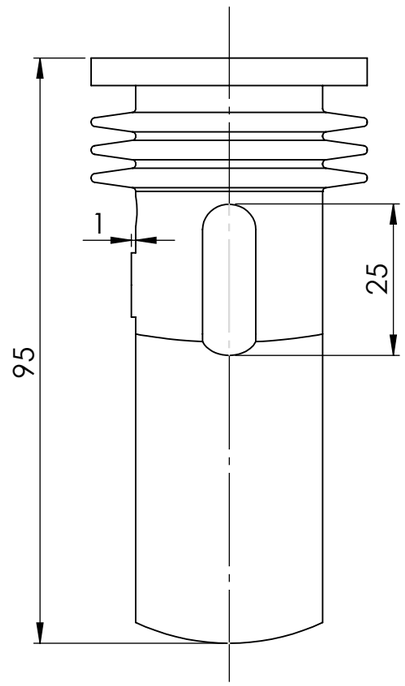

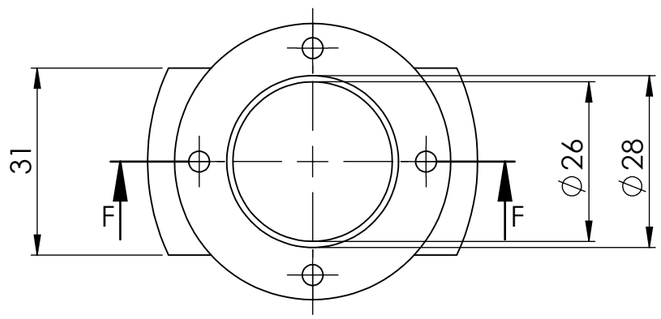

Università di Pisa - Scuola di ingegneria	
Albero	Scala 1:1
	Data: 29/05/2025
Rugosità generale: 3.2 µm (salvo diversa indicazione)	Materiale: G.Al-Si 13
Disegnatori Spinelli Michele Sofia La Spina	Foglio 1/1
Tolleranze generali secondo UNI ISO 2768-mK	

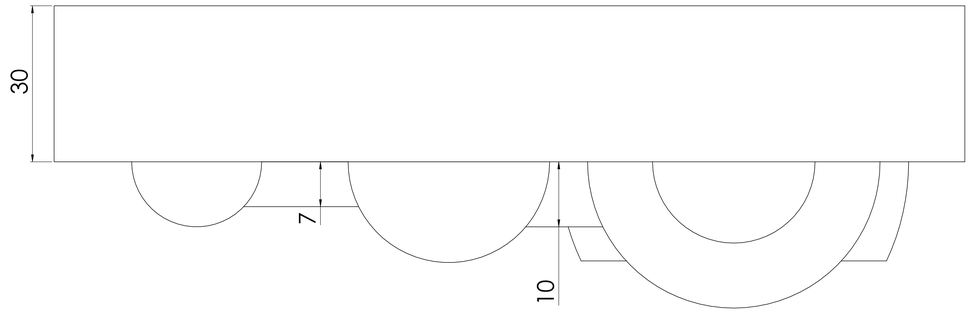

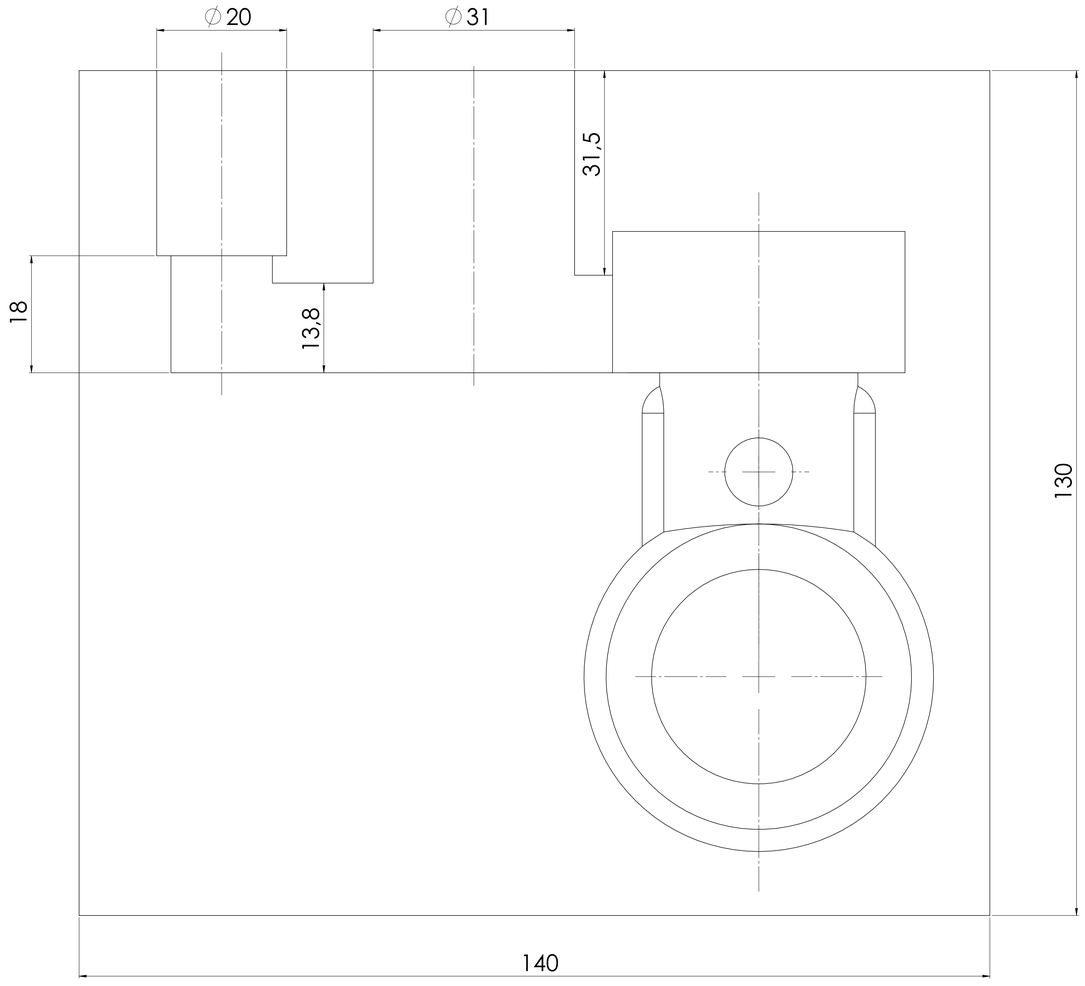

UNIVERSITA' DI PISA	Scuola Di Ingegneria
particolare	Mat.: sabbia silicea
placca modello inferiore	Foglio: 1:1
Disegnatori: Spinelli Michele La Spina Sofia	Data: 05/06/2025 Scala: 3:1

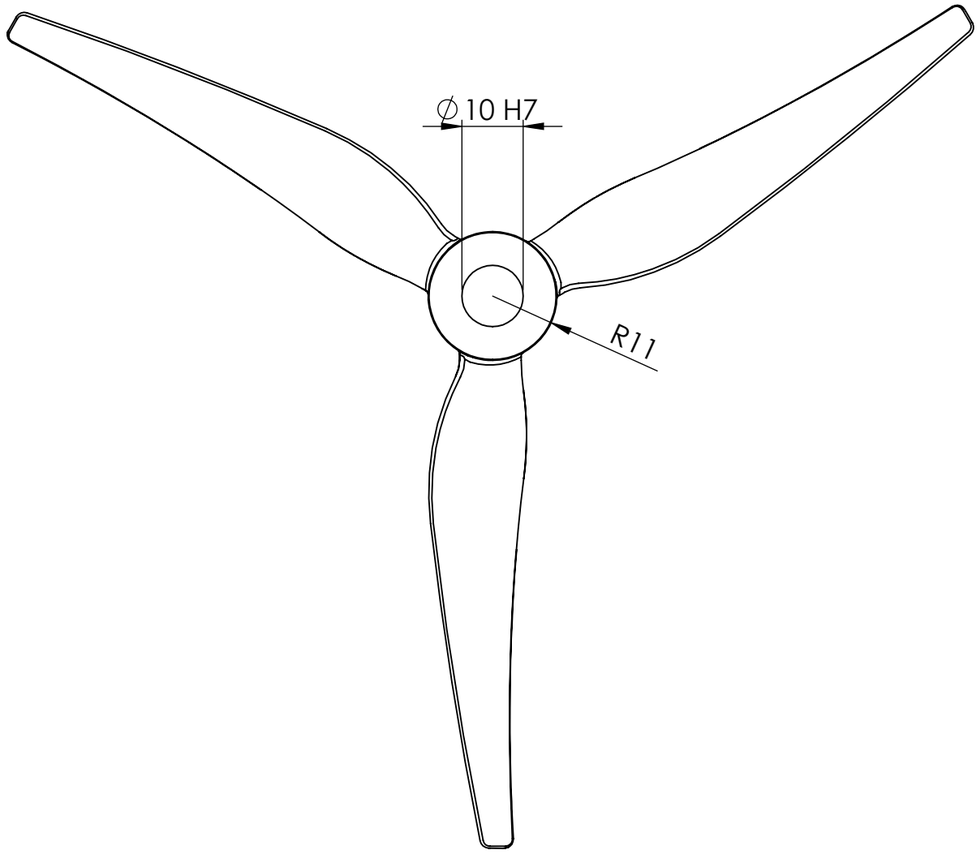

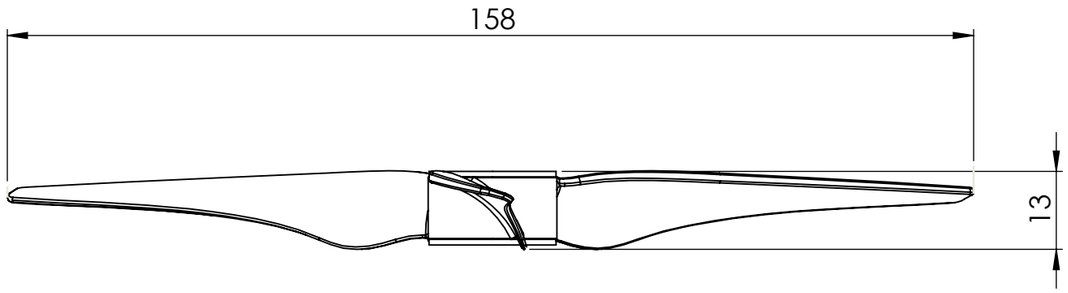

Università di Pisa - Scuola di ingegneria	
Elica	Scala 1:1
Materiale: ABS	Data: 19/04/2025
Disegnatori Spinelli Michele Sofia La Spina	Foglio 1/1

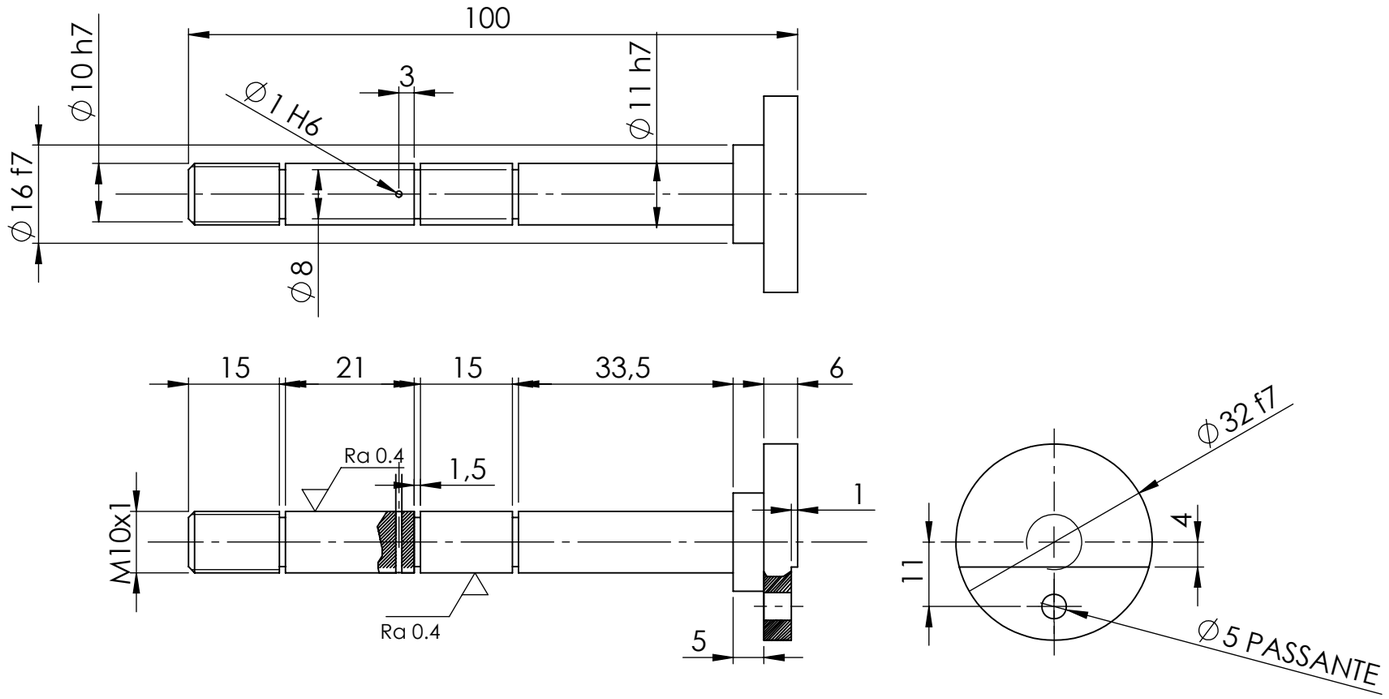

smussi non quotati 1x45°

Università di Pisa - Scuola di ingegneria	
Albero	Scala 1:1
Rugosità generale: 3.2 µm (salvo diversa indicazione)	Data: 12/05/2025
Disegnatori Spinelli Michele Sofia La Spina	Materiale: S355JR
	Foglio 1/1
Tolleranze generali secondo UNI ISO 2768-fH	

University of Pisa School of Engineering	Shaft Man. Cycle	Blank (cylindrical bar): diameter 35 mm, length 100 mm Material: S355JR			
Surfaces	Phase	Operation	Machine	Equipment	Clamping
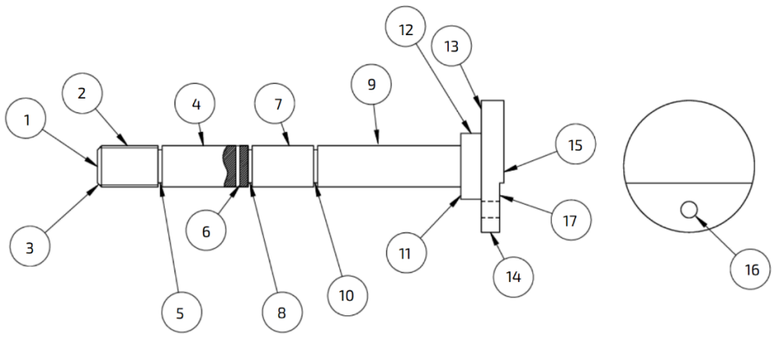	10	Parting-off	Bandsaw		
	20a	Facing Surface 1	Lathe	Self-Centering Chuck	Surface 14 (Provisional)
		Centering Surface 1			
		Roughing Surface 9			
		Finishing Surface 9			
	20b	Roughing Surface 12			
		Finishing Surface 12			
	20c	Grooving Surfaces 5-8-10			
	20d	Chamfering Surface 3			
	20e	Threading Surface 2			
	20f	Facing Surface 15			Sur. 9
		Centering Surface 15			
		Roughing Surface 14			
		Finishing Surface 14			
	30a	Marking and Drilling Surface 6	Milling Machine		Sur. 14
	30b	Surfacing Surface 17			Sur. 9
		Finishing Surface 17			
	30c	Marking and Drilling Surface 16			
	40	Grinding Surfaces 4-7	Grinding Machine	Grinding Wheel	Sur. 14

University of Pisa School of Engineering					Phase 10: Parting-off			
					Cutting Parameters			
Sub Phase	Process Sketch	No.	Tool	Inspection	Machine Power	Cutting Power	Cutting Speed	Spindle RPM
					Efficiency	Number of Passes	Cutting Depth	Feed Rate
		1	Bandsaw	Caliper			30 m/min	
						1	35 mm	300 mm/min

University of Pisa School of Engineering						Phase 20: Turning			
						Cutting Parameters			
Sub Phase	Process Sketch	No.	Operation	Tool	Inspection	Machine Power	Cutting Power	Cutting Speed	Spindle RPM
				Insert		Efficiency	Number of Passes	Cutting Depth	Feed Rate
A	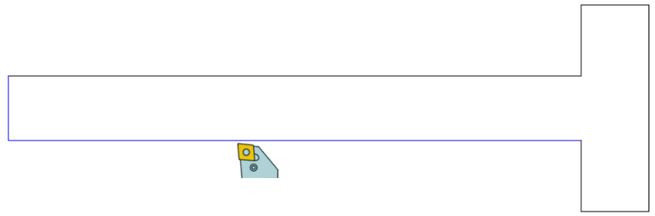	1	Facing Surface 1 from 104 mm to 102 mm	**DCLNR 2020K 12**	Vernier Caliper	0,67 kW	0,473 kW	55 m/min	1000 RPM
				CNMG 12 04 16-MR 4405		0,7 η	1	2 mm	0,3 mm/min
		2	Centering Surface 1	**Punta da centratura DIN 333-A**				10 m/min	
							1	2 mm	manuale
		3	Roughing Surface 9 from 35 mm to 12.5 mm	**DCLNR 2020K 12**		0,72 kW	0,51 kW	55 m/min	737 RPM
				CNMG 12 04 16-MR 4405		0,7 η	6	2.2 mm	0,3 mm/min
		4	Finishing Surface 9 from 12.5 mm to 10 mm	**SDJCL 12 3B**		0,05 kW	0,05 kW	50 m/min	1415 RPM
				DCMX 07 02 08-WF 1125		0,7 η	5	0.3 mm	0,1 mm/min
B	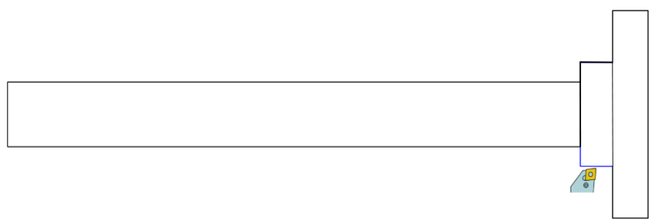	5	Roughing Surface 12 from 35 mm to 18 mm	**DCLNR 2020K 12**	Vernier Caliper	0,67 kW	0,473 kW	55 m/min	660 RPM
				CNMG 12 04 16-MR 4405		0,7 η	5	2 mm	0,3 mm/min
		6	Finishing Surface 12 from 18 mm to 16 mm	**SDJCL 12 3B**		0,07 kW	0,05 kW	70 m/min	1311 RPM
				DCMX 07 02 08-WF 1125		0,7 η	4	0.3 mm	0,1 mm/min

C	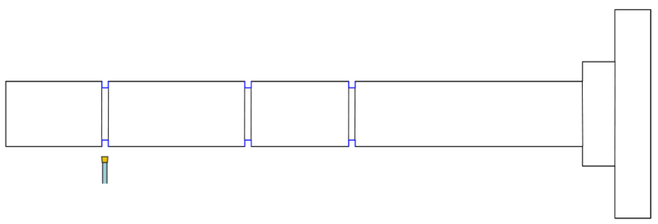	7	Grooving Surfaces 5-8-10	**N123T3-0100-00 00-GS 1125** **N123K55-25A2**	Vernier Caliper	0,47 kW 0,7 η	0,33 kW 1	50 m/min 1 mm	1676 RPM 0,1 mm/min
D	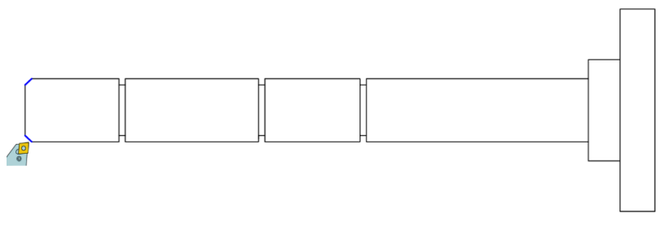	8	Chamfering Surface 3	**CNMG 12 04 16-MR 4405** **DCLNR 2020K 12**	Vernier Caliper	0,13 kW 0,7 η	0,09 kW 1	45 m/min 1 mm	1508 RPM 0,1 mm/min
E	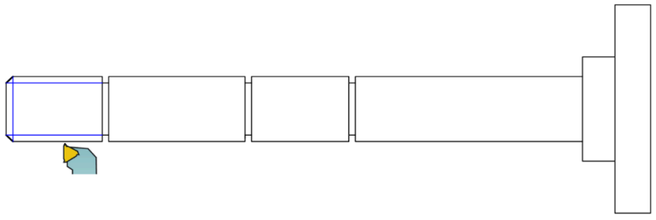	9	Threading Surface 2	**266RG-16MM02A 150M 112** **266RFA-2020-16**	Vernier Caliper	0,08 kW 0,7 η	0,05 kW 1	40 m/min 0,8 mm	1340 RPM 0,1 mm/min

F	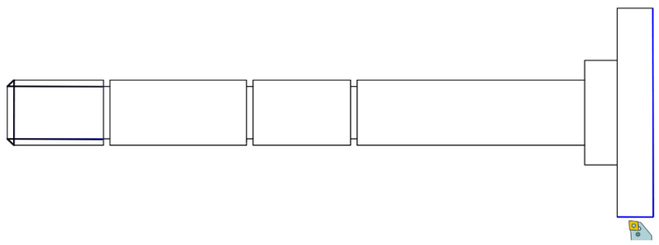	10	Facing Surface 15 from 102 mm to 100 mm	**DCLNR 2020K 12**	Self-Centering Chuck	0,67 kW	0,473 kW	55 m/min	1000 RPM
				CNMG 12 04 16-MR 4405		0,7 η	1	2 mm	0,3 mm/min
		11	Centering Surface 15	**Center Drill DIN 333-A**				10 m/min	
							1	2 mm	Manual
		12	Roughing Surface 14 from 35 mm to 33 mm	**DCLNR 2020K 12**		0,72 kW	0,51 kW	55 m/min	515 RPM
				CNMG 12 04 16-MR 4405		0,7 η	1	2 mm	0,3 mm/min
		13	Finishing Surface 14 from 33 mm to 32 mm	**SDJCL 12 3B**		0,08 kW	0,05 kW	80 m/min	783 RPM
				DCMX 07 02 08-WF 1125		0,7 η	2	0.3 mm	0,1 mm/min

University of Pisa School of Engineering						Phase 30: Milling			
						Cutting Parameters			
Sub Phase	Process Sketch	No.	Operation	Tool Insert	Inspection	Machine Power Efficiency	Cutting Power Number of Passes	Cutting Speed Cutting Depth	Spindle RPM Feed Rate
A	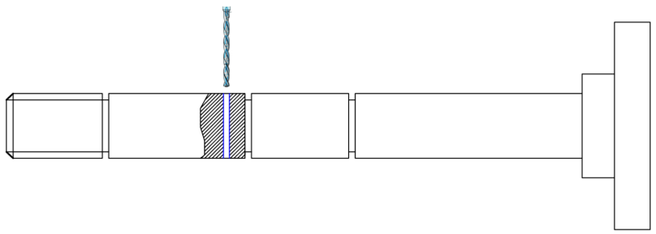	1	Marking and Drilling Surface 6	**DIN 333-A and N123K55-25A2**	Dividing Head, Tailstock	0,12 kW 0,7 η	0,08 kW 1	5 m/min 10 mm	1592 RPM 1273 mm/min
B	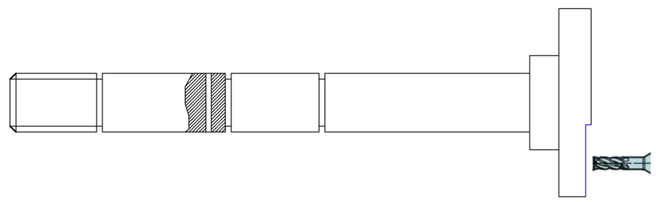	2	Roughing Surface 17	**2P342-0500-PA P2BM N123K55-25A2**	Vernier Caliper	0,27 kW 0,7 η	0,19 kW 1	20 m/min 1 mm	1273 RPM 1018 mm/min
		3	Finishing Surface 17	**SDJCL 12 3B** **DCMX 07 02 08-WF 1125**		0,58 kW 0,7 η	0,41 kW 2	25 m/min 0.25 mm	1592 RPM 955 mm
C	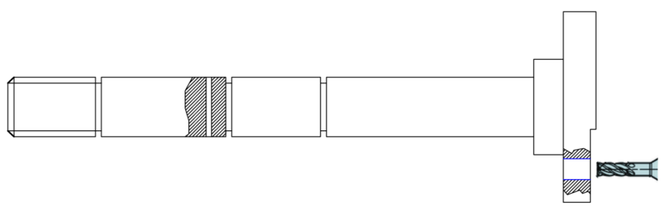	4	Marking and Drilling Surface 16	**DIN 333-A and 2P342-0500-PA P2BM N123K55-25A2**	Dividing Head, Tailstock	0,81 kW 0,7 η	0,57 kW 1	15 m/min 5.5 mm	955 RPM 764 mm

University of Pisa School of Engineering						Phase 40: Grinding			
						Cutting Parameters			
Sub Phase	Process Sketch	No.	Operation	Tool	Inspection	Machine Power	Cutting Power	Cutting Speed	Spindle RPM
				Insert		Efficiency	Number of Passes	Cutting Depth	Feed Rate
A	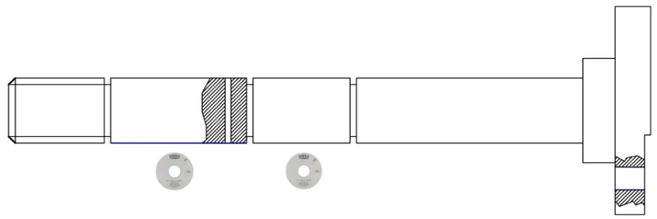	1	Grinding Surfaces 4 and 7	**89A 802 J5A V217 50**	Surface Roughness Tester	0,7 kW	0,5 kW	20 m/min	1273 RPM
						0,7 η	4	0,002 mm	0,1 mm/min

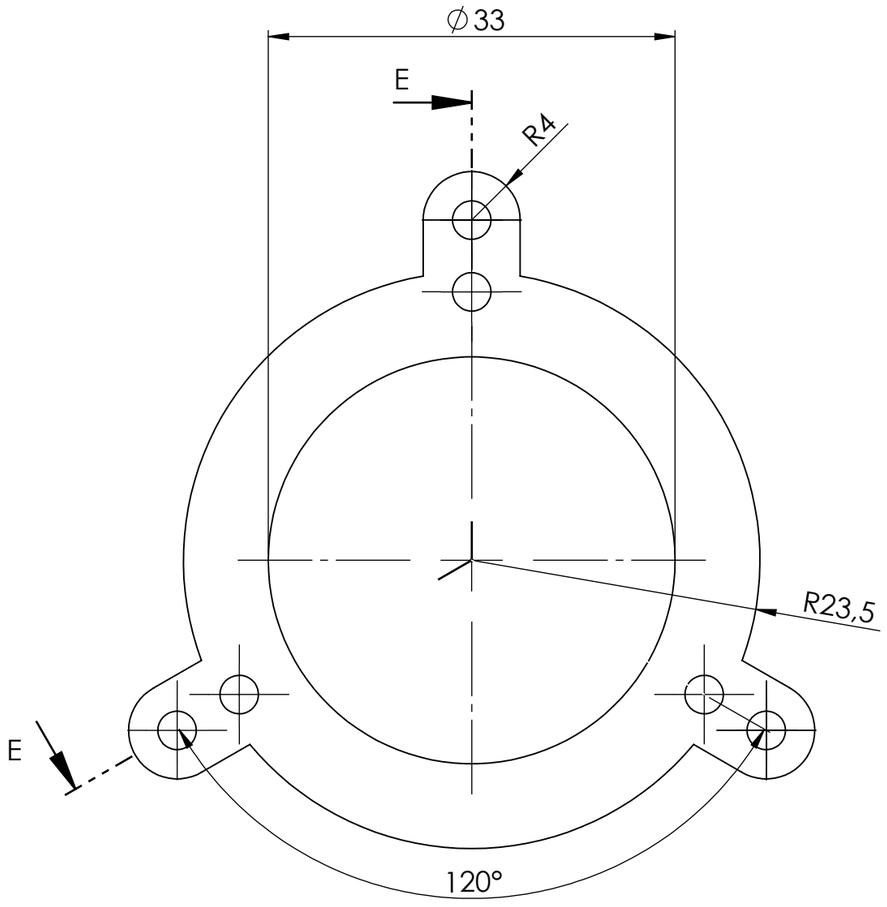

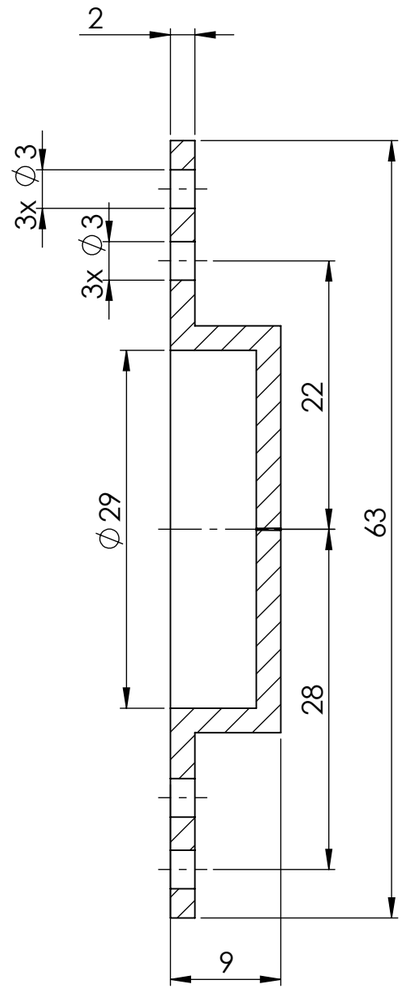

SEZIONE E-E

Coperchio	Scala 1:1
Rugosità generale: 3.2 µm	Data: 12/05/2025
Disegnatori Spinelli Michele Sofia La Spina	Materiale: Al serie 3003
	Foglio 1/1
Tolleranze generali secondo UNI ISO 2768-mK	

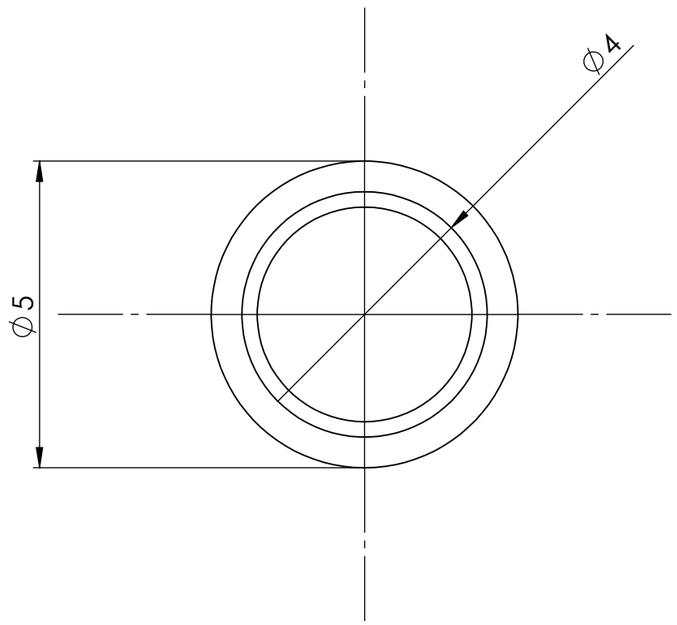

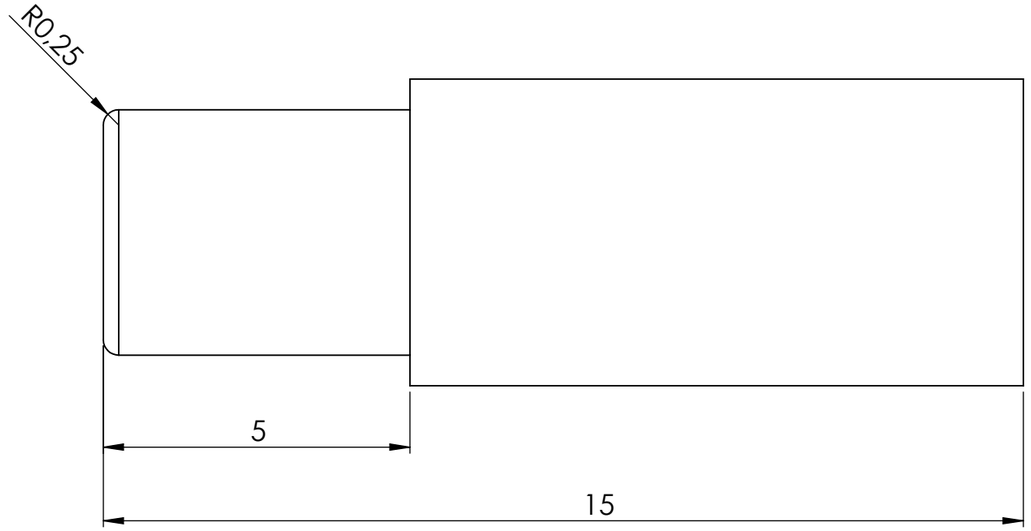

Università di Pisa - Scuola di ingegneria	
P.Di Manovella	Scala 10:1
Rugosità generale: 3.2 µm (salvo diversa indicazione)	Data: 30/05/2025
Disegnatori Spinelli Michele Sofia La Spina	Materiale: S355JR
Tolleranze generali secondo UNI ISO 2768-fH	Foglio 1/1